Climate data and climate-based seed zones for Mexico: guiding reforestation under observed and projected climate change

by

Dante Castellanos-Acuna

A thesis submitted in partial fulfillment of the requirements for the degree of

Doctor of Philosophy

in

Forest Biology and Management

Department of Renewable Resources
University of Alberta

Abstract

Seed zones for forest tree species have been used for decades to guide seed movement in reforestation programs, ensuring that seedlings are well adapted to their planting environments. Seeds may be collected and planted anywhere within a zone, but not across zone boundaries. The zones are geographic delineations that often track ecosystem boundaries, and comprise areas of similar climate and other environmental conditions. However, under climate change, this management approach is no longer valid. Local seed sources become increasingly lagged behind the environments to which they are optimally adapted.

Here, I develop a climate-based seed zone system for Mexico to address observed and projected climate change. For climate-based geographical delineations, I develop an interpolated climate database for past conditions (1901-2015) as well as for future projections for the 2020s, 2050s. and 2080s. While high quality interpolated climate data for temperature variables are widely available, existing datasets for precipitation have a number of shortcomings. Precipitation patterns in complex terrain, such as orographic lift effects and rain shadows, are generally difficult to model, and high quality products are only available for some regions of the world, namely for the United States, western Canada, and Europe.

To address this issue for Mexico and other parts of the world where high quality precipitation grids are not available, I start with the compilation of precipitation weather station records from nine open-access databases (CRU, GHCN, FAO, WMO, ECA, R-HydroNet and USFS). The database was cross-checked for errors, duplicates were removed, location and elevation errors corrected, and missing precipitation values were estimated where possible. The database was then spatially subsampled, retaining only the most reliable records with a balanced

spatial and elevational distribution, targeting one station per 40km grid cell and per 100m elevation interval. The resulting database contained 45,888 stations from an original 98,631 stations, excluding duplicates. This represents an approximately 50% larger compilation than any of the original databases, even after spatial subsampling.

Subsequently, I developed a new interpolation approach that models monthly long-term precipitation patterns for the 1961-1990 normal period, based on weather station data, wind measurements, and topographical exposure. The model was implemented through a local, universal kriging approach that uses wind speed, wind direction, as well as topographic aspect and slope to build an exposure covariate. This covariate was used to improve predictions of precipitation patterns, such as orographic lift on windward facing slopes and rain shadows on leeward facing slopes of mountain ranges. The resulting product consists of monthly estimates of precipitation at a resolution of 2.5 arcminutes (approximately 4km) with global coverage.

The new precipitation layers were integrated with existing data products for temperature, monthly historical anomalies layers for 110 years, and 90 future climate projections from the CMIP5 multimodel database into a comprehensive data package for Latin America. Estimates of more than 50 monthly, seasonal, and annual variables, including many biologically relevant climate variables such as growing and chilling degree days, beginning and end of the frost-free period, and drought indices are included. In total, the database includes approximately 18,000 climate surfaces that are accessible with a software front-end to query the database. I provide guidance for researchers and natural resource managers to select relevant climate variables, and future projections for climate change impact and adaptation planning and research.

In collaboration with the Government of Mexico, I then use the new database to develop climate change adaptation strategies to guide reforestation and afforestation programs. I propose

a new seed zone classification system that is based on bands of climate variables that are often related to local adaptation of tree populations of climate, delineating 32 zones that cover most of Mexico. I find that climate change observed over the last decades (1961-1990 reference period versus 1991-2015) has already resulted in substantial shifts of these seed zones towards warmer and drier conditions, with an additional shift of a similar magnitude expected by the 2050s. We recommend moving seed sources from warm, dry locations towards currently wetter and cooler planting sites, to compensate for climate change that has already occurred and is expected to continue for the next decades.

Preface

Chapter 2 of this thesis has been submitted to the *Geoscience Data Journal* as "Castellanos-Acuna, D. and Hamann, A. 2019. A global monthly weather station database for precipitation over the period 1901 to 2015. (MS# GDJ-2019-03-0008, revisions invited)". The study was conceived and designed by myself and AH. I assembled the database and conducted the error checking and analysis. I wrote the first draft of the chapter and AH contributed to editing the manuscript.

Chapter 3 of this thesis is being prepared for submission as a journal article to the *International Journal of Climatology*, entitled "Castellanos-Acuna, D. and Hamann, A. 20XX. Global, high-resolution monthly precipitation grids for 1961-1990 climate normal period". The study was conceived and designed by myself and AH. I conducted model development and validation, and wrote the first draft of the chapter. AH contributed to editing the manuscript.

Chapter 4 of this thesis is being prepared for submission as a journal article, entitled "Castellanos-Acuna, D. and Hamann, A., Wang, T. 20XX. A comprehensive database of historical and projected future climate for Latin America". The study was conceived and designed by myself and AH. I conducted data gathering and analysis and generated a new precipitation layer (Chapter 3). TW programmed a software package to access the database. I wrote the first draft of the chapter and all co-authors contributed to editing the manuscript.

Chapter 5 of this thesis has been published as Castellanos-Acuña, D., Vance-Borland, K.W., St. Clair, J.B., Hamann, A., López-Upton, J., Gómez-Pineda, E., Ortega-Rodríguez, J.M., Sáenz-Romero, C., 2018. Climate-based seed zones for Mexico: guiding reforestation under observed and projected climate change. *New Forests* **49**: 297-309. This study is a collaboration between the University of Alberta and the forest services of the U.S. and Mexico. It was originally conceived by CSR, JBSC, AH, and myself. KWVB, EGP, JMOR and myself collaborated on the analysis. Myself and CSR jointly developed the first draft of the paper and the other co-authors edited the manuscript.

Acknowledgements

Table of Contents

List of Tables

List of Figures

Chapter 1. General introduction

1.1. Climate change and observed climate trends

Emission of greenhouse gases from human activities have been identified as the main factor driving climate change observed over the last 100 years (Stott et al. 2001, Estrada et al. 2013, Lean 2018). Observed directional temperature trends attributed to human activities have been estimated to be between +0.6°C and +0.9°C for the last century, compared to an average temperature trend of less than +0.2°C estimated for the last several millennia (Jones and Mann 2004). The main greenhouse gases in the atmosphere causing climate change are water vapor, carbon dioxide (CO_2), methane (CH_4), and nitrous oxide (N_2O). The higher the concentrations of these gases in the atmosphere, the more infrared radiation emitted from the ground will be intercepted, causing warming of the atmosphere.

Although methane and nitrous oxide have a stronger greenhouse gas effect than carbon dioxide per molecule (10 times and 200 times more, respectively), their low concentrations in the atmosphere makes them overall less important greenhouse gasses compared to CO_2 (Lashof and Ahuja 1990). Water vapor is a strong greenhouse gas at relatively high concentrations, but its overall concentration has not significantly changed over the last century. The main changes in greenhouse gas concentrations have occurred for carbon dioxide, methane, and nitrous oxide. Ice cores from Antarctica and Greenland, show that from 1800 to 2005, the atmospheric concentrations of these gases have increased from 283 ppm to 379 ppm for CO_2 (a 34% increase), 742 ppb to 1754 ppb for CH_4 (a 136% increase), and 274 ppb to 319 ppb for N_2O (a 16% increase) (Meinshausen et al. 2011). The increments of carbon dioxide are due mostly to the burning of fossil fuels. Livestock husbandry, farming, landfills, and mining are the main

producers of methane, and the widespread use of fertilizers and byproducts of burning fossil fuels are the main causes for increases of nitrous oxide in the atmosphere (IPCC 2014).

Observed global warming first became apparent in the 1990s and has since been increasing at 0.2°C per decade. For global mean annual temperature, the observed climate change amounts to an increase of 0.78 °C between the average value for the 1850–1900 period and the 2003–2012 period (IPCC 2014). Regarding regional variation, southeastern United States, regions around the Mediterranean Sea, eastern India and southeast Asia, have experienced warming of less than 1°C, while the rest of the globe has experienced warming greater than 1°C (IPCC 2014). Changes to precipitation can only be analyzed with certainty back to the 1950s because a lack of weather stations prior. From 1951 to 2010, there have been increases in precipitation in eastern North America, southern South America, northern Europe and Eurasia, India and northern Australia (IPCC 2014), with most of these increases occurring as more intense precipitation events (Min et al. 2011). Decreases of precipitation for the 1951 to 2010 period, mostly in the form of seasonal or multi-annual droughts (Cook et al. 2018), have been observed in Mexico and Central America, northern South America, southern Europe, northern and central Africa, Southeast Asia, and eastern Australia (IPCC 2014).

The magnitude of temperature changes during the 20th century have no equivalent over the past two millennia, according to climate reconstructions based on global tree-rings, lake sediments and ice cores (Jones and Mann 2004). In contrast, changes in precipitation over the last centuries are more difficult to relate to directional trends associated with anthropogenic climate change. Severe drought episodes in the Northern Hemisphere have occurred in the past, and have, for example, be associated to solar activity (Ljungqvist et al. 2016).

1.2. Climate change projections

Given that significant climate change that has already occurred, and the strong dependence of agricultural and natural systems on climate, predictions of future climate change and their impacts are needed to develop climate change adaptation strategies. The earliest models to simulate atmospheric conditions and the effect of radiative forcing on these systems were developed in the 1960s (Manabe and Wetherald 1967, Manabe and Bryan 1969). Since then, institutions around the world have developed complex mathematical models that simulate the atmosphere and ocean dynamics (Atmosphere-Ocean General Circulations Models, or AOGCMs). The models are built based on observed atmospheric flows and ocean currents, and then make short and long term climate change predictions (Meehl et al. 2007). Atmospheric flows and ocean currents are modeled in three dimensions with mathematical fluid dynamics equations on high performance computers (Flato et al. 2013). The latest generations of models (usually denoted with an –ES extension for Earth Systems) also incorporate other factors that influence the Earth's atmospheric circulation patterns, such as changes to global vegetation, changes to global nutrient cycles, changes to ice cover at the poles, and their resulting effects on local and global climate conditions, atmospheric circulation and ocean currents (Flato 2011).

Even the most advanced AOGCM Earth Systems models are not without important conceptual and technical limitations. Technical limitations include computational resources that require the models to be run at low spatial resolutions, typically with resolutions of approximately 200km grid cells, too coarse to model changes to local weather patterns (Bader et al. 2008). For higher resolution models, the number of variables included in the model may have to be limited, reducing its predictive power (Randall 2010). Furthermore, some processes are too complex to be directly incorporated in the model (i.e. biochemical processes in plants, or the formation of

clouds). To solve this limitation, independent models are run for such processes, and the results are then incorporated in the general model in the form of statistical associations rather than functional modeling (Moorthi and Suarez 1992, Pan and Randall 1998, Randall et al. 2003, Miura et al. 2007).

There are also broader, conceptual concerns why AOGCMs from different research groups may all be systematically biased in their projections. The evolution and development of AOGCMs is not independent among research groups, and it could be argued that all AOGCMs are essentially small variations of the same general modeling approach (Knutti et al. 2013). They are describing the same data, collected for the same system, and rely on similar procedures to simplify, parameterize, select or omit processes to be modeled. In addition, models share components due to the exchange of ideas and code among research groups. As a consequence, variance in projections from different AOGCMs may underestimate the true uncertainty associated with AOGCM-based future climate projections. With the same errors, assumptions, and simplifications implemented in all or most AOGCMs, what appears to be agreement in results could also be the same bias in projections (Giorgi and Mearns 2002, Knutti et al. 2013).

Even though we cannot fully quantify the bias or true error of future projections, AOGMCs have by now proven their ability to forecast climate change. The first IPCC report, published in 1990, summarizes results from early generation general circulation models that were developed in the 1980s. The report includes average "future" predictions for a normal period centered around the year 2010 of approximately 1°C (IPCC 1990), a projection made at a time when an anthropogenic warming signal was not statistically detectable. The actual global increase of mean annual temperature for a 20 year period centered around 2010 (2000-2019) was in fact 0.85°C warmer than the first half of the 20th century (Hansen et al. 2010, GISTEMP 2019).

4

From 2010 forward, a comparable near-future projection from the latest generation AOGCMs for the 2030s, points towards an increase of global mean annual temperature around 1.2°C relative to the first half of the 20th century, resulting in substantial increases in the duration, intensity and extent of heat waves (Kirtman et al. 2013). For precipitation, a strengthening of spatial and temporal variation in precipitation events is expected for the near term future, i.e. generally, increases of precipitation are expected for regions that already receive high precipitation in both high latitudes and the tropics, whereas decreases are expected for many dry subtropical and arid regions (Chou et al. 2007, Muller and O'Gorman 2011, Kirtman et al. 2013).

1.3. Climate change impacts on forest ecosystems

The effects of climate change on natural ecosystems has also been well documented over the last two decades (e.g., reviewed by Parmesan and Yohe 2003, Rosenzweig et al. 2008, Maclean and Wilson 2011, Wiens 2016). Some of the impacts on natural systems are the reduction of the ice sheets on the poles, thawing of the permafrost in the arctic (Osterkamp 2007, Anthony et al. 2018), late freezing and early breaking of rivers and lakes (Magnuson et al. 2000, Sharma et al. 2016), and increase in the frequency and intensity of wildfires (Westerling et al. 2006, Flannigan et al. 2009). For oceans, a decrease of 6% of primary productivity since the 1980s, associated with increased ocean surface temperature of 0.6°C and an acidification of 0.1 pH units, has been reported (Hoegh-Guldberg and Bruno 2010). Impacts directly observed on organisms include changes to the timing of biological events in plants, insects, and animals, such as the time of year when budbreak or flowering occurs (Beaubien and Hamann 2011), or the time of insect and bird activity (Visser and Both 2005, Memmott et al. 2007). Changes on the distribution of plants, mostly tracking their climate niche in poleward directions (Boisvert-Marsh et al. 2014), or upward on the elevational gradient (Penuelas et al. 2007, Lenoir et al. 2008) have also been reported.

Regarding trees and forest ecosystems, the focus of this thesis, their inability to track their climate niche due to their immobility and long generation time exposes them to increased risk of mortality when exposed to extended periods of extreme temperatures and droughts (McDowell et al. 2011). Even if a moderate increase of average temperatures does not cause the death of the trees, the stress associated with having to cope with conditions outside the climate niche for which they are optimally adapted, leaves individuals or local populations weakened (e.g., Aitken et al. 2008). In northern latitudes, where many insect pests, like bark beetles, have not been able to build significant populations due to cold winter temperatures that kill their dormant eggs, weakened forests and ecosystems face additional new threats from pests and diseases (Breshears et al. 2005).

Forests declines due to biotic factors, climate and their interactions have been comprehensively reviewed (Allen et al. 2010, Birdsey and Pan 2011, Pravalie 2018). To give some notable examples across the globe: A drought spanning the years from 2000 to 2008 in northern Africa, has been linked to nearly 40% mortality of the Atlas cedar conifer in the dry regions of the species distribution (Matyas 2010). In Uganda, an extreme drought period in 1999 caused 19% mortality of tropical tree species (Lwanga 2003). Warm winters and increased drought from 2003-2008 in South Korea caused 30% mortality of *Abies koreana* (Koo et al. 2017). In Argentina, increased temperatures and drought in 1998-2000 caused widespread mortality of *Nothofagus dombeyi* (Suarez et al. 2004). In the Amazon, extreme droughts in 2005 and 2010 caused dieback and mortality in rainforest ecosystems (Lewis et al. 2011).

In North America, the most notable impact of climate change on forest ecosystems is arguably the mountain pine beetle epidemic centered around the sub-boreal forests of British Columbia,

6

resulting in 18.3 million hectares of affected pine forests, or 435 million m^3 lost, with an estimated 270 million tons of carbon released to the atmosphere by 2020 (Kurz et al. 2008). In Alaska, from 1990 to 2000, the spruce beetle caused widespread mortality across 1.2 million ha, approximately 40% more than the 800,000 ha infected from 1920-1990 (Werner et al. 2006). In Alberta and Saskatchewan, 50% mortality of *Populus tremuloides* was related to increased temperatures and droughts across 11.5 million ha, with potential carbon emissions of 14 million tons (Michaelian et al. 2011). In the US, extreme droughts in the period 2000 to 2003, led to almost 90% death of *Pinus edulis* across 1.2 million ha. In the later stages of this massive mortality, increased presence of the bark beetle *Ips confusus* was observed (Breshears et al. 2005).

1.4. Climate change adaptation strategies in forestry

To mitigate or prevent large-scale tree mortality, climate change adaptation strategies need to be developed for forestry and for management of forest ecosystems, which may include a variety of different approaches (Millar et al. 2007). For forests of high conservation value, management that increases resistance to climate change may be appropriate. This may include bans of forest harvesting that would result in microclimate conditions that would no longer support the regeneration of the current forest ecosystem. For forests that are not in extreme danger due to climate change, management practices that enhance resilience may be appropriate. For example, planting nursery stock that is larger than normal would give seedlings a better chance to successfully regenerate in climate conditions that are not optimal. For forests that can no longer be maintained in place, management approaches need to focus on facilitating change towards ecosystems that can be sustained under climate change, for example through human-assisted migration.

In the context of forestry, assisted migration prescriptions could be implemented through regular reforestation programs, where seed sources are collected in one location, grown in a nursery, and then transported to a new reforestation site (Pedlar et al. 2011, Pedlar et al. 2012). This type of assisted migration would not only occur beyond the current range of species, but would also be applicable for moving seed sources among locally adapted populations within a species range, sometimes referred to as assisted gene flow (Aitken et al. 2008, Aitken and Bemmels 2016). For implementing assisted migration or assisted geneflow, information is required on how forest species and their populations are adapted to local climate conditions. This information can then be used to delineate tree populations with similar adaptations to climate that may be used as seed zones to regulate seed transfer (Liepe et al. 2016).

Seed zones for forest tree species have been used for decades to guide seed movement in reforestation programs, ensuring that seedlings are well adapted to their planting environments. Seeds may be collected and planted anywhere within a zone, but not across zone boundaries. Ideally, these seed zones are based on extensive provenance field testing across multiple environments to delineate genetically homogenous populations (Ying and Yanchuk 2006, Hamann et al. 2011), but such trial series are only available for a few commercially important tree species, and typically only for the portions of their natural range where commercial forestry operations take place. An alternative for species, where only a few or no trials are available to estimate genetic differentiation is to guide reforestation practices by proxy information. Forest trees are generally adapted to landscape-scale climatic and physiogeographic features, thus seed zone delineations are often first drawn based on ecosystem delineations, and later refined as genetic information from long-term provenance trials becomes available (Morgenstern 1996, Ying and Yanchuk 2006).

However, under climate change, the seed-zone based management approach is no longer valid. Local seed sources become increasingly lagged behind the environments to which they are optimally adapted. To address this problem, recent seed zone delineations have been based on climate conditions rather than ecosystem delineations. The rationale for this change is that climatic regions can be re-drawn under observed and projected climate change to match genotypes to new environmental conditions. Examples for climate-based seed zones include delineations that largely reflect climatic gradients in temperature and precipitation for the United States (Bower et al. 2014). In Canada, climate-based seed zones have been developed based on minimum temperature for applications in agriculture, forestry and horticulture (McKenney et al. 2001), and provincial climate-based seed zones have been developed to guide reforestation efforts under current and anticipated future climates (Gray and Hamann 2011, O'Neill et al. 2017).

1.5. Interpolated climate data to support adaptation

A required tool for developing climate-based seed zones are high quality interpolated climate grids that represent normal climate conditions, often represented by the 1961-1990 climate average, but also annual historical climate data to evaluate observed climate trends and future projections of climate change of adaptation planning. A number of climate data products with varying spatial and temporal resolution and extent have been developed. However, the quality of the climate data is partially driven by historical factors and economic development. Some European countries have weather station records that date back to the 1700s, and the United States has thousands of stations with records dating back to the early 1900s (Peterson and Vose 1997). In other parts of the World, such as Canada, Latin America, Asia and Africa, station records are quite scarce before the 1960s (Lawrimore et al. 2011).

This difference in the quality and density of weather station coverage is reflected in the interpolated products derived from these weather stations. For the United States, there are several well regarded high-resolution datasets that date back to 1895 in monthly time steps, such as the Parameter Elevation Regression on Independent Slopes Model database (PRISM) (Daly et al. 2008), or the North America Land Data Assimilation System database (NLDAS) (Mitchell et al. 2004). Even daily time steps are available since 1980 through Daymet: Daily Surface Weather and Climatological Summaries (Thornton et al. 1997). These databases typically cover 3 basic climate variables originally obtained as daily minimum temperature, daily maximum temperature and daily precipitation, and subsequently summarized in various ways (monthly, seasonal, annual, decadal, and 30-year averages).

Interpolated climate databases at the global scale are typically limited to moderate spatial resolutions (0.5° or approximately 50km), due to a lack of a reliable network of weather stations for many regions of the world. Widely used data sets include the Climate Research Unit Time Series (CRU-TS) from the University of East Anglia (Harris et al. 2014), and a similar database by Wilmott & Matsura from the University of Delaware (Willmott and Matsuura 1995). Other datasets with the same spatial and temporal resolution and time coverage, include a precipitation database by the Global Precipitation Climatology Centre (GPCC) operated by the German Weather Service (DWD) (Becker et al. 2013), and the Precipitation REConstruction Land (PRECL) database from NOAA (Chen et al. 2002). While these datasets have a useful monthly temporal resolution for historical research, the absolute climate values can be unreliable because of their coarse spatial resolution of about 50km.

WorldClim, a high spatial resolution database (30 arcseconds or approximately 1km) (Hijmans et al. 2005) is widely used, but provides only a 30-year climate normal period and no explicit historical data is provided. Additionally, the methodology employed by WorldClim is not as

advanced as the PRISM approach to model precipitation patterns in topographically complex landscapes.

1.6. Developing climate data products for easy use by researchers and practitioners

To plan adequate management strategies for climate change for natural and managed resources, researchers often need to access and combine various databases that come in different spatial and temporal resolutions, and also different file formats. Depending on the location of the study area and the type of climate data required, this might require hundreds of files. For example, for historical sample-based research, the historical values might come from a historical database such as the time series of CRU. However, the low spatial resolution of 0.5° of its grid makes the absolute values unreliable, and absolute values have to be obtained from other sources. To facilitate this task, Hamann and Wang (2005) have developed a software solution that combines various databases, and performs extractions, historical time overlays, and lapse-rate based elevation adjustments.

This software tool was first developed for British Columbia, but subsequently expanded to Alberta and western Canada (Mbogga et al. 2009, Mbogga et al. 2010), western North America (Wang et al. 2012), and all of North America (Wang et al. 2016). The size of the databases is kept small by relying on a single high resolution base climate surface (a 1961-1990 climate normal period), and storing all historical or future data layers as anomalies (or deviations from the 1961-1990 normal period) at a much lower resolution of 0.5°. The program then uses the delta method that consists of overlaying the low resolution anomalies over the high resolution baseline to quickly generate time series or gridded data for a selected study area in any projection, at any resolution, and for any time period. The software has proven useful for applied

11

research in many disciplines and is cited in hundreds of research papers for North America every year (Wang et al. 2016).

1.7. Objectives and thesis structure

My focus in this thesis will be the development of a new methodology to create long term averaged precipitation data, and use it for the development of a climate-based seedzone system for Mexico. However, I also intend to use the databases and tools developed in this thesis to provide useful databases for climate change impact and adaptation planning for developing countries that have imperfect weather station networks and also lack high-quality interpolated data products. This thesis comprises an effort to compile global weather station data from various sources, cross-check and validate the quality of station data, and then develop a high-quality global precipitation layer for the world. Conceptually emulating the PRISM methodology used for North America, I will use additional covariates such as, topographic aspect and slope, and wind speed and direction, to model unusual precipitation patterns, such as orographic lift on windward facing slopes and rain shadows on leeward facing slopes. Secondly, building on the existing code base developed by Hamann and Wang (Hamann et al. 2013, Wang et al. 2016), I will co-develop a software package of historical and future projected climate data for Latin America, including a wide range of biologically relevant climate variables. Lastly I provide an example of how these climate databases can be applied to develop climate change adaptations strategies for natural resource management. In collaboration with the government of Mexico, the COmision NAcional FORestal (CONAFOR), and the Instituto de Investigaciones Agropecuarias y Forestales of the Universidad Michoacana (UMSNH-IIAF), I develop general climate-based seed zones and seed transfer guidelines for Mexico to address observed and projected climate change.

My thesis contains four research chapters with the following specific objectives:

Chapter 2. In order to develop a high quality global precipitation surface, I start by assembling and cross-checking a monthly weather station database for precipitation that combines several regional and global databases that are publicly available. I use duplicate entries, digital elevation models and nearby stations to search for inconsistencies in recorded climate values in weather station records that may be due to unit conversion errors, location and elevation inaccuracies. To improve the estimates of long term averages (e.g. 30-year climate normals), I estimate missing values in monthly station time series records with a linear model approach based on interpolated anomaly surfaces. The reliability of estimated values was documented with model fit statistics and quality scores. Lastly, I subsample this database for a pre-determined three dimensional filter to retain only the most reliable and complete station records for a given area.

Chapter 3. Using the weather station database from the previous chapter, I develop a new high resolution precipitation layer with a global extent. I implement a novel approach to interpolate precipitation similar to the PRISM methodology, by including covariates such as topographic aspect and slope, wind speed and direction, as well as local interpolations, to model precipitation patterns such as orographic lift on windward facing slopes, and rain shadows on leeward facing slopes. I statistically and visually evaluate the generated surfaces and compare the reliability of climate estimates with other widely used interpolated data products.

Chapter 4. Similar to the software package ClimateNA for North America (Wang et al 2016), I assemble and validate a database for Mexico, Central and South America (ClimateSA). I evaluate whether local lapse-rate based elevation adjustments result in more precise estimates of temperature for complex mountainous terrain, and also calculate errors associated with estimates of historical climate values by means of delta method overlays of moderate resolution monthly

13

historical anomalies for the last century on a high-resolution 1961-1990 climate normal surface for South America. I also intend to visualize future projections of climate from different AOGCMs to provide guidance for researchers and professionals on how to best select relevant scenarios for their area of interest.

Chapter 5. Using improved climate data from the previous research chapters, I develop climate-based seed zones for Mexico. Changes to climatic conditions that have been observed over the last three decades are quantified for existing, ecosystem-based seed zones. Similarly, changes expected for the near term future (2050s) are compiled for each seed zone to analyze how observed trends compare to future predictions in direction and magnitude. Subsequently, I develop climate-based seed zones to visualize observed and projected shifts of geographic areas with comparable climate conditions over time. I use an overlay of ten intervals of mean coldest month temperature and seven intervals of a dryness index to arrive at 32 major climate-based seed zones for Mexico. I subsequently evaluate climate envelope shifts for these zones to derive assisted migration recommendations that compensate for observed and anticipated climate change.

1.8. References

Aitken, S. N., and J. B. Bemmels. 2016. Time to get moving: assisted gene flow of forest trees. Evolutionary Applications **9**:271-290.

Aitken, S. N., S. Yeaman, J. A. Holliday, T. Wang, and S. Curtis-McLane. 2008. Adaptation, migration or extirpation: climate change outcomes for tree populations. Evolutionary Applications **1**:95-111.

Allen, C. D., A. K. Macalady, H. Chenchouni, D. Bachelet, N. McDowell, M. Vennetier, T. Kitzberger, A. Rigling, D. D. Breshears, E. H. Hogg, P. Gonzalez, R. Fensham, Z. Zhang, J. Castro, N. Demidova, J. H. Lim, G. Allard, S. W. Running, A. Semerci, and N. Cobb.

2010. A global overview of drought and heat-induced tree mortality reveals emerging climate change risks for forests. Forest Ecology and Management **259**:660-684.

Anthony, K. W., T. S. von Deimling, I. Nitze, S. Frolking, A. Emond, R. Daanen, P. Anthony, P. Lindgren, B. Jones, and G. Grosse. 2018. 21st-century modeled permafrost carbon emissions accelerated by abrupt thaw beneath lakes. Nature Communications **9**:3262. DOI: 3210.1038/s41467-41018-05738-.

Bader, D., C. Covey, W. Gutowski, I. Held, K. Kunkel, R. Miller, R. Tokmakian, and M. Zhang. 2008. Climate models: an assessment of strengths and limitations. Geological and Atmospheric Sciences Reports. 3. Accessed March 6, 2017 at http://lib.dr.iastate.edu/ge_at_reports/3.

Beaubien, E., and A. Hamann. 2011. Spring Flowering Response to Climate Change between 1936 and 2006 in Alberta, Canada. Bioscience **61**:514-524.

Becker, A., P. Finger, A. Meyer-Christoffer, B. Rudolf, K. Schamm, U. Schneider, and M. Ziese. 2013. A description of the global land-surface precipitation data products of the Global Precipitation Climatology Centre with sample applications including centennial (trend) analysis from 1901–present. Earth System Science Data **5**:71-99.

Birdsey, R., and Y. D. Pan. 2011. Ecology: drought and dead trees. Nature Climate Change **1**:444-445.

Boisvert-Marsh, L., C. Périé, and S. de Blois. 2014. Shifting with climate? Evidence for recent changes in tree species distribution at high latitudes. Ecosphere **5**:art83. doi:10.1890/ES1814-00111.00111.

Bower, A. D., J. B. S. Clair, and V. Erickson. 2014. Generalized provisional seed zones for native plants. Ecological Applications **24**:913-919.

Breshears, D. D., N. S. Cobb, P. M. Rich, K. P. Price, C. D. Allen, R. G. Balice, W. H. Romme, J. H. Kastens, M. L. Floyd, J. Belnap, J. J. Anderson, O. B. Myers, and C. W. Meyer. 2005. Regional vegetation die-off in response to global-change-type drought. Proceedings of the National Academy of Sciences 102:15144-15148.

Chen, M., P. Xie, J. E. Janowiak, and P. A. Arkin. 2002. Global land precipitation: a 50-yr monthly analysis based on gauge observations. Journal of Hydrometeorology **3**:249-266.

Chou, C., J. Y. Tu, and P. H. Tan. 2007. Asymmetry of tropical precipitation change under global warming. Geophysical Research Letters **34**:Artn L17708, DOI:17710.11029/12007gl030327

Cook, B. I., J. S. Mankin, and K. J. Anchukaitis. 2018. Climate change and drought: from past to future. Current Climate Change Reports **4**:164-179.

Daly, C., M. Halbleib, J. I. Smith, W. P. Gibson, M. K. Doggett, G. H. Taylor, J. Curtis, and P. P. Pasteris. 2008. Physiographically sensitive mapping of climatological temperature and precipitation across the conterminous United States. International Journal of Climatology **28**:2031-2064.

Estrada, F., P. Perron, and B. Martinez-Lopez. 2013. Statistically derived contributions of diverse human influences to twentieth-century temperature changes. Nature Geoscience **6**:1050-1055.

Flannigan, M. D., M. A. Krawchuk, W. J. de Groot, B. M. Wotton, and L. M. Gowman. 2009. Implications of changing climate for global wildland fire. International Journal of Wildland Fire **18**:483-507.

Flato, G., J. Marotzke, B. Abiodun, P. Braconnot, S. C. Chou, W. Collins, P. Cox, F. Driouech, S. Emori, V. Eyring, C. Forest, P. Gleckler, E. Guilyardi, C. Jakob, V. Kattsov, C. Reason, and M. Rummukaine. 2013. Evaluation of Climate Models.*in* T. F. Stocker, D. Qin, G.-K. Plattner, M. Tignor, S. K. Allen, J. Boschung, A. Nauels, Y. Xia, V. Bex, and P. M. Midgley, editors. Climate Change 2013: The Physical Science Basis. Contribution of Working Group I to the Fifth Assessment Report of the Intergovernmental Panel on Climate Change. Cambridge University Press, Cambridge, UK.

Flato, G. M. 2011. Earth system models: an overview. Wiley Interdisciplinary Reviews: Climate Change **2**:783-800.

Giorgi, F., and L. O. Mearns. 2002. Calculation of average, uncertainty range, and reliability of regional climate changes from AOGCM simulations via the "reliability ensemble averaging" (REA) method. Journal of Climate **15**:1141-1158.

GISTEMP. 2019. GISS Surface Temperature Analysis (GISTEMP). NASA Goddard Institute for Space Studies. Dataset accessed 2019-04-10 at data.giss.nasa.gov/gistemp/.

Gray, L. K., and A. Hamann. 2011. Strategies for reforestation under uncertain future climates: guidelines for Alberta, Canada. PLOS ONE **6**:e22977.

Hamann, A., T. Gylander, and P.-y. Chen. 2011. Developing seed zones and transfer guidelines with multivariate regression trees. Tree Genetics & Genomes **7**:399-408.

Hamann, A., and T. L. Wang. 2005. Models of climatic normals for genecology and climate change studies in British Columbia. Agricultural and Forest Meteorology **128**:211-221.

Hamann, A., T. L. Wang, D. L. Spittlehouse, and T. Q. Murdock. 2013. A Comprehensive, High-Resolution Database of Historical and Projected Climate Surfaces for Western North America. Bulletin of the American Meteorological Society **94**:1307-1309.

Hansen, J., R. Ruedy, M. Sato, and K. Lo. 2010. Global Surface Temperature Change. Reviews of Geophysics **48**:RG4004.

Harris, I., P. D. Jones, T. J. Osborn, and D. H. Lister. 2014. Updated high-resolution grids of monthly climatic observations – the CRU TS3.10 Dataset. International Journal of Climatology **34**:623-642.

Hijmans, R. J., S. E. Cameron, J. L. Parra, P. G. Jones, and A. Jarvis. 2005. Very high resolution interpolated climate surfaces for global land areas. International Journal of Climatology **25**:1965-1978.

Hoegh-Guldberg, O., and J. F. Bruno. 2010. The impact of climate change on the world's marine ecosystems. Science **328**:1523-1528.

IPCC. 1990. Working Group I: Scientific Assesment of Climate Change. Cambridge University Press, Cambridge UK.

IPCC. 2014. Climate Change 2014: Synthesis Report. Contribution of Working Groups I, II and III to the Fifth Assessment Report of the Intergovernmental Panel on Climate Change [Core Writing Team, R.K. Pachauri and L.A. Meyer (eds.)]. IPCC, Geneva, Switzerland.

Jones, P. D., and M. E. Mann. 2004. Climate over past millennia. Reviews of Geophysics **42**.

Kirtman, B., S.B. Power, J.A. Adedoyin, G.J. Boer, R. Bojariu, I. Camilloni, F.J. Doblas-Reyes, A.M. Fiore, M. Kimoto, G.A. Meehl, M. Prather, A. Sarr, C. Schär, R. Sutton, G.J. van Oldenborgh, G. Vecchi, and H. J. Wang. 2013. Near-term Climate Change: Projections and Predictability.*in* T. F. Stocker, D. Qin, G.-K. Plattner, M. Tignor, S. K. Allen, J. Boschung, A. Nauels, Y. Xia, V. Bex, and P. M. Midgley, editors. Climate Change 2013: The Physical Science Basis. Contribution of Working Group I to the Fifth Assessment Report of the Intergovernmental Panel on Climate Change. Cambridge University Press, Cambridge, UK.

Knutti, R., D. Masson, and A. Gettelman. 2013. Climate model genealogy: Generation CMIP5 and how we got there. Geophysical Research Letters **40**:1194-1199.

Koo, K. A., W. S. Kong, S. U. Park, J. H. Lee, J. Kim, and H. Jung. 2017. Sensitivity of Korean fir (*Abies koreana* Wils.), a threatened climate relict species, to increasing temperature at an island subalpine area. Ecological Modelling **353**:5-16.

Kurz, W. A., C. C. Dymond, G. Stinson, G. J. Rampley, E. T. Neilson, A. L. Carroll, T. Ebata, and L. Safranyik. 2008. Mountain pine beetle and forest carbon feedback to climate change. Nature **452**:987-990.

Lashof, D. A., and D. R. Ahuja. 1990. Relative Contributions of Greenhouse Gas Emissions to Global Warming. Nature **344**:529-531.

Lawrimore, J. H., M. J. Menne, B. E. Gleason, C. N. Williams, D. B. Wuertz, R. S. Vose, and J. Rennie. 2011. An overview of the Global Historical Climatology Network monthly mean temperature data set, version 3. Journal of Geophysical Research: Atmospheres **116**:D19121. doi:19110.11029/12011JD016187.

Lean, J. L. 2018. Observation-based detection and attribution of 21st century climate change. Wiley Interdisciplinary Reviews-Climate Change **9**:e511. DOI: 510.1002/wcc.1511.

Lenoir, J., J. C. Gegout, P. A. Marquet, P. de Ruffray, and H. Brisse. 2008. A significant upward shift in plant species optimum elevation during the 20th century. Science **320**:1768-1771.

Lewis, S. L., P. M. Brando, O. L. Phillips, G. M. F. van der Heijden, and D. Nepstad. 2011. The 2010 Amazon drought. Science **331**:554-554.

Liepe, K. J., A. Hamann, P. Smets, C. R. Fitzpatrick, and S. N. Aitken. 2016. Adaptation of lodgepole pine and interior spruce to climate: implications for reforestation in a warming world. Evolutionary Applications **9**:409-419.

Ljungqvist, F. C., P. J. Krusic, H. S. Sundqvist, E. Zorita, G. Brattstrom, and D. Frank. 2016. Northern Hemisphere hydroclimate variability over the past twelve centuries. Nature **532**:94-98.

Lwanga, J. S. 2003. Localized tree mortality following the drought of 1999 at Ngogo, Kibale National Park, Uganda. African Journal of Ecology **41**:194-196.

Maclean, I. M. D., and R. J. Wilson. 2011. Recent ecological responses to climate change support predictions of high extinction risk. Proceedings of the National Academy of Sciences USA **108**:12337-12342.

Magnuson, J. J., D. M. Robertson, B. J. Benson, R. H. Wynne, D. M. Livingstone, T. Arai, R. A. Assel, R. G. Barry, V. Card, E. Kuusisto, N. G. Granin, T. D. Prowse, K. M. Stewart, and V. S. Vuglinski. 2000. Historical trends in lake and river ice cover in the Northern Hemisphere. Science **289**:1743-1746.

Manabe, S., and K. Bryan. 1969. Climate calculations with a combined ocean-atmosphere model. Journal of the Atmospheric Sciences **26**:786-&.

Manabe, S., and R. T. Wetherald. 1967. Thermal equilibrium of the atmosphere with a given distribution of relative humidity. Journal of the Atmospheric Sciences **24**:241-259.

Matyas, C. 2010. Forecasts needed for retreating forests. Nature **464**:1271-1271.

Mbogga, M. S., A. Hamann, and T. Wang. 2009. Historical and projected climate data for natural resource management in western Canada. Agricultural and Forest Meteorology **149**:881-890.

Mbogga, M. S., X. Wang, and A. Hamann. 2010. Bioclimate envelope model predictions for natural resource management: dealing with uncertainty. Journal of Applied Ecology **47**:731-740.

McDowell, N. G., D. J. Beerling, D. D. Breshears, R. A. Fisher, K. F. Raffa, and M. Stitt. 2011. The interdependence of mechanisms underlying climate-driven vegetation mortality. Trends in Ecology & Evolution **26**:523-532.

McKenney, D. W., M. F. Hutchinson, J. L. Kesteven, and L. A. Venier. 2001. Canada's plant hardiness zones revisited using modern climate interpolation techniques. Canadian Journal of Plant Science **81**:129–143.

Meehl, G. A., C. Covey, T. Delworth, M. Latif, B. McAvaney, J. F. B. Mitchell, R. J. Stouffer, and K. E. Taylor. 2007. The WCRP CMIP3 multimodel dataset - A new era in climate change research. Bulletin of the American Meteorological Society **88**:1383-1394.

Meinshausen, M., S. J. Smith, K. Calvin, J. S. Daniel, M. L. T. Kainuma, J. F. Lamarque, K. Matsumoto, S. A. Montzka, S. C. B. Raper, K. Riahi, A. Thomson, G. J. M. Velders, and D. P. P. van Vuuren. 2011. The RCP greenhouse gas concentrations and their extensions from 1765 to 2300. Climatic Change **109**:213-241.

Memmott, J., P. G. Craze, N. M. Waser, and M. V. Price. 2007. Global warming and the disruption of plant-pollinator interactions. Ecology Letters **10**:710-717.

Michaelian, M., E. H. Hogg, R. J. Hall, and E. Arsenault. 2011. Massive mortality of aspen following severe drought along the southern edge of the Canadian boreal forest. Global Change Biology **17**:2084-2094.

Millar, C. I., N. L. Stephenson, and S. L. Stephens. 2007. Climate change and forests of the future: managing in the face of uncertainty. Ecological Applications **17**:2145-2151.

Min, S.-K., X. Zhang, F. W. Zwiers, and G. C. Hegerl. 2011. Human contribution to more-intense precipitation extremes. Nature **470**:378.

Mitchell, K. E., D. Lohmann, P. R. Houser, E. F. Wood, J. C. Schaake, A. Robock, B. A. Cosgrove, J. Sheffield, Q. Duan, L. Luo, R. W. Higgins, R. T. Pinker, J. D. Tarpley, D. P. Lettenmaier, C. H. Marshall, J. K. Entin, M. Pan, W. Shi, V. Koren, J. Meng, B. H. Ramsay, and A. A. Bailey. 2004. The multi-institution North American Land Data Assimilation System (NLDAS): Utilizing multiple GCIP products and partners in a continental distributed hydrological modeling system. Journal of Geophysical Research: Atmospheres **109**:D07S90. doi:10.1029/2003JD003823

Miura, H., M. Satoh, H. Tomita, A. T. Noda, T. Nasuno, and S. Iga. 2007. A short-duration global cloud-resolving simulation with a realistic land and sea distribution. Geophysical Research Letters **34**:Artn L02804. DOI: 02810.01029/02006gl027448.

Moorthi, S., and M. J. Suarez. 1992. Relaxed Arakawa-Schubert - a parameterization of moist convection for General-Circulation Models. Monthly Weather Review **120**:978-1002.

Morgenstern, K. 1996. Geographic Variation in Forest Trees. Genetic Basis and Application of Knowledge in Silviculture University of British Columbia Press, Vancouver, British Columbia.

Muller, C. J., and P. A. O'Gorman. 2011. An energetic perspective on the regional response of precipitation to climate change. Nature Climate Change **1**:266-271.

O'Neill, G., T. Wang, N. Ukrainetz, L. Charleson, L. McAuley, A. Yanchuk, and S. Zedel. 2017. A proposed climate-based seed transfer system for British Columbia. Prov. BC, Victoria. BC Tech. Rep. 099. www. for. gov. bc. ca/hfd/pubs/Docs/Tr/Tr099. htm.

Osterkamp, T. E. 2007. Characteristics of the recent warming of permafrost in Alaska. Journal of Geophysical Research-Earth Surface **112**.

Pan, D.-M., and D. D. A. Randall. 1998. A cumulus parameterization with a prognostic closure. Quarterly Journal of the Royal Meteorological Society **124**:949-981.

Parmesan, C., and G. Yohe. 2003. A globally coherent fingerprint of climate change impacts across natural systems. Nature **421**:37-42.

Pedlar, J., D. McKenney, J. Beaulieu, S. Colombo, J. McLachlan, and G. O'Neill. 2011. The implementation of assisted migration in Canadian forests. The Forestry Chronicle **87**:766-777.

Pedlar, J. H., D. W. McKenney, I. Aubin, T. Beardmore, J. Beaulieu, L. Iverson, G. A. O'Neill, R. S. Winder, and C. Ste-Marie. 2012. Placing forestry in the assisted migration debate. BioScience **62**:835-842.

Penuelas, J., R. Ogaya, M. Boada, and A. S. Jump. 2007. Migration, invasion and decline: changes in recruitment and forest structure in a warming-linked shift of European beech forest in Catalonia (NE Spain). Ecography **30**:829-837.

Peterson, T. C., and R. S. Vose. 1997. An Overview of the Global Historical Climatology Network Temperature Database. Bulletin of the American Meteorological Society **78**:2837-2849.

Pravalie, R. 2018. Major perturbations in the Earth's forest ecosystems. Possible implications for global warming. Earth-Science Reviews **185**:544-571.

Randall, D., M. Khairoutdinov, A. Arakawa, and W. Grabowski. 2003. Breaking the cloud parameterization deadlock. Bulletin of the American Meteorological Society **84**:1547-1564.

Randall, D. A. 2010. The evolution of complexity in general circulation models.*in* L. Donner, W. Schubert, and R. C. J. Somerville, editors. The development of atmospheric general circulations models: complexity, synthesis, and computation. Cambridge University Press, Cambridge UK.

Rosenzweig, C., D. Karoly, M. Vicarelli, P. Neofotis, Q. G. Wu, G. Casassa, A. Menzel, T. L. Root, N. Estrella, B. Seguin, P. Tryjanowski, C. Z. Liu, S. Rawlins, and A. Imeson. 2008. Attributing physical and biological impacts to anthropogenic climate change. Nature **453**:353-357.

Sharma, S., J. J. Magnuson, R. D. Batt, L. A. Winslow, J. Korhonen, and Y. Aono. 2016. Direct observations of ice seasonality reveal changes in climate over the past 320-570 years. Scientific Reports **6**:Artn 25061. DOI: 25010.21038/Srep25061

Stott, P. A., S. F. B. Tett, G. S. Jones, M. R. Allen, W. J. Ingram, and J. F. B. Mitchell. 2001. Attribution of twentieth century temperature change to natural and anthropogenic causes. Climate Dynamics **17**:1-21.

Suarez, M. L., L. Ghermandi, and T. Kitzberger. 2004. Factors predisposing episodic drought-induced tree mortality in Nothofagus - site, climatic sensitivity and growth trends. Journal of Ecology **92**:954-966.

Thornton, P. E., S. W. Running, and M. A. White. 1997. Generating surfaces of daily meteorological variables over large regions of complex terrain. Journal of Hydrology **190**:214-251.

Visser, M. E., and C. Both. 2005. Shifts in phenology due to global climate change: the need for a yardstick. Proceedings of the Royal Society Biological Sciences **272**:2561-2569.

Wang, T., A. Hamann, D. Spittlehouse, and C. Carroll. 2016. Locally downscaled and spatially customizable climate data for historical and future periods for North America. PLOS ONE **11**:e0156720. DOI: 0156710.0151371/journal.pone.0156720.

Wang, T., A. Hamann, D. L. Spittlehouse, and T. Q. Murdock. 2012. ClimateWNA—High-resolution spatial climate data for Western North America. Journal of Applied Meteorology and Climatology **51**:16-29.

Werner, R. A., E. H. Holsten, S. M. Matsuoka, and R. E. Burnside. 2006. Spruce beetles and forest ecosystems in south-central Alaska: A review of 30 years of research. Forest Ecology and Management **227**:195-206.

Westerling, A. L., H. G. Hidalgo, D. R. Cayan, and T. W. Swetnam. 2006. Warming and earlier spring increase western US forest wildfire activity. Science **313**:940-943.

Wiens, J. J. 2016. Climate-related local extinctions are already widespread among plant and animal species. Plos Biology **14**:ARTN e2001104. DOI:2001110.2001371/journal.pbio.2001104

Willmott, C. J., and K. Matsuura. 1995. Smart interpolation of annually averaged air temperature in the United States. Journal of Applied Meteorology **34**:2577-2586.

Ying, C. C., and A. D. Yanchuk. 2006. The development of British Columbia's tree seed transfer guidelines: Purpose, concept, methodology, and implementation. Forest Ecology and Management **227**:1-13.

Chapter 2. A cross-checked global monthly weather station database for precipitation covering the period 1901 to 2010.

2.1. Summary

Comprehensive monthly weather station databases are the foundation for many gridded climate data products that are widely used to characterize regional climate conditions, track climate change, and research the impact of climate on natural and managed ecosystems. However, station database coverage is often regional, there can be extensive gaps in station coverage over time, as well as errors in climate records, station coordinates or elevation. In order to support researchers that rely on monthly weather station databases, we assemble a monthly weather station database for precipitation from multiple reputable data sources. We use digital elevation models and nearby stations to search for inconsistencies in reported station locations and recorded precipitation values. We also estimated missing values in weather station time series using a linear model approach based on interpolated anomaly surfaces. The resulting station records were ranked into ten classes, according to the completeness of records, the reliability of missing value estimations and other criteria. We corrected incomplete or erroneous location and elevation information for 12% of all available station records. A total of 23% of monthly records that had missing values could be estimated with high or moderate confidence. We sub-sampled our global database of more than 80,000 stations with various spatial filters, so that only the highest quality station for a given area was retained. Our contribution significantly enhances global data coverage compared to other databases currently available. Even when accepting only the stations within the top two quality ranks in our combined database, and applying the coarsest spatial filter of one station per approximately 1,600 km², the remaining station count of more than 20,000 stations exceeds the largest alternative database (without a spatial filter applied) by approximately 50%.

2.2. Introduction

Comprehensive monthly weather station databases are the foundation for characterizing regional climate conditions, and for tracking climate change over time. For the purpose of climatic characterizations, monthly summaries represent a good compromise between capturing seasonal climate variation without having to manage large amounts of daily weather data. Once these monthly weather summaries have been recorded for 30 years, also referred to as a climate normal period, calculating an average allows to infer a long-term expectation of climate conditions that is not usually biased by cyclical or random anomalies (Guttman 1989, Arguez and Vose 2011). With a sufficient density of weather station data for a region, interpolation methods can be used to derive grids of baseline climate data for complex landscapes, modeling various climate phenomena, such as changes in temperature along elevation gradients, orographic precipitation and rain shadows (Hutchinson 1995, Daly et al. 2002). Once the baseline climatology of a region has been established, additional questions can be addressed with monthly time series records, such as how the climate has changed in the past, or how the climatology of a region may change in the future (Sáenz-Romero et al. 2010, Ramirez-Villegas et al. 2013).

Many gridded climate data products that are widely used to research the impact of climate variability and climate change on natural and managed ecosystems rely on monthly weather station databases. For the United States, PRISM is a well-regarded database of gridded climate that benefits from the extensive network of weather stations available for this region. Gridded climate products with global coverage also include the CRU database from the University of East Anglia (Harris et al. 2014), a gridded database from the University of Delaware (Willmott and Matsuura 1995), the Global Precipitation Climatology Centre (GPCC) product (Becker et al. 2013), or the Precipitation REConstruction Land (PRECL) database from NOAA (Chen et al. 2002). These databases with monthly historical resolution are limited to low spatial resolutions (0.5° or coarser). Alternative products, with high spatial resolutions (30 arc-seconds or

approximately 1km) are usually restricted to 30-year normal summaries and provide no inter-annual historical data, e.g. WorldClim (Hijmans et al. 2005).

For researchers that develop climate grids, there are a number of important challenges in assembling the required regional or global weather station databases. First, the placement of the weather stations is usually biased towards population centers or agricultural lands, whereas climate conditions of mountainous or desert areas are usually not well documented (New et al. 1999, Menne et al. 2012). Another important limitation of weather station data is temporal coverage. Before the 1950s the density of weather stations tends to be low, reaching its highest global density around the 1970s before declining again (Menne et al. 2012). Additionally, many of these stations were operational only for a few years, containing extensive gaps in the records or operating only seasonally, especially in mountainous regions. Finally, it is not uncommon to encounter errors in recorded climate values, such as errors of unit conversions in countries using the Imperial system, or mistakes associated with the location of the station, such as inaccuracies in the reported coordinates or elevation. Before the widespread use of global positioning systems, coordinates were typically recorded to the nearest minute, implying a location error of hundreds of meters, which can be problematic on mountainous terrain where the elevation and topographic gradients are an important determinant of the weather patterns.

In order to support researchers that rely on monthly weather station databases to develop interpolated grids or other climate data products, we assemble and cross-check a monthly weather station database for precipitation that combines several regional and global databases that are publicly available, including the GHCN v2 database (Lawrimore et al. 2011, Menne et al. 2012), the station database corresponding to the CRU v3.21 interpolated dataset (Harris et al. 2014), the WMO-CLINO database (WMO. 1996), the FAOCLIM 2 database (Bogaert et al. 1995), the R-Hydronet database (Vorosmarty et al. 1998), the ECA&D database (Tank et al. 2002, Van Den Besselaar et al. 2015) and the USFS database (Rehfeldt 2006). We use duplicate entries, digital elevation models and nearby stations to search for inconsistencies in recorded

climate values in weather station records that may be due to unit conversion errors, location and elevation inaccuracies.

This study provides a consolidated database of more than 80,000 observations ranked into ten quality classes, according to the completeness of records, the reliability of missing value estimates and other criteria. Specifically, we contribute the following corrections and enhancements for users of monthly precipitation databases: (1) When errors could be corrected without ambiguity, corrections were made and indicated by flags in the database. Alternatively, the records were flagged with the lowest quality score for removal; (2) We estimate missing values in monthly station time series records with a linear model approach based on interpolated anomaly surfaces. The reliability of estimated values was documented with model fit statistics and quality scores. Missing value estimates are primarily provided to estimate adjusted long term averages (e.g. 30-year climate normals); (3) Lastly, we provide subsamples of this database that select the best station records for pre-determined three dimensional filters (with different intervals for latitude, longitude, and elevation). The sub-sampled datasets retain only the most reliable and complete station records for a given area, with global coverage and with as little spatial sample bias as possible.

2.3. Methods

2.3.1. Databases used

The public weather station databases that we use in this study (Table 2.1) have already been subjected to rigorous quality control methodology. The CRU and GHCN database have been screened for duplicate records, outliers, tests for violation of logical or physical relations between variables (Tmax<Tmin), unrealistic peaks or dips in time series, spatial consistency tests by comparing with surrounding stations, etc. (New et al. 1999, Durre et al. 2010). The FAOCLIM 2 database from FAO was established in the 1980s to evaluate the global agricultural

production potential in developing countries, and provides additional regional coverage in Central America, agricultural areas of South America, the Sahel zone of Africa. The ECA&D monthly database provides good additional coverage for mountainous regions in Europe, such as the Alps, the Carpathians, the Balkans, the Caucasus, and the Scandinavian mountains. The R-HydroNET database for South America provides useful additions for Amazonian precipitation data, and the USGS database has excellent additional coverage for mountainous regions in North America, including the United States, Canada and Mexico.

Table 2.1. Databases included in this study with statistics describing their spatial and temporal coverage. The databases are ordered by preference, based on documented quality control efforts, accuracy of location information, temporal coverage, and overlap with other databases. The latest data used was 2010 as most databases were incomplete beyond this date (Fig 2.1).

Database*	Spatial Extent	Temporal extent	Temporal resolution	Number of stations
1. Climate Research Unit Time-series v3.21 observations (CRU)	Global	1901-2010	Monthly time-series	11,702
2. Global Historic Climate Network Dataset v2 (GHCN)	Global	1850-2010	Monthly time-series	20,541
3. FAOCLIM 2.0 global climate database (FAO)	Global	1901-1999	Monthly time-series	13,529
4. World Meteorological Organization normals (WMO)	Global	1961-1990	1961-1990 Normals	4,259
5. European Climate Assessment Dataset (ECA)	Europe, Russia, North Africa	1901-2010	Monthly time-series	10,085
6. R-HydroNET (R-HN)	South America	1920-1990	Monthly or 1961-1990 Normal	3,256
7. Daily Global Historical Climatology Network (dGHCN)	Global	1901-2010	Daily data	45,603
8. United States Forest Service (USFS)	North America	1961-1990	1961-1990 Normals	14,635

*) References: 1. Harris et al. (2014), 2. Lawrimore et al. (2011), 3. Bogaert et al. (1995), 4. WMO. (1996), 5. Tank et al. (2002), Van Den Besselaar et al. (2015), 6. Vorosmarty et al. (1998), 7. Menne et al. (2012), 8. Rehfeldt (2006)

After removal of duplicates from the combined weather station database, temporal coverage used in this study extends from the beginning of the last century to 2010, reaching their highest spatial density from the 1960s to the 1990s for most regions of the world (Fig. 2.1). The drop of station coverage in recent years is partially due to several databases not including recent records (Fig. 2.1). Excellent temporal and spatial coverage for the 1961 to 1990 period is one reason why baseline grids are often developed for this 1961-1990 normal period (New et al. 1999, Menne et al. 2012). Another reason why 1961-1990 normal period is a useful reference period is that it largely precedes anthropogenic climate change (Tett et al. 1999, Lawrimore et al. 2011), and can therefore be used as a reference period when future climate projections are expressed as an anomaly (e.g. +2°C warming relative to a reference period). In the database that we develop in this study we therefore also rank weather stations highly that have complete records for this 1961-1990 normal period.
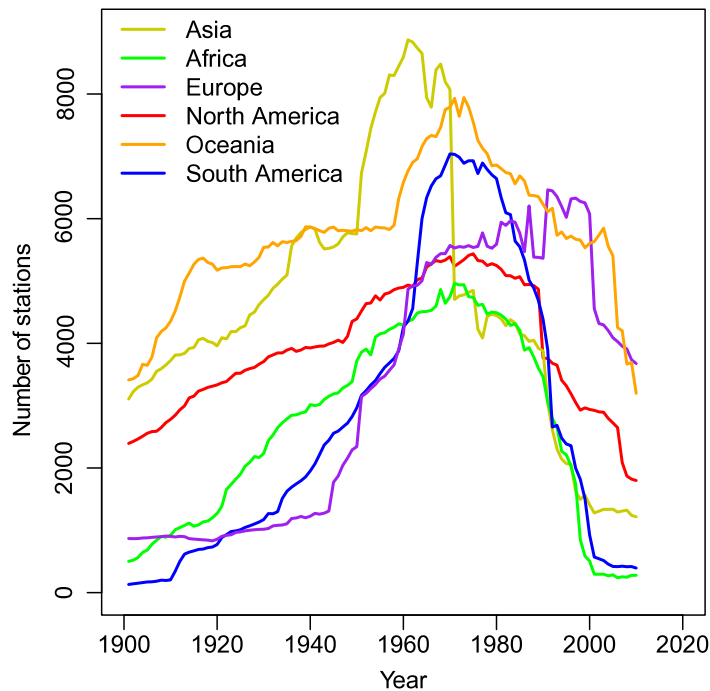
Fig. 2.1. Temporal coverage of weather station records from all databases listed in Table 2.1. combined, after removal of duplicate station records.

2.3.2. Elevation match with DEM

As a first check of station records, we compared the reported elevation for each weather station against a digital elevation model (DEM) of 1km resolution (Gesch et al. 1999). Missing elevation values in weather station records, usually indicated by flags in the elevation field, such as -9999, -999, -99, or 9999 were replaced with the DEM value. Elevation records of exactly zero were also replaced with the DEM value. The rationale for this replacement was that many databases had at least some records, where an elevation value of zero actually indicated a missing value as well. Recorded elevation values of zero that represented a correct measurement were usually located near the coast, where the DEM replacement resulted in a very similar elevation estimate. Further, we recorded the difference between the reported elevation value and the DEM, and performed a more detailed inspection of any station that had a difference exceeding ±250m. We checked those stations for potential errors of unit conversions, potential errors of location that may have led to an elevation discrepancy, or implausible elevation values given the topography in the vicinity of the recorded station. Determining the correct value for weather stations is important, because the elevation value is normally used as a covariate in any climate modeling or interpolation effort.

2.3.3. Outlier detection and missing value estimation

A second useful check of weather station records is to determine consistency of records with other nearby stations to detect recording errors or unit conversion issues. However, in this study we use a different approach, relying on the well regarded CRU TS database of monthly grids of climate anomalies from 1901 to 2010 (Mitchell and Jones 2005, Harris et al. 2014). Our criterion for potentially problematic station records were low correlations of station data with the CRU TS monthly anomalies for the location of the weather station. For this purpose, we calculated correlation coefficients for each month of the year between weather station records and the

corresponding CRU grid cell. Stations with low correlation coefficients were flagged as potentially problematic.

If the correlation between CRU TS data and weather station records were high, we used a simple linear model with a fixed intercept at zero to predict missing values in the temporal record of station data. The weather station record needed to have at least 20 years for the 1961–1990 period and the linear model an $R^2 > 0.7$ to be considered for estimating missing values. A less reliable missing value estimation, resulting in a lower quality rank was based on linear models with R^2 values between 0.5 and 0.7 and at least 27 years of data for the 1901–2010 period. A special case for missing value estimation were stations located in desert areas, where a linear model could not be established due to the majority of monthly precipitation values being zero. For stations with at least 10 years of monthly data for the 1901–2010 period, but located in desert areas, we filled any missing values in the observed weather station data with the corresponding CRU TS values directly (i.e. not using a linear model). These estimates were flagged as filled and assigned a lower quality score (see next section), allowing users of our database to select various quality criteria to filter the database according to their needs.

2.3.4. Quality criteria

For each station, we assigned a quality score based on the completeness of the station record, the quality of the linear model to estimate missing values, and a number of other criteria (Table 2.2). The best station quality score (1) was assigned to stations that had at least 90% complete data for the 1961-1990 period, either as monthly time series, or reported as average for the 1961-1990 normal period (i.e. from WMO or R-HydroNET databases). The next best score (2) was assigned to the stations that had at least 66% of the data for the 1961-1990 period complete, and where missing values could be estimated with a linear model that had an R^2 of at least 0.7. The following score (3) was assigned to stations with a similar criteria, but between 33% and 66% of the data of the 1961-1990 was complete (i.e. 10 years), plus a total of 25% of the data complete

30

for the 1901-2010 period (i.e. 27 years of data in total), and an R^2 of at least 0.7 for estimation of missing values. The fourth score (4) was given to records that did not report monthly time series, but only 1961-1990 normal period averages (i.e., from WMO and R-HydroNET) with completeness of annual records between 66% and 90%. The next lower score (5) was given to station records that did not cover the 1961-1990 period well, but that still contained a substantial time series with at least 25% of the data complete for 1901-2010 time series (i.e. 27 years), and with a total of 90% of data either observed or estimated for 61-90 time series with $R^2>0.7$. Score (6) was assigned to stations with at least 25% of the data complete for 1901-2010 time series (i.e. 27 years and missing values estimable with $R^2>0.5$. Score (7) includes all seasonal stations that covered three to ten months of the season, and that otherwise covered at least quality score 6. The score of (8) was given to stations that, independently of its other statistics, had a difference between the reported elevation and the DEM larger than 250m that could not be corrected. The score of (9) was applied to entries that did not have monthly time series but only a 1961-1990 normal period average with between 33% and 66% completeness of the data (i.e. applicable to some entries of the WMO database) or data completeness was not reported (applicable to the USGS database). Finally, the score of (10) was given to all remaining stations that did not fulfill any of the above stated requirements.

The monthly consolidated database contains all entries from our source databases (Table 2.1), without duplicates removed at this stage. In addition to the original entries, we report the DEM value for the station location, a linear model estimate for any missing value for the 1901-2010 period, the R^2 value for the linear model estimate, and a flag that indicates whether the precipitation value was recorded, estimated, filled with CRU estimates for desert stations, or not estimable. Additional columns specify percent of complete records for the 1901-2010 period, the percent of complete records for the 1961-1990 period, a database quality score according to Table 2.1, a station quality score according to Table 2.2, and a combined quality score that ranks database scores within station quality scores (e.g. 23 would indicate a station quality score of 2 for an FAO database entry). Smaller numbers indicate overall higher quality records.

31

Table 2.2. Data quality scores based on the completeness of the station record for the 1961-1990 period, the completeness of station records for the 1901-2010 period, the quality of the linear model to estimate missing values, and a number of other criteria.

Score	Data requirements for station quality score
1	At least 90% complete for 61-90 time series or normal averages (i.e., 3 missing values allowed)
2	At least 66% complete for 61-90 time series & missing values estimated with $R^2>0.7$
3	At least 33% complete for 61-90 time series (i.e. 10 years), 25% complete for 1901-2010 time series (i.e. 27 years), and missing values estimated with $R^2>0.7$
4	At least 66% complete values for reported 61-90 normal average (i.e., uncorrected)
5	At least 25% complete for 1901-2010 time series (i.e. 27 years), and 90% observed or estimated for 61-90 time series with $R^2>0.7$
6	At least 25% complete for 1901-2010 time series (i.e. 27 years), and missing values estimable with $R^2>0.5$
7	Seasonal stations (three to ten months) that otherwise ranked at least quality score 6
8	Stations with elevation versus DEM differences >250m that could not be corrected, but that otherwise ranked at least quality score 6
9	At least 33% complete values for reported 61-90 normal average (i.e., uncorrected), or completeness of record unreported.
10	All remaining stations that did not meet any of the above quality criteria

2.3.5. Duplicate removal and database subsets

Duplicate stations among the databases were common and were removed based on reported weather station IDs and location information. Most databases used station IDs derived from those of the World Meteorological Organization. Where possible, we parsed the ID field to generate station IDs that conformed to the WMO format. This occasionally resulted in duplicate station IDs among different databases that were located in different states, countries, or continents that used similar but independent ID schemes. To avoid these false positive duplicate detections, we assigned to each station a global code related to the country, state or province where they were located. The final ID-based duplicate removal retained the station with the highest overall quality score for a given station ID in the same jurisdiction. This step did not

remove all duplicates, as some databases did not use the WMO station IDs for some or all of their records.

The second duplicate removal step was location-based. We generated grids of 2.5 arcminutes (~5km), 5 arcminutes (~10km), 10 arcminutes (~20km), and 20 arcminutes (~40km). In addition, we want to retain stations in the same general area that are located at different elevations. For this purpose we created elevation intervals of 100m for each of the above grids. To sub-sample the original database at different spatial densities and to remove any additional duplicates that were missed in the previous step, we retained a single station with the highest overall quality score in each of the three dimensional grid cells.

2.4. Results and Discussion

2.4.1. Recorded station elevation vs. DEM

From the total consolidated record of 123,000 stations (no duplicates removed), 9% had missing values for elevation indicated by a flag of -9999 or similar. In addition several databases contained a sizable number of records that had zero recorded for elevation. (0.11% of CRU, 3.5% of GHCN, 0.4% of FAO, 0.05% of ECA, and 1.5 of dGHCN). Not all of these zero values were plausible measurements, e.g. indicated in blue in Fig. 2.2, typically located across India, Australia and Brazil. Here, zero values were presumably used when the record should indicate missing values. For simplicity, we replaced all zero values with records from the digital elevation model, even when zero values were plausible measurements, i.e. for the Netherlands and other coastal locations.
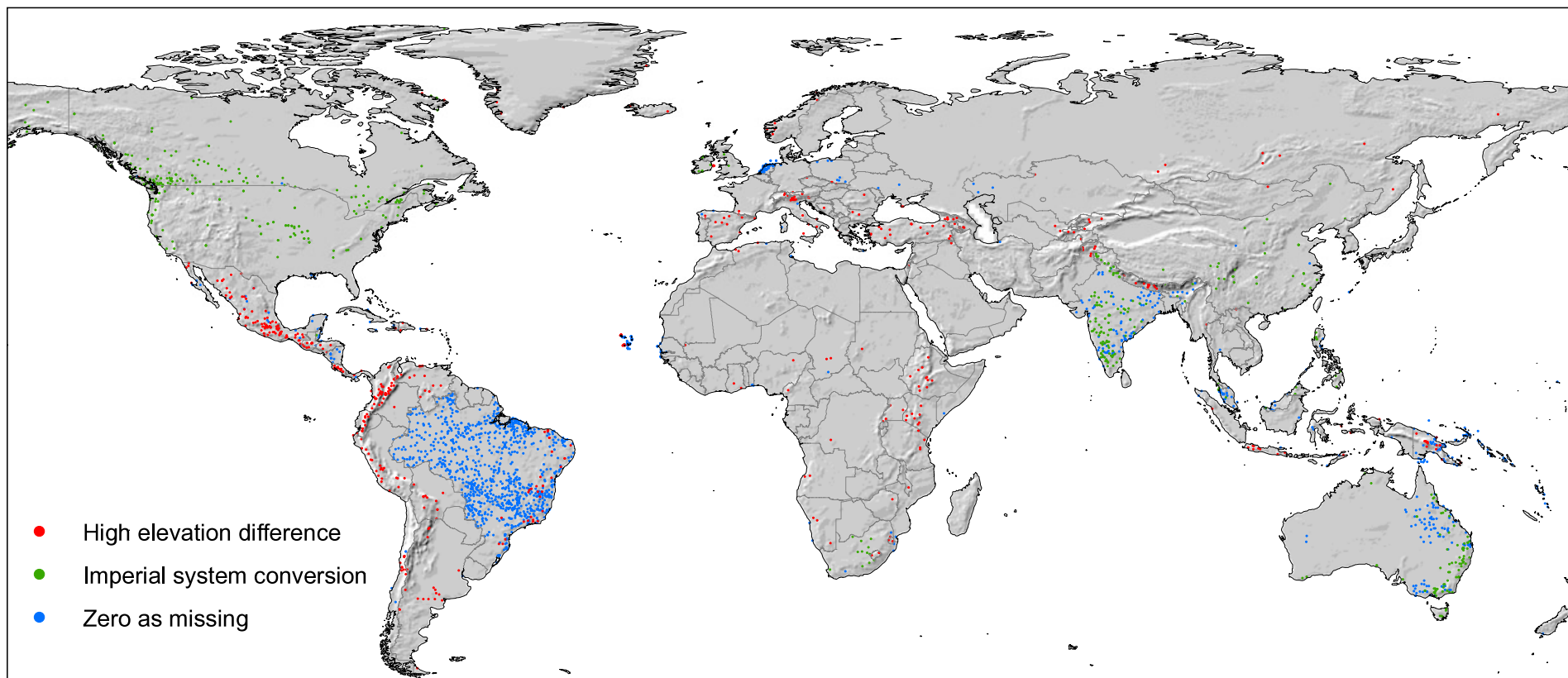
Fig. 2.2. Stations with recorded elevations of zero (blue), with double-conversions or omission of conversions from feet to meters (green), and other station with elevation differences >250m (red) between a digital elevation model and the value recorded for the station location.

For all other records we screened for substantial discrepancies between the digital elevation model and the recorded station elevation. This yielded a number of stations where conversions from the imperial system to the metric system was either omitted, or applied twice (Fig. 2.3. rows of green points). We found that most databases were affected by this type of error, but to varying degrees (0.7% of CRU, 4.4% of GHCN, 0.6% in FAO, 0.1% of ECA, 0.4% of dGHCN, and 0.3% of USFS). Even within local regions only a subset of stations had these conversion errors. The errors were corrected by either multiplying by 3.281 or dividing by 0.305. We only carried out the corrections for countries that in some point in their history used the Imperial system, and where these errors were almost exclusively located (Fig. 2.2). For stations with elevation conversion issues, we also checked if precipitation conversions may have been incorrect, but this was generally not the case.

Lastly, other stations with large elevation discrepancies were flagged, but retained unchanged. These stations are usually located in mountainous regions (Fig. 2.2. red circles), and the recorded elevation is likely a more reliable indicator of the true elevation of the weather station than the DEM value for these locations.
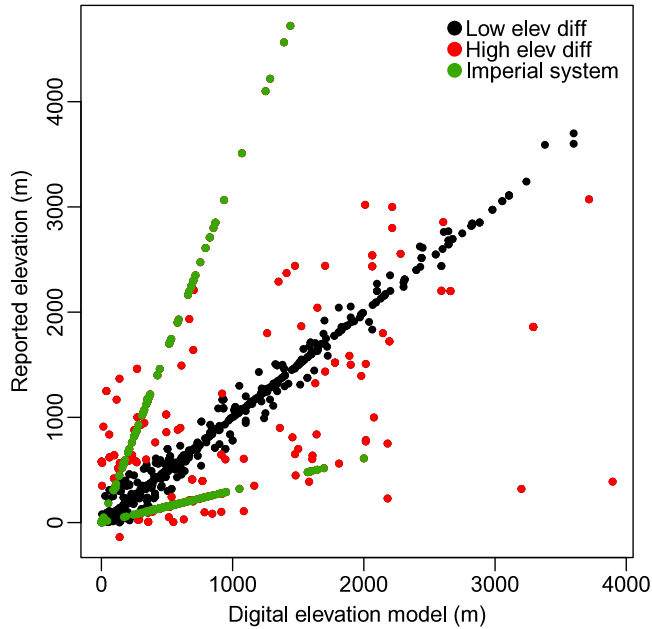
Fig. 2.3. Scatter plot of recorded station elevation over the elevation value from a digital elevation model for the station. Double conversions or omission of conversions from feet to meters are visible as off-diagonal rows of green dots, other stations with an elevation difference >250m are indicated in red. The location of these stations is mapped with the same colors in Fig. 2.2.

2.4.2. Missing value estimation

For the purpose of calculating long-term climate averages, we provide missing value estimations that may be used in lieu of accepting a certain number of missing values in estimation of climate normals. The missing value estimation relies on a linear model with interpolated CRU-TS anomaly grids that have a coarse resolution (30 arcminutes), but nevertheless often yield strong correlations with recorded weather station data. The interpolated grids allow missing value estimation because of spatial interpolation from nearby stations that have records for the missing target value. While the correlations of station values with the monthly interpolated grids is often quite high and suitable for prediction (Fig. 2.4a), the relationship is also often biased with a slope considerably deviating from the diagonal (e.g. Fig. 2.4c). A moderate proportion of missing

values could be estimated based on a linear model with R^2 values between 0.5 and 0.7 (Fig. 2.4b, and Table 2.3)
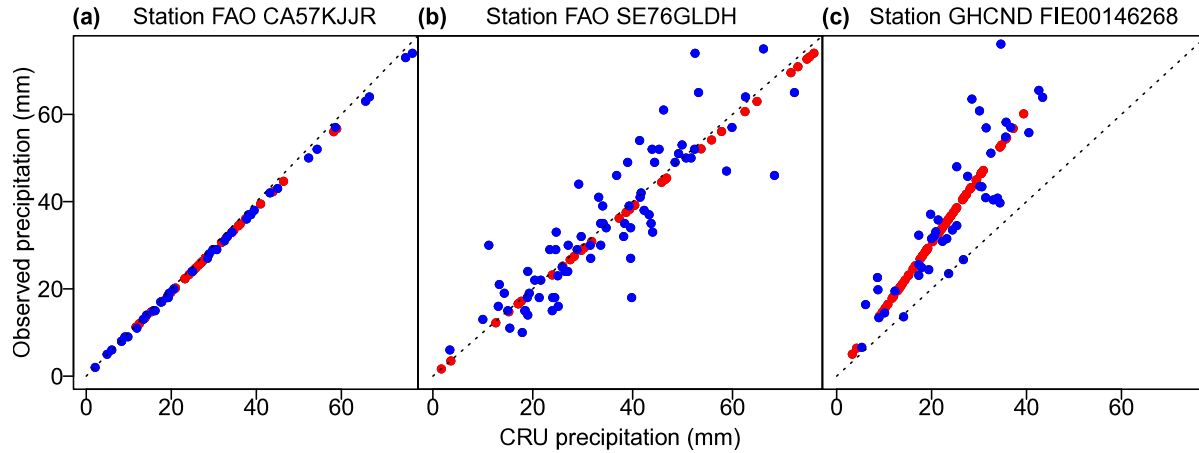
Fig. 2.4. Examples for estimation of missing values in January precipitation (red circles) using a linear model with high confidence indicated by an $R^2 > 0.7$ (a), moderate confidence with an R^2 between 0.5 and 0.7 (b), and moderate confidence as well as a biased relationship (c), leading to different quality scores as outlined in Table 2.2.

Table 2.3. Percentage of observed records and estimable missing values by station database.

Database	Observed records	Predicted ($R^2 > 0.7$)	Predicted (R^2 0.5-0.7)	Zero & filled	Not estimated
CRU	60.3	28.9	3.5	4.1	1.5
GHCN	44.6	29.7	9.7	3.7	6.7
FAO	43.6	28.8	6.2	5.5	12.1
ECA	36.2	46.4	3.0	0.0	13.6
R-HN	14.4	29.2	10.0	1.1	38.9
dGHCN	29.2	33.5	7.9	1.0	25.1

2.4.3. Final spatially sub-sampled databases

Spatial and elevational sub-sampling by elevation intervals and various grid sizes (2.5, 5, 10, and 20 arcminutes) is meant to provide users with databases where local duplications (nearby

37

stations) are removed, retaining only a single station with the highest overall quality for a given

grid cell. As the grid size for subsamples increases, we therefore retain slightly higher

proportions of high quality stations while the overall database size decreases (Table 2.4). The

WMO and CRU databases have the highest proportion of high quality station records, but the

database size is relatively small compared to our combined and sub-sampled databases. Even

when sampling one station at the coarsest 20 arcminute grid resolution, we retain more than

20,000 stations with a quality score of 1 or 2 (Table 2.4). The spatial distribution of stations

using the coarsest subsample at 20 arcminute resolution is shown in Fig. 2.4, where the quality is

indicated by a color legend. Low quality stations are typically restricted to mountainous areas

and specific countries. For example, most of India's weather station coverage has gaps after 1970

in all databases (Fig. 2.3).

Table 2.4. Size and the proportion of records with different quality scores for the individual
databases used in this study, for all databases combined prior to the removal of duplicates, and
for subsets that select the highest quality station for various grid sizes.

Database	Number of stations	Station quality (see Table 2)									
		1	2	3	4	5	6	7	8	9	10
CRU	11,702	71	19	<1	0	0	5	0	4	0	<1
GHCN	20,541	35	13	3	0	4	32	1	5	0	7
FAO	13,493	44	12	5	0	1	22	<1	4	0	11
WMO	4,149	92	0	0	5	0	0	0	1	0	1
ECA	9998	46	11	4	0	<1	20	3	2	0	14
R-Hydronet	3,256	52	9	0	4	0	8	0	8	0	20
dGHCN	44,763	18	11	6	0	5	31	2	1	0	25
USFS	14,629	0	0	0	0	0	0	0	0	100	0
Combined	122,531	32	10	4	<1	3	21	1	3	12	13
No Dupl.	98,631	31	9	4	<1	3	22	1	3	13	14
2.5' Grid	78,409	30	9	4	<1	3	23	2	3	13	13
5' Grid	71,136	31	9	4	<1	3	22	1	3	14	13
10' Grid	60,143	32	9	3	<1	3	22	1	3	15	11
20' Grid	45,888	36	8	3	<1	2	20	1	4	16	10
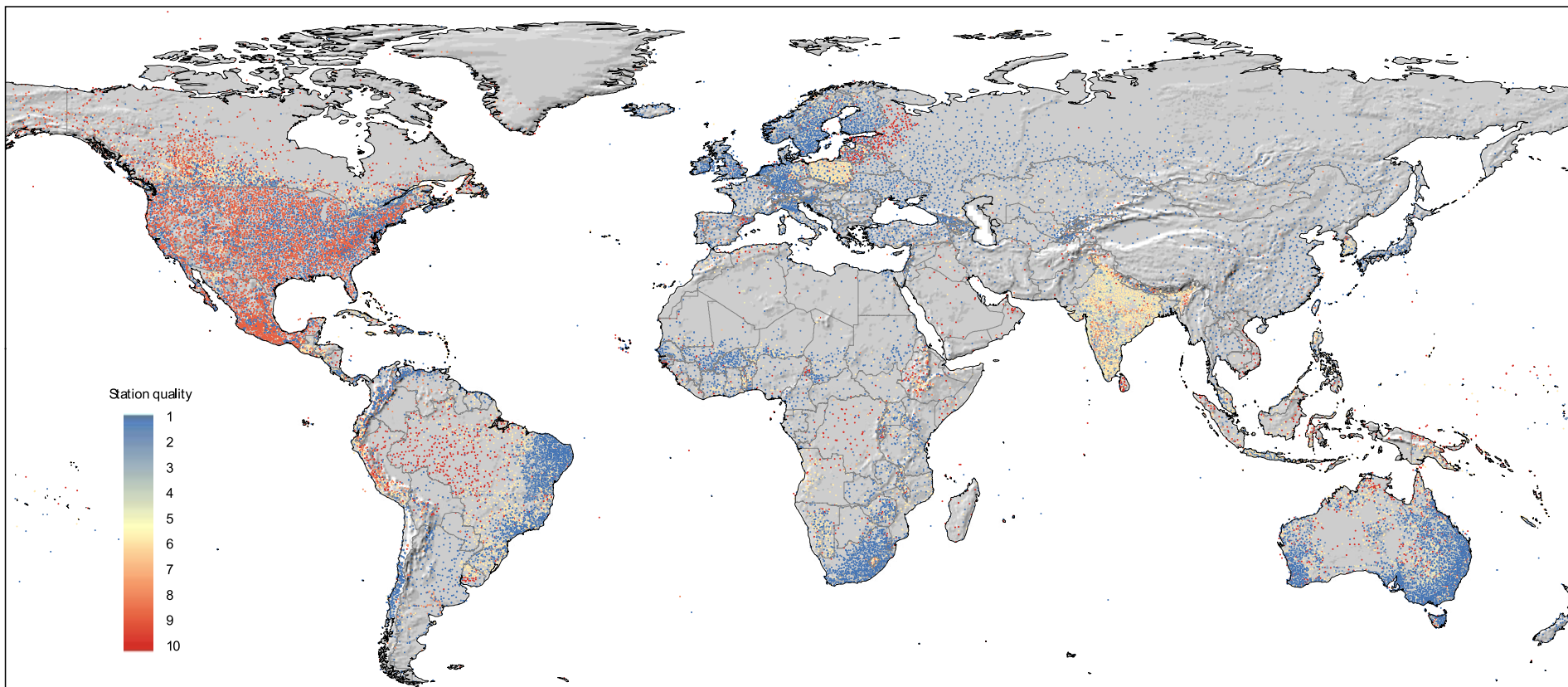
Fig 2.5. Map of stations colored by quality score (blue = high quality, red = poor records, see Table 2.2), for the subsample where one station is selected for each 20 arcminute grid cell (approximately 1600km²) and 100m elevation interval.

2.4.4. Applications and limitations

In this data management and data cleaning effort, we made a number of subjective choices that are guided by particular applications that this database may be useful for, namely for the development of long-term climate normal surfaces that can serve as reference periods for ecological research on adaptation of organisms with climate, biological response of organisms to interannual climate variability, and response of organisms to historical and future climate trends. As a useful normal reference period, we advocate the use of the 1961-1990 climate normal, which strikes a good balance between excellent global weather station coverage, and largely preceding a strong anthropogenic warming signal (Tett et al. 1999, Lawrimore et al. 2011, Estrada et al. 2013). Therefore, our station quality ranks specifically take this period into account. Nevertheless, users that are interested in other periods can easily modify the ranking system. All records of the combined database were retained, and all decision criteria for quality ranks for each station are included to specify other preferences.

For generating interpolated surfaces of climate normal periods other than the 1961-1990 period, or for generating surfaces with a monthly resolution, for example to study response of organisms to climate variability or climate trends at a monthly time step, we recommend using an anomaly or delta approach, described for example by Mitchell and Jones (2005) and Wang et al. (2006). Relying on our missing value estimation for stations up to a quality score of 8, an adjusted 1961-1990 normal average can be obtained for a large majority of the stations contained in this database (75% of stations). Deviations from this 1961-1990 normal estimate can then be calculated for all observed values in station time series. Interpolated monthly anomalies, or interpolated normal anomalies can then provide robust climate estimates for years outside the 1961-1990 period, even if weather station coverage is not as dense.

Our general recommendations for developing global climate products with this database would be to use our 20 arcminute sub-sample and station records with a quality score of at least 8. For the 1961-1990 period, this subset would include stations with the following summary statistics: 69% of records complete, 17% of monthly records being estimated with high confidence (linear model estimates with an $R^2 > 0.7$), 6% of monthly records being estimated with moderate confidence (linear model estimates with an R^2 between 0.5 and 0.7), and 2% of records being filled with CRU estimates for desert stations. For the development of local climatology products, a higher density station coverage may be used (i.e., one station per 2.5, 5, or 10 arcminute grid cell), especially if local station coverage is generally poor. If the study area is not mountainous, stations with quality scores 7 and 8 may be dropped, removing seasonal stations and stations with uncorrected elevation discrepancies.

2.5. Conclusion

The databases that we generated in this study should be of value to a variety of users who create gridded precipitation data or other climate data products derived from weather station data. We corrected a sizable number of errors in reported station elevations due to unit conversions, or due to missing values being reported as zero. Elevation errors can be detrimental for the quality of interpolated surfaces, as elevation is almost always used as a predictor variable or covariate in interpolation techniques for climate data. In addition, the estimation of missing values with linear models should render some stations useful that did not have appropriate coverage to calculate a specific 30-year climate normal due to missing values, but that had enough records from other years available to infer long-term climate conditions. Finally, the sub-sampling procedure guarantees that poorer records from various source databases are replaced by other, better quality records for nearby locations within the same elevation band. Our contribution significantly

enhances the global data coverage compared to databases currently available. Even when accepting only the stations within the top two quality ranks in our combined database, and applying the coarsest spatial filter of one station per approximately 1,600 km², the resulting station count of more than 20,000 stations exceeds the largest alternative database (without a spatial filter applied) by 50%.

2.6. References

Arguez, A., and R. S. Vose. 2011. The definition of the standard WMO climate normal: the key to deriving alternative climate normals. Bulletin of the American Meteorological Society **92**:699-U345.

Becker, A., P. Finger, A. Meyer-Christoffer, B. Rudolf, K. Schamm, U. Schneider, and M. Ziese. 2013. A description of the global land-surface precipitation data products of the Global Precipitation Climatology Centre with sample applications including centennial (trend) analysis from 1901–present. Earth System Science Data **5**:71-99.

Bogaert, P., P. Mahau, and F. Beckers. 1995. The Spatial Interpolation of Agro-Climatic Data. Cokriging software and source data. User's Manual v1.0b. Agrometeorology Series Working Paper 12. Environmental Information Management Service. Sustainable Development Department. Agrometeorology Group. FAO. Rome, Italy.

Chen, M., P. Xie, J. E. Janowiak, and P. A. Arkin. 2002. Global land precipitation: a 50-yr monthly analysis based on gauge observations. Journal of Hydrometeorology 3:249-266.

Daly, C., W. P. Gibson, G. H. Taylor, G. L. Johnson, and P. Pasteris. 2002. A knowledge-based approach to the statistical mapping of climate. Climate Research **22**:99-113.

Durre, I., M. J. Menne, B. E. Gleason, T. G. Houston, and R. S. Vose. 2010. Comprehensive automated quality assurance of daily surface observations. Journal of Applied Meteorology and Climatology **49**:1615-1633.

Estrada, F., P. Perron, and B. Martinez-Lopez. 2013. Statistically derived contributions of diverse human influences to twentieth-century temperature changes. Nature Geoscience **6**:1050-1055.

Gesch, D. B., K. L. Verdin, and S. K. Greenlee. 1999. New land surface digital elevation model covers the Earth. Eos, Transactions: American Geophysical Union **80**:69-70.

Guttman, N. B. 1989. Statistical descriptors of climate. Bulletin of the American Meteorological Society **70**:602-607.

Harris, I., P. D. Jones, T. J. Osborn, and D. H. Lister. 2014. Updated high-resolution grids of monthly climatic observations – the CRU TS3.10 Dataset. International Journal of Climatology **34**:623-642.

Hijmans, R. J., S. E. Cameron, J. L. Parra, P. G. Jones, and A. Jarvis. 2005. Very high resolution interpolated climate surfaces for global land areas. International Journal of Climatology 25:1965-1978.

Hutchinson, M. F. 1995. Interpolating mean rainfall using thin-plate smoothing splines. International Journal of Geographical Information Systems **9**:385-403.

Lawrimore, J. H., M. J. Menne, B. E. Gleason, C. N. Williams, D. B. Wuertz, R. S. Vose, and J. Rennie. 2011. An overview of the Global Historical Climatology Network monthly mean temperature data set, version 3. Journal of Geophysical Research: Atmospheres **116**:D19121. doi:19110.11029/12011JD016187.

Menne, M. J., I. Durre, R. S. Vose, B. E. Gleason, and T. G. Houston. 2012. An overview of the Global Historical Climatology Network-Daily database. Journal of Atmospheric and Oceanic Technology **29**:897-910.

Mitchell, T. D., and P. D. Jones. 2005. An improved method of constructing a database of monthly climate observations and associated high-resolution grids. International Journal of Climatology **25**:693-712.

New, M., M. Hulme, and P. Jones. 1999. Representing twentieth-century space-time climate variability. Part I: Development of a 1961-90 mean monthly terrestrial climatology. Journal of Climate **12**:829-856.

Ramirez-Villegas, J., A. J. Challinor, P. K. Thornton, and A. Jarvis. 2013. Implications of regional improvement in global climate models for agricultural impact research. Environmental Research Letters **8**:Artn 024018. DOI: 024010.021088/021748-029326/024018/024012/024018

Rehfeldt, G. E. 2006. A spline model of climate for the Western United States. General Technical Report RMRS-GTR-165. Department of Agriculture, Forest Service, Rocky Mountain Research Station, Fort Collins, Colorado, U.S.

Sáenz-Romero, C., G. E. Rehfeldt, N. L. Crookston, P. Duval, R. St-Amant, J. Beaulieu, and B. A. Richardson. 2010. Spline models of contemporary, 2030, 2060 and 2090 climates for Mexico and their use in understanding climate-change impacts on the vegetation. Climatic Change **102**:595-623.

Tank, A. M. G. K., J. B. Wijngaard, G. P. Konnen, R. Bohm, G. Demaree, A. Gocheva, M. Mileta, S. Pashiardis, L. Hejkrlik, C. Kern-Hansen, R. Heino, P. Bessemoulin, G. Muller-Westermeier, M. Tzanakou, S. Szalai, T. Palsdottir, D. Fitzgerald, S. Rubin, M. Capaldo, M. Maugeri, A. Leitass, A. Bukantis, R. Aberfeld, A. F. V. Van Engelen, E. Forland, M. Mietus, F. Coelho, C. Mares, V. Razuvaev, E. Nieplova, T. Cegnar, J. A. Lopez, B. Dahlstrom, A. Moberg, W. Kirchhofer, A. Ceylan, O. Pachaliuk, L. V. Alexander, and P. Petrovic. 2002. Daily dataset of 20th-century surface air temperature and precipitation series for the European Climate Assessment. International Journal of Climatology **22**:1441-1453.

Tett, S. F. B., P. A. Stott, M. R. Allen, W. J. Ingram, and J. F. B. Mitchell. 1999. Causes of twentieth-century temperature change near the Earth's surface. Nature **399**:569-572.

Van Den Besselaar, E. J. M., A. M. G. K. Tank, G. Van Der Schrier, M. S. Abass, O. Baddour, A. F. V. Van Engelen, A. Freire, P. Hechler, B. I. Laksono, Iqbal, R. Jilderda, A. K. Foamouhoue, A. Kattenberg, R. Leander, R. M. Guingla, A. S. Mhanda, J. J. Nieto, Sunaryo, A. Suwondo, Y. S. Swarinoto, and G. Verver. 2015. International climate assessment & dataset: climate services across borders. Bulletin of the American Meteorological Society **96**:16-21.

Vorosmarty, C. J., C.F-Jauregui, and M. C. Donoso. 1998. A Regional, Electronic Hydrometeorological Data Network for South America, Central America, and the Caribbean. University of New Hampshire, Durham, New Hampshire, U.S.

Wang, T., A. Hamann, D. L. Spittlehouse, and S. N. Aitken. 2006. Development of scale-free climate data for Western Canada for use in resource management. International Journal of Climatology **26**:383-397.

Willmott, C. J., and K. Matsuura. 1995. Smart interpolation of annually averaged air temperature in the United States. Journal of Applied Meteorology 34:2577-2586.

WMO. 1996. Climatological Normals (CLINO) for the period 1961-1990. World Meteorological Organization. Geneva, Switzerland.

Chapter 3. Global, high-resolution precipitation grids for the 1961-1990 climate normal period.

3.1. Summary

Interpolated grids of historical climate normal data serve as an important reference point for any research that investigates observed or projected climate change. While temperature variables are relatively easy to model, as they vary with elevation due to adiabatic lapse rates, interpolating precipitation from weather station data is more difficult. Most widely used interpolation methods have severe shortcomings in predicting rain shadows and precipitation due to orographic lift. Some expert systems have these capabilities, but they are not easily replicable by other researchers and lack global coverage. Here, we contribute a modeling approach that uses wind speed, wind direction, slope, and aspect to arrive at an exposure metric that is suitable to predict orographic lift on the windward side, and rainshadows on the leeward side of mountain ranges. This exposure metric is used in addition to elevation as covariates to predict precipitation with a universal kriging method. Statistics for independent validation with a withheld set of weather stations match or exceed other currently available climate normal products for precipitation. Our weather station data collection and the climate normal surfaces from this study are publicly available.

3.2. Introduction

When describing the climatic condition for a location or region, climatologists rely on a long time series of weather station observations to reliably calculate an average that is not affected by inter-annual climate variability, or short to medium term cyclical climate events, such as El-Nino climate anomalies. By convention, a 30-year time series of weather station observations are

averaged, which is also referred to as a climate normal (Guttman 1989, Arguez and Vose 2011). Climate normals represent the basis for climate-dependent management decisions, such as crop selection and timing of agricultural activities for food production (Alcamo et al. 2007, Campbell et al. 2016), for estimating water supply (Vanham et al. 2009), infrastructure planning (Koetse and Rietveld 2009, Schweikert et al. 2014), etc. Climate normals are also required as reference to study past climate trends and make predictions for future climate (i.e. projections for the 2050s refer to the average of 2041-2070). For these purposes, the 1961-1990 normal period is often used because it is preceding a strong anthropogenic warming signal, and by the 1960s a fairly comprehensive global weather station network had been established.

In order to estimate the climate conditions for any location on the earth's surface, interpolation methods are used to derive grids of climate variables from weather station records. Accuracy of these interpolation estimates vary with weather station density, topographic complexity, proximity to water bodies, and the type of climate variable. Since temperature has a strong relationship with elevation due to adiabatic lapse rates, it is relatively straight forward to accurately interpolate temperature by using just elevation as a covariate (Daly 2006). On the contrary, precipitation has a more complex relationships with topography that is driven by wind direction and terrain barriers resulting in high precipitation due to orographic lift and sharp rain shadows behind mountain ridges (Daly 2006). Also the proximity to large water bodies influences precipitation values (Daly 2006).

Traditional interpolation methods that use just elevation as a co-variate, such as interpolation by kriging, and tri-variate splines, have difficulty in accurately modeling topographically-driven precipitation patterns. Nevertheless, such interpolated products are widely used for research and management, and include the NOAA's Merged Analysis of Precipitation product (Xie and Arkin 1997) and Unified Gauge Based Analysis of Global Precipitation product (Chen et al. 2008),

46

WMO's Global Precipitation Analysis products (Schneider et al. 2014), as well as the WorldClim database (Hijmans et al. 2005, Fick and Hijmans 2017).

An alternative method to estimate precipitation for any location on earth are satellite-derived products such as PERSIANN-CDR (Ashouri et al. 2015a) and CHOMPS (Joseph et al. 2009), as well as NASA's TRMM product (Huffman et al. 2007). However, these products do not tend to perform well when validated against weather station data, partially because of their tendency to underestimate topography-driven precipitation (Hughes 2006, Mendelsohn et al. 2007, Derin and Yilmaz 2014, Bartsotas et al. 2018). Another limitation is that visible or infrared satellite sensors measure the brightness or temperature of clouds, but this does not always correlate well with precipitation. Passive microwave satellite sensors are able to directly measure precipitation droplets, but they are limited by their low earth orbits resulting in low spatiotemporal coverage (Sun et al. 2018, Varma 2018). Additionally, both types of sensors are influenced by water vapor concentrations, surface temperatures, and other emissions or reflections from the earth's surface (Varma 2018).

Lastly, expert systems have been developed to estimate precipitation, such as Parameter Regression of Independent Slope Model (PRISM) from Oregon State University (Daly et al. 2008). This method primarily relies on the interpolation of weather station data, but also allows for the input of expert knowledge in the form of additional variables, such as elevation, topographic facets, terrain barriers, to weigh the importance of weather stations in determining the value for a target location. However, PRISM-derived precipitation grids have only been developed for North America and the methodology and software is not publicly available for applications elsewhere.

Here, we contribute an interpolation approach that is similar to PRISM methodology by incorporating terrain complexity measures into universal kriging. However, we use a more generic and easily repeatable approach, relying on publicly available data for covariates such as topographic aspect and slope, wind speed and direction, as well as local interpolations to model terrain-driven precipitation patterns such as orographic lift on windward facing slopes and rain shadows on leeward facing slopes. Our databases are publicly available for use in regional studies with locally available weather station networks.

3.3. Methods

3.3.1. Weather station data

The methodology used to assemble the weather station database to generate interpolated climate normal surfaces is described in detail in Chapter 2 of this thesis. Briefly, we gathered monthly weather station data for the 1901- 2010 period from multiple sources, including GHCN v2 (Lawrimore et al. 2011, Menne et al. 2012), CRU v3. (Harris et al. 2014), WMO-CLINO (WMO. 1996), FAOCLIM 2 (Bogaert et al. 1995), R-Hydronet (Vorosmarty et al. 1998), ECA&D (Tank et al. 2002, Van Den Besselaar et al. 2015), and the USFS database (Rehfeldt 2006). We checked for inconsistencies in location, elevation, and precipitation values by using duplicate entries, digital elevation models, and comparing to nearby stations. Missing monthly precipitation values in the time series of each station were predicted by regressing CRU TS v3.23 anomaly grids with weather station records that were available between 1901-2010. Depending on the percentage of observed and predicted data for the 1961-1990 period and other quality criteria, all station records for the 1961-1990 normal period were assigned a quality score from 1-10. The total size of the combined database was 122,531 stations, and 98,631 stations after removal of duplicates that arose from combining multiple databases.

We then spatially subsampled this database by selecting the weather station with the highest quality score for a global grid of 20 arcminutes (approximately 40 x 40 km) as well as one station per 100m elevation band in each cell in the grid. The final database used for interpolation in this study contained 45,888 stations. For those stations, 69% of all monthly records used to calculate the 1961-1990 normal were direct station observations, 17% and 6% were estimated with high ($R^2 > 0.7$) and moderate ($R^2 > 0.5$) confidence respectively, and 2% of the records were filled with zero or near zero values from the CRU TS for stations in desert regions, which could not be predicted with a linear model but that could nevertheless be estimated reliably as a simple average of available station records (of mostly zero values). Stations where missing values for the 1961-1990 period could not be estimated with moderate reliability were excluded (6%).

3.3.2. Additional covariates and target resolution

The global 30 Arc-Second GTOPO30 Digital Elevation Model (DEM) (Gesch et al. 1999), was used to generate a lower-resolution DEM of 2.5 arcminutes. This resolution is sufficient to model the interaction between topography and general global prevailing wind patterns at a monthly temporal resolution that drive precipitation (Daly 2006). We then created slope layers in both West to East (270º azimuth) and South to North (180º azimuth) directions with the hillshade tool of ArcGIS (ESRI 2008). The slope layers were scaled from -1, indicating maximum west or south exposure, zero indicating no slope, and +1 indicating maximum east or north exposure (Figs. 3.1 a and d).

Wind data for each month of the year was obtained from the MERRA2 monthly meteorological fields v5.1 at intervals of 500m of elevation in the atmosphere (Gelaro et al. 2017). The data was resampled from the original of 0.625°x0.5° to the 2.5 arcmin resolution of our target DEM, and

then the corresponding level for each elevation was selected to form a stacked layer of wind speed in West to East and South to North directions (Figs. 3.1 b and e). We subsequently calculated leeward and windward exposure for each month of the year, by multiplying the 270º azimuth exposure layers with West to East wind data (Figs. 3.1 c) and the 180º azimuth exposure layers with South to North wind data (Figs. 3.1 f).

The final exposure layer to be used in the interpolation was calculated for each month as the average of the South to North and West to East exposure layers (Fig 3.1 h). The resulting wind exposure surfaces for each month of the year had a value of zero for flat terrain or zero wind speed, positive values for West to East facing mountain sides, and negative values for East to West facing mountain sides. The intent of these exposure layers was to simulate the way in which the prevailing winds interact with the mountainous terrain causing effects such as rain shadows (putatively driven by negative exposure values) and orographic lift (putatively driven by positive exposure values). To give an example of how slope and wind layers interact to create these exposure layers, note for example the strong westward slope of the California Sierra rising from the Central Valley (Fig 3.1a) that ultimately does not result in westward exposure (Fig 3.1 c) due to easterly winds (Fig 3.1 b, red shades).
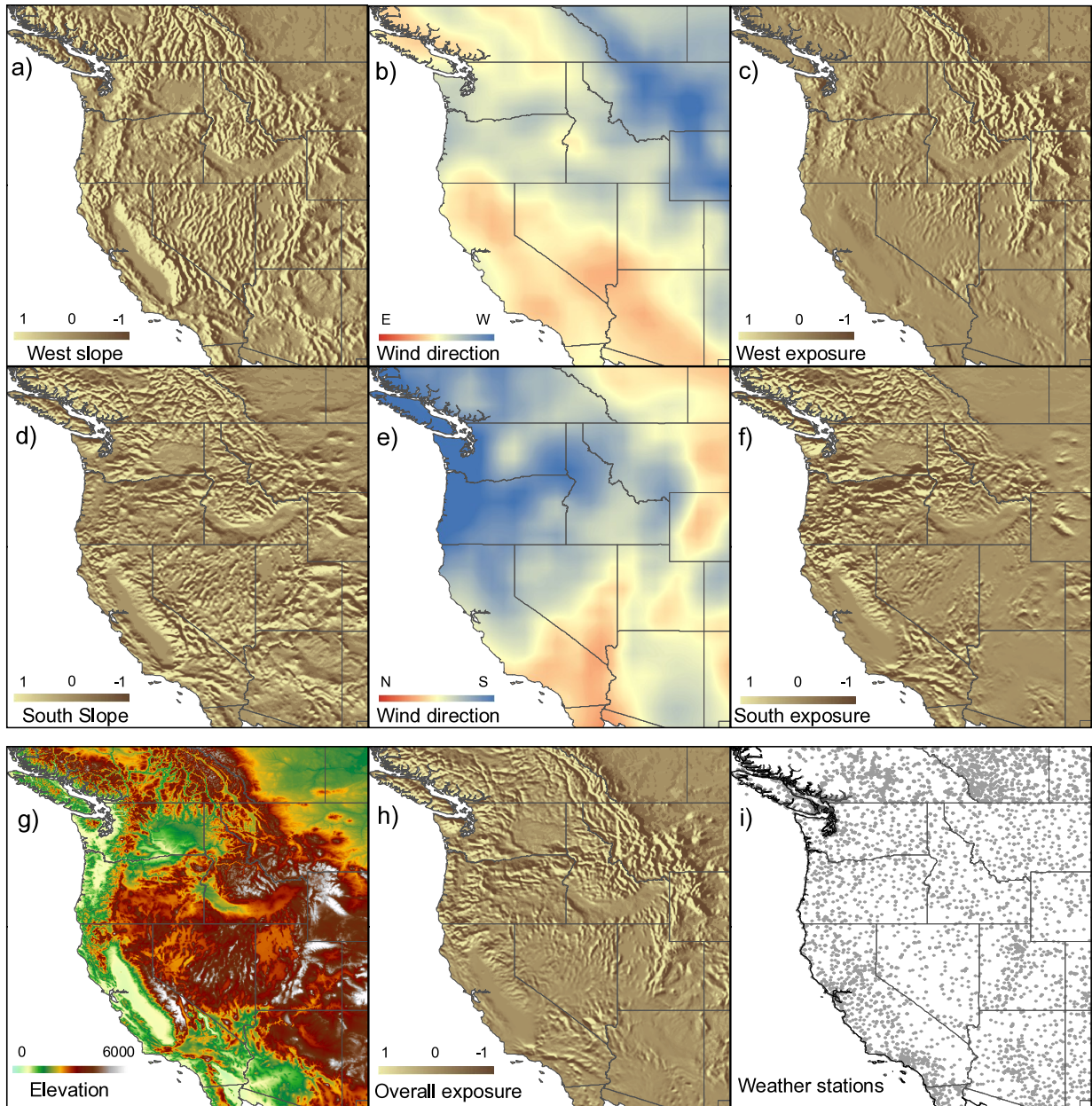
Fig. 3.1. Creating an exposure layer from topography and wind speed and direction by multiplying a west slope layer (a), scaled from -1 (maximum east slope) to +1 (maximum west slope) with a layer of wind speed in east-west wind direction (b) to result in a west exposure layer (c). The same procedure is repeated for north-south exposure (d-f). A digital elevation model (g) and an average of west and south exposure (h) are used as covariates for the interpolation of weather station data (i). Separate exposure layers are generated for each month, with January wind speed, wind direction, and exposure layers shown in this example.

3.3.3. Interpolation and validation

We selected a universal kriging interpolation method from the *gstat* package (Pebesma 2004, Graler et al. 2016) of the R statistical programming environment for interpolation (R Core Team 2016). We use elevation and overall exposure as co-variates to predict precipitation grids from weather station data. For computational reasons and also due to the high regionalization of the precipitation patterns, the task was subdivided into 4° tiles. If the tile did not contain at least 20 weather stations, the training data for predictions was extended by 2° in all directions repeatedly, until the 20 station criteria was met. We empirically determined that this was the minimum number of stations required to build robust local models with covariates that consistently predict rainshadows and orographic lift and that resulted in good validation statistics. To avoid artifacts between the resulting tiles of the regional interpolations, overlapping 4° tiles were generated in 2° intervals, and then a weighted average was calculated where a 100% weight was assigned to the center of each tile, and a 0% weight to its edge.

To test the quality of the surfaces generated, we performed both independent and a non-independent evaluations. The non-independent evaluations allow us to compare our results to other studies that report non-independent statistics where training and validation data are identical. For the independent evaluation, we used 66% of the weather stations sampled randomly for training and used the remaining 33% of stations to calculate validation statistics for each month, each season, and annualy. Because of our spatial sub-sampling of weather stations, any validation station was at least 40km distant from a training data station, reducing spatial autocorrelations. We report variance explained (R^2) by the interpolation estimate in validation station observations, as well as the mean absolute error (MAE) among interpolation estimates and station data. The MAE was obtained by averaging the difference, independent of sign, between observed and predicted for each validation station, and we choose this measure over the

root mean square error (RMSE) because it is less sensitive to extreme values and easy to interpret as an average deviation from the true measurement (Willmott 1982). For concise summaries, we report R² and MAE by continent but we also provide maps of deviations to describe smaller scale patterns in the quality of interpolation estimates.

3.4. Results & Discussion

3.4.1. Precipitation layers

As pointed out by Appelhands et al (2015), different methods of interpolation can have very similar validation statistics, but nevertheless diverge visually in areas of low weather station coverage or where topography influences the climate estimates. A good example to illustrate this divergence is western Canada, where weather station coverage is fairly dense in the southern British Columbia, but becomes increasingly sparse toward the Northwest Territories. We can see that the interpolations significantly diverge in the northern areas, with our interpolation approach (Fig 3.2a) resembling Daly et al's (2008) PRISM interpolation (b) more than Hijmans et al's (2005) Anuspline interpolation (c). This is expected, as our methodology was designed in principle to emulate PRISM methodology that takes account of precipitation patterns induced by topography, such as orographic lift and rain shadows. Another example can be seen in Mexico's mountain ranges of the eastern Gulf coast (Fig 3.3). From June to October, the moisture-laden trade winds coming from the east are intercepted by either the Sierra Madre Oriental or the Sierra of Oaxaca, causing intense precipitation on the east facing slopes, and rain shadows on the west facing slopes (Fig 3.3 inset and arrow).
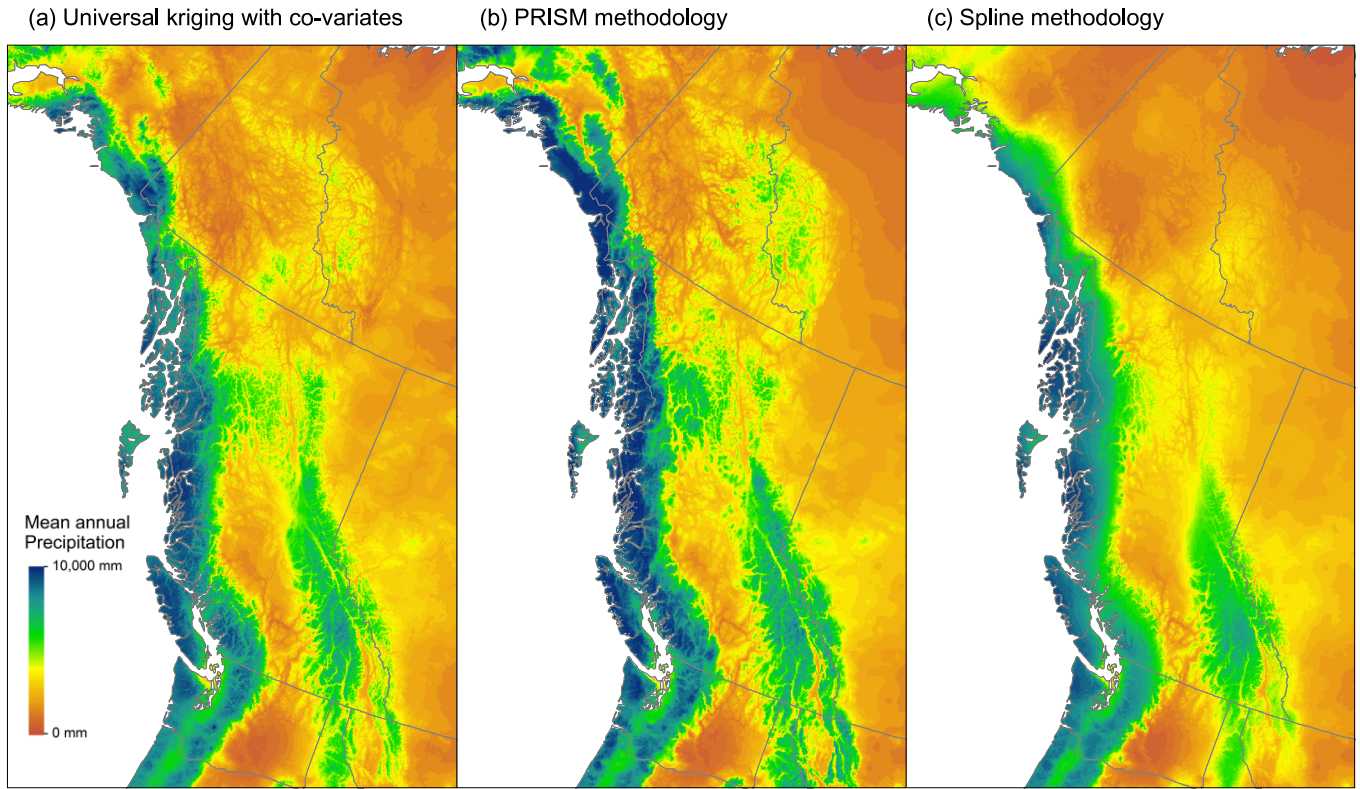
Fig. 3.2. Mean annual precipitation grids from three different interpolation methods for a region with sparse weather station coverage, including (a) universal kriging from this study, (b) PRISM interpolation by Daly et al (2008), and (c) spline interpolation by Hijmans et al (2005).
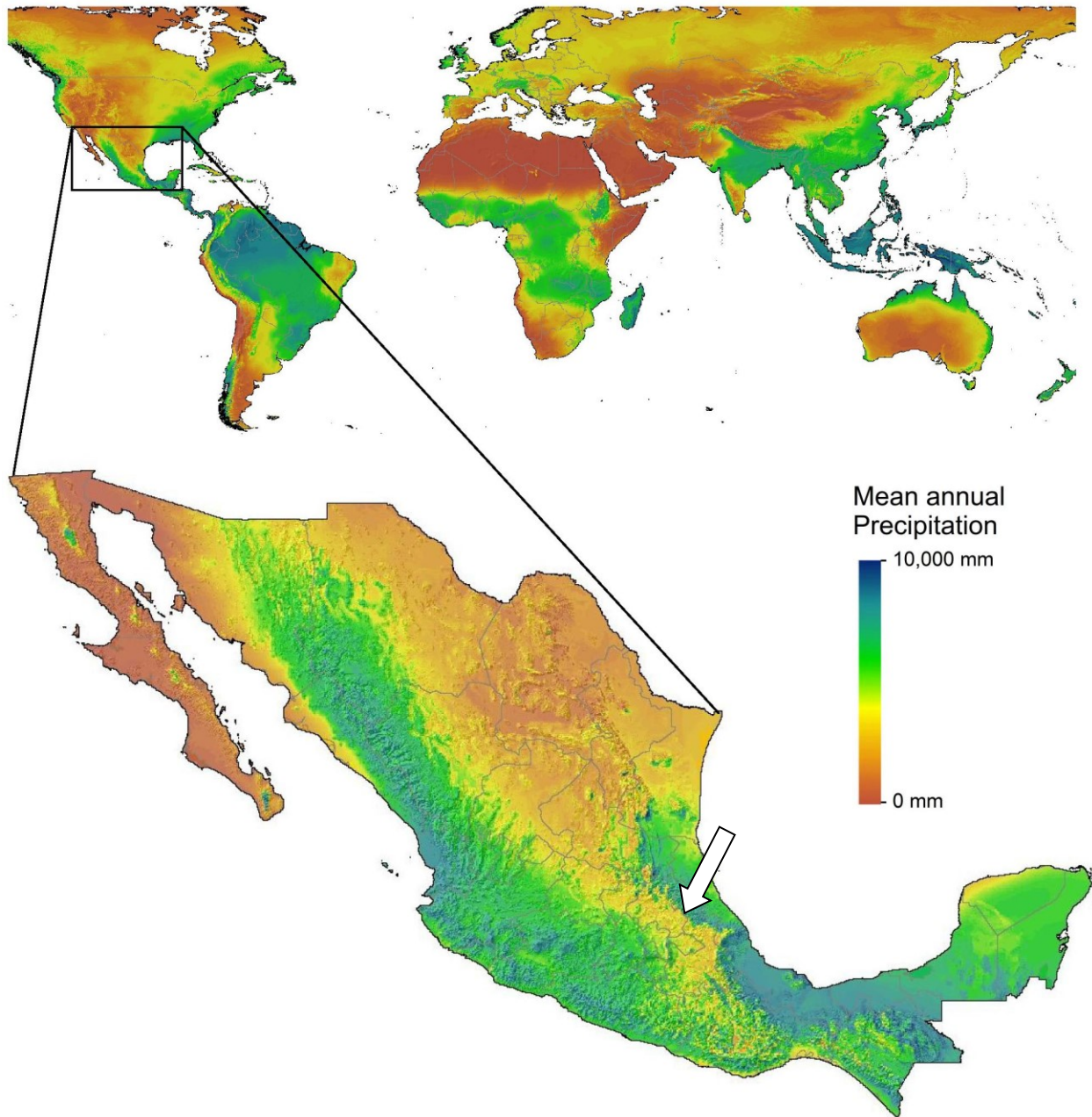
Fig. 3.3. Mean annual precipitation from universal kriging methodology, including a detailed map for Mexico. Abrupt rain shadows west of the cordillera mountain ranges that are driven by easterly winds from the Gulf of Mexico during the hurricane season are well defined (arrow).

3.4.2. Statistical evaluation

For the independent statistical evaluation, where we withheld 33% of stations at least 40km distant from the nearest weather station in the training dataset, we report mean absolute error (MAE) values in mm, as well as the absolute error expressed as a percentage of total precipitation. Our interpretation focuses on the relative percentage value because the MAE varies with the length of time the variable represents (i.e. the MAE for mean annual precipitation is expected to be twelve times larger than MAE for January precipitation). Similarly, geographic regions with high precipitation (e.g. tropical rain forests) are expected to have much larger MAEs than those with low precipitation (e.g. deserts).

In a broad continental comparison, the lowest error percentages were obtained for North America, Europe, and Oceania with a 6-12% relative error. Africa, South America and Asia typically had relative errors of 15-20% (Table 3.1). The good validation statistics for Europe and North America are likely due to dense, high quality weather station networks, while Oceania, including Australia, lacks major mountain ranges that are more difficult to model. The paucity of weather station coverage for mountain ranges such as the Andes in South America, or the Himalaya in Asia, makes modeling the precipitation patterns in these regions more difficult.

Table 3.1. Mean absolute error (MAE) of interpolated surfaces in mm and also expressed as median percentage of observed precipitation values in parentheses. Values are reported for a non-independent validation, including all stations as training data, and for a cross-validation that excludes 33% of stations for validation.

Continent	33% for validation			All stations		
	Monthly	Seasonal	Annual	Monthly	Seasonal	Annual
Asia	24 (20%)	64 (16%)	215 (12%)	14 (13%)	37 (10%)	128 (8%)
Africa	12 (20%)	30 (15%)	100 (8%)	5 (10%)	13 (8%)	44 (4%)
Europe	10 (9%)	28 (8%)	104 (7%)	4 (5%)	12 (4%)	44 (4%)
North America	10 (10%)	27 (8%)	92 (6%)	5 (6%)	14 (5%)	46 (4%)
Oceania	13 (12%)	34 (10%)	120 (7%)	5 (6%)	12 (5%)	42 (4%)
South America	25 (21%)	67 (17%)	236 (13%)	13 (12%)	35 (10%)	122 (7%)

When mapping the relative error values of predictions for individual weather stations (Fig. 3.4), high deviations are generally confined to mountainous regions and deserts. In the deserts, the high positive percentages are due to overestimations of precipitation, which can lead to very high percentage values if the observed record is near zero, as for example for the Sahara.

The summary statistics for relative deviations (Table 3.1) also suggests that climate estimates become more accurate for longer time periods. The values for mean annual precipitation tend to be twice as precise as the values for monthly precipitation, with seasonal precipitation estimates intermediate in precision. For North America and Europe, precision increases from around 10% for monthly precipitation to 8% for seasonal variables, to 6% for mean annual precipitation. The sequence for Asia, Africa and South America is from around 20% to 16% to 12%, respectively. This is not an unexpected result as summaries for longer time periods are always easier to estimate due to stochasticity being reduced. Such increases in precision would similarly apply to estimating 30-year climate normals, as in this study versus decadal or annual averages (Mbogga et al. 2009).
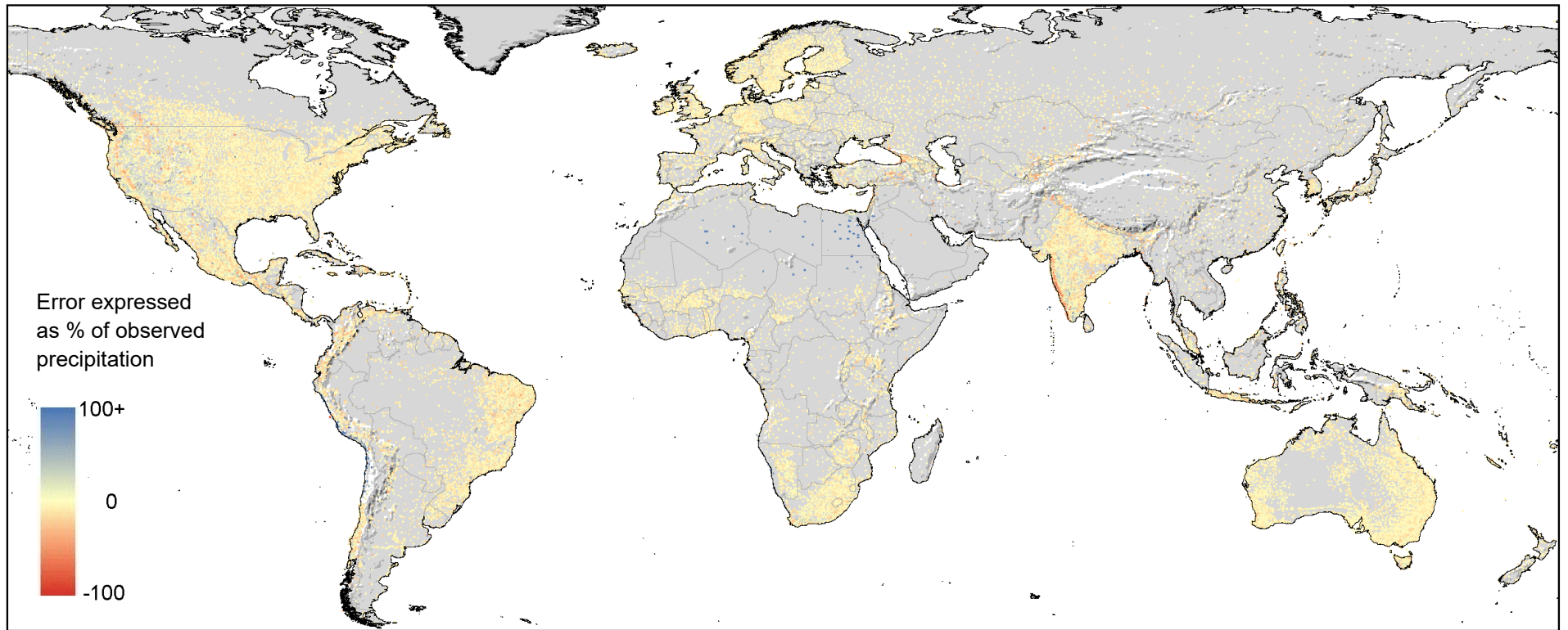
Fig. 3.4. Error estimated for mean annual precipitation for weather station locations. Because the errors are much larger for locations of high precipitation, such as tropical rainforest regions than for areas of low precipitation, such as desert regions, we express the errors as percentages of the observed mean annual precipitation.

In order to compare our validation statistics to other studies, we also report R^2 values, or variance explained by the interpolation estimates for the observed weather station data (Table 3.2). R^2 values are to some extent driven by the range of precipitation. Regions with a higher range of precipitation values tend to yield higher R^2 values than climatically more homogenous regions. Africa, with large areas of tropical rainforests and large deserts yields relatively high R^2 values, although the relative errors from Table 3.1 indicate that the precision is not very high.

Table 3.2. Variance explained (R^2) by interpolated surfaces for weather station data. Values are reported for a non-independent validation, including all stations as training data, and for a cross-validation that excludes 33% of stations for validation.

Continent	33% for validation			All stations		
	Monthly	Seasonal	Annual	Monthly	Seasonal	Annual
Asia	0.73	0.78	0.76	0.90	0.91	0.91
Africa	0.85	0.86	0.85	0.97	0.97	0.96
Europe	0.74	0.76	0.72	0.96	0.97	0.96
North America	0.82	0.84	0.83	0.95	0.96	0.96
Oceania	0.66	0.67	0.66	0.98	0.99	0.99
South America	0.76	0.78	0.70	0.94	0.95	0.93

That said, the R^2 values from Table 3.2 conform to r values reported for the WorldClim dataset, which yielded a variance explained of 0.86 for monthly precipitation variables for the entire world in an independent evaluation (Fick and Hijmans 2017). We should note that the independent evaluation by the authors of WorldClim is even more rigorous than ours in controlling for spatial autocorrelation. They divided the validation and training dataset with a systematic chessboard pattern with a grid size of 3°, building the model with the "white" cells and validating the interpolation estimates with the weather stations contained in the "black" grids, and then repeated the process in reverse. Our validation approach is more traditional with a 33% randomly withheld subset for validation and controlling less stringently for autocorrelation with the requirement that the nearest training data station must be at least 40km distant from a validation station.

Fick and Hijmans (2017) also report an MAE of 22mm for monthly precipitation variables for a worldwide evaluation of their WorldClim product, which appear comparable to our MAE values. Our values are somewhat smaller on average, but also less well controlled for inflation of precision estimates due to autocorrelations. For a global precipitation product for the 1961-1990 normal period, developed with a spline interpolation approach, New et al (1999) report cross-validation errors from 5mm to 120mm for different seasons and different regions of the world (New et al. 1999). For the PRISM database, Daly et al. (2008) report MAE values from a single deletion jackknife cross-validation. Their statistics vary regionally with MAE of 8 mm for the Western US, 5 mm for Central US, and 6 mm for Eastern US for monthly precipitation averaged across all months. Our corresponding MAE value for North America is larger with 10 mm, but in this case, our control for autocorrelations may be slightly more stringent with a minimum distance set. For a USDA interpolated precipitation product for the Western United States, Rehfeldt (2006) reports R^2 values of 0.92 for monthly precipitation variables, where they withheld 8% of the stations for validation.

Several other studies that evaluate interpolated precipitation surfaces carry out non-independent tests, where all weather stations were used for model building and evaluations. Mbogga et al. (2009) evaluated the PRISM surfaces for Western Canada for the 1961-1990 climate normal period. They reported comparable R^2 values of 0.97 and MAEs of 93mm for mean annual precipitation. For seasonal precipitation the MAE statistics were $R^2=0.97$ and MAE=27mm. Wang et al. (2012) report R^2 values of 0.96 for monthly precipitation in a non-independent evaluation, again similar to what we obtained in a comparable validation (Table 3.2). In summary, our independent and non-independent validation statistics appear similar to what has been obtained by other authors, and would not by themselves indicate that any one product is clearly more precise than another. This is partially due to the fact that any validation statistics vary regionally and due to different implementations. It appears that for

precipitation variables, the MAE statistic, expressed as percent of the observed precipitation at a location, provides the best guidance as to where precipitation estimates are most reliable.

3.4.3. Limitations and Applications

While a visual assessment of our precipitation layers suggest that topographically-driven precipitation patterns, such as orographic lift and rain shadows are well captured, we still encountered some issues when modeling regions of high topographic complexity that did not have a dense weather station network, such as the Andes and the Himalayas. In these regions we tend to see an underestimation on the windward slopes of a mountainous range where effects of orographic lift may not be reliably modeled (Fig. 3.4). Nevertheless, our global precipitation layer for the 1961-1990 normal period should match or exceed the quality of other products, not least because it is based on a significantly larger database of weather stations than other studies that we are aware of, even after spatially filtering and only retaining one station per 20 arcminutes. While we only provide the 1961-1990 normal as a reference period here, other normal periods, monthly historical data, or future projections can easily be developed using the delta method and available anomaly layers, such as CRU-TS (Harris et al. 2014).

We provide gridded surfaces at 30arcsecond and 2.5arcminute resolution that are publicly available for download at Zenodo.org (links will be activated when this manuscript has undergone peer-review). We should note that the higher resolution 30 arcsecond estimates were generated with an up-sampled 2.5 arcminute exposure covariate because the climatic features driven by this covariate (rain shadows or orographic lift are not driven by fine-scale topographic variation, but rather by larger topographic features such as mountain ranges. These 30 arcseconds estimates are provided to assure compatibility with other climate databases (Fick and Hijmans 2017). While our databases should not be able to provide useful information beyond a resolution of approximately 2.5 arcminutes, temperature variables in

complex terrain can certainly be estimated with enough precision to warrant 30 arcsecond resolution. Our 30 arcsecond precipitation surfaces are provided for convenience to be jointly used with temperature products from other authors.

The global interpolation grids generated in this study should be of interest to researchers who require baseline climatologies at high resolution in complex terrain. Applications may include species distribution modeling, where precipitation patterns have a direct impact on whether a vegetation community occurs at a particular sampling location. Estimating local runoff and erosion risk in complex mountainous terrain is also highly dependent on correctly modeling orographic lift and rainshadows (Guan et al. 2009, Scholl and Murphy 2014). Our data layers may also have use for infrastructure planning, hydrological power generation, or risk management against floods and mudslides by government and industry (Schär and Frei 2005). To make this dataset easily accessible to researchers and managers, we also provide a software package to query the 1961-1990 baseline data layer, and to overlay anomaly (delta) layers to arrive at different normal periods, monthly historical data, or future projections (e.g. Wang et al. 2016, and Chapter 4 of this thesis).

3.5. References

Alcamo, J., N. Dronin, M. Endejan, G. Golubev, and A. Kirilenkoc. 2007. A new assessment of climate change impacts on food production shortfalls and water availability in Russia. Global Environmental Change-Human and Policy Dimensions **17**:429-444.

Appelhans, T., E. Mwangomo, D. R. Hardy, A. Hemp, and T. Nauss. 2015. Evaluating machine learning approaches for the interpolation of monthly air temperature at Mt. Kilimanjaro, Tanzania. Spatial Statistics **14**:91-113.

Arguez, A., and R. S. Vose. 2011. The definition of the standard WMO climate normal: the key to deriving alternative climate normals. Bulletin of the American Meteorological Society **92**:699-U345.

Ashouri, H., K.-L. Hsu, S. Sorooshian, D. K. Braithwaite, K. R. Knapp, L. D. Cecil, B. R. Nelson, and O. P. Prat. 2015. PERSIANN-CDR: daily precipitation climate data record from multisatellite observations for hydrological and climate studies. Bulletin of the American Meteorological Society **96**:69-83.

Bartsotas, N. S., E. N. Anagnostou, E. I. Nikolopoulos, and G. Kallos. 2018. Investigating satellite precipitation: uncertainty over complex terrain. Journal of Geophysical Research-Atmospheres **123**:5346-5359.

Bogaert, P., P. Mahau, and F. Beckers. 1995. The Spatial Interpolation of Agro-Climatic Data. Cokriging software and source data. User's Manual v1.0b. Agrometeorology Series Working Paper 12. Environmental Information Management Service. Sustainable Development Department. Agrometeorology Group. FAO. Rome, Italy.

Campbell, B. M., S. J. Vermeulen, P. K. Aggarwal, C. Corner-Dolloff, E. Girvetz, A. M. Loboguerrero, J. Ramirez-Villegas, T. Rosenstock, L. Sebastian, P. K. Thornton, and E. Wollenberg. 2016. Reducing risks to food security from climate change. Global Food Security-Agriculture Policy Economics and Environment **11**:34-43.

Chen, M., W. Shi, P. Xie, V. B. S. Silva, V. E. Kousky, R. Wayne Higgins, and J. E. Janowiak. 2008. Assessing objective techniques for gauge-based analyses of global daily precipitation. Journal of Geophysical Research: Atmospheres **113**:D04110. doi: 04110.01029/02007JD009132.

Daly, C. 2006. Guidelines for assessing the suitability of spatial climate data sets. International Journal of Climatology **26**:707-721.

Daly, C., M. Halbleib, J. I. Smith, W. P. Gibson, M. K. Doggett, G. H. Taylor, J. Curtis, and P. P. Pasteris. 2008. Physiographically sensitive mapping of climatological temperature and precipitation across the conterminous United States. International Journal of Climatology **28**:2031-2064.

Derin, Y., and K. K. Yilmaz. 2014. Evaluation of multiple satellite-based precipitation products over complex topography. Journal of Hydrometeorology **15**:1498-1516.

Fick, S. E., and R. J. Hijmans. 2017. WorldClim 2: new 1-km spatial resolution climate surfaces for global land areas. International Journal of Climatology **37**:4302-4315.

Gelaro, R., W. McCarty, M. J. Suarez, R. Todling, A. Molod, L. Takacs, C. A. Randles, A. Darmenov, M. G. Bosilovich, R. Reichle, K. Wargan, L. Coy, R. Cullather, C. Draper, S. Akella, V. Buchard, A. Conaty, A. M. da Silva, W. Gu, G. K. Kim, R. Koster, R. Lucchesi, D. Merkova, J. E. Nielsen, G. Partyka, S. Pawson, W. Putman, M. Rienecker, S. D. Schubert, M. Sienkiewicz, and B. Zhao. 2017. The Modern-Era Retrospective Analysis for Research and Applications, Version 2 (MERRA-2). Journal of Climate **30**:5419-5454.

Gesch, D. B., K. L. Verdin, and S. K. Greenlee. 1999. New land surface digital elevation model covers the Earth. Eos, Transactions: American Geophysical Union **80**:69-70.

Graler, B., E. Pebesma, and G. Heuvelink. 2016. Spatio-Temporal Interpolation using gstat. R Journal **8**:204-218.

Guan, H. D., C. T. Simmons, and A. J. Love. 2009. Orographic controls on rain water isotope distribution in the Mount Lofty Ranges of South Australia. Journal of Hydrology **374**:255-264.

Guttman, N. B. 1989. Statistical descriptors of climate. Bulletin of the American Meteorological Society **70**:602-607.

Harris, I., P. D. Jones, T. J. Osborn, and D. H. Lister. 2014. Updated high-resolution grids of monthly climatic observations – the CRU TS3.10 Dataset. International Journal of Climatology **34**:623-642.

Hijmans, R. J., S. E. Cameron, J. L. Parra, P. G. Jones, and A. Jarvis. 2005. Very high resolution interpolated climate surfaces for global land areas. International Journal of Climatology **25**:1965-1978.

Huffman, G. J., D. T. Bolvin, E. J. Nelkin, D. B. Wolff, R. F. Adler, G. Gu, Y. Hong, K. P. Bowman, and E. F. Stocker. 2007. The TRMM multisatellite precipitation analysis (TMPA): quasi-global, multiyear, combined-sensor precipitation estimates at fine scales. Journal of Hydrometeorology **8**:38-55.

Hughes, D. A. 2006. Comparison of satellite rainfall data with observations from gauging station networks. Journal of Hydrology **327**:399-410.

Joseph, R., T. M. Smith, M. R. P. Sapiano, and R. R. Ferraro. 2009. A new high-resolution satellite-derived precipitation dataset for climate studies. Journal of Hydrometeorology **10**:935-952.

Koetse, M. J., and P. Rietveld. 2009. The impact of climate change and weather on transport: an overview of empirical findings. Transportation Research Part D-Transport and Environment **14**:205-221.

Lawrimore, J. H., M. J. Menne, B. E. Gleason, C. N. Williams, D. B. Wuertz, R. S. Vose, and J. Rennie. 2011. An overview of the Global Historical Climatology Network monthly mean temperature data set, version 3. Journal of Geophysical Research: Atmospheres **116**:D19121. doi:19110.11029/12011JD016187.

Mbogga, M. S., A. Hamann, and T. Wang. 2009. Historical and projected climate data for natural resource management in western Canada. Agricultural and Forest Meteorology **149**:881-890.

Mendelsohn, R., P. Kurukulasuriya, A. Basist, F. Kogan, and C. Williams. 2007. Climate analysis with satellite versus weather station data. Climatic Change **81**:71-83.

Menne, M. J., I. Durre, R. S. Vose, B. E. Gleason, and T. G. Houston. 2012. An overview of the Global Historical Climatology Network-Daily database. Journal of Atmospheric and Oceanic Technology **29**:897-910.

New, M., M. Hulme, and P. Jones. 1999. Representing twentieth-century space-time climate variability. Part I: Development of a 1961-90 mean monthly terrestrial climatology. Journal of Climate **12**:829-856.

Pebesma, E. J. 2004. Multivariable geostatistics in S: the gstat package. Computers & Geosciences **30**:683-691.

Rehfeldt, G. E. 2006. A spline model of climate for the Western United States. General Technical Report RMRS-GTR-165. Department of Agriculture, Forest Service, Rocky Mountain Research Station, Fort Collins, Colorado, U.S.

Schär, C., and C. Frei. 2005. Orographic Precipitation and Climate Change. Pages 255-266 *in* U. M. Huber, H. K. M. Bugmann, and M. A. Reasoner, editors. Global Change and Mountain Regions: An Overview of Current Knowledge. Springer Netherlands, Dordrecht, Netherlands.

Schneider, U., A. Becker, P. Finger, A. Meyer-Christoffer, M. Ziese, and B. Rudolf. 2014. GPCC's new land surface precipitation climatology based on quality-controlled in situ data and its role in quantifying the global water cycle. Theoretical and Applied Climatology **115**:15-40.

Scholl, M. A., and S. F. Murphy. 2014. Precipitation isotopes link regional climate patterns to water supply in a tropical mountain forest, eastern Puerto Rico. Water Resources Research **50**:4305-4322.

Schweikert, A., P. Chinowsky, X. Espinet, and M. Tarbert. 2014. Climate change and infrastructure impacts: comparing the impact on roads in ten countries through 2100. Humanitarian Technology: Science, Systems and Global Impact 2014 **78**:306-316.

Sun, Q. H., C. Y. Miao, Q. Y. Duan, H. Ashouri, S. Sorooshian, and K. L. Hsu. 2018. A review of global precipitation data sets: data sources, estimation, and intercomparisons. Reviews of Geophysics **56**:79-107.

Tank, A. M. G. K., J. B. Wijngaard, G. P. Konnen, R. Bohm, G. Demaree, A. Gocheva, M. Mileta, S. Pashiardis, L. Hejkrlik, C. Kern-Hansen, R. Heino, P. Bessemoulin, G. Muller-Westermeier, M. Tzanakou, S. Szalai, T. Palsdottir, D. Fitzgerald, S. Rubin, M. Capaldo, M. Maugeri, A. Leitass, A. Bukantis, R. Aberfeld, A. F. V. Van Engelen, E. Forland, M. Mietus, F. Coelho, C. Mares, V. Razuvaev, E. Nieplova, T. Cegnar, J.

A. Lopez, B. Dahlstrom, A. Moberg, W. Kirchhofer, A. Ceylan, O. Pachaliuk, L. V. Alexander, and P. Petrovic. 2002. Daily dataset of 20th-century surface air temperature and precipitation series for the European Climate Assessment. International Journal of Climatology **22**:1441-1453.

Team, R. D. C. 2016. R: A language and environment for statistical computing. R Foundation for Statistical Computing, Vienna, Austria. URL https://www.R-project.org/.

Van Den Besselaar, E. J. M., A. M. G. K. Tank, G. Van Der Schrier, M. S. Abass, O. Baddour, A. F. V. Van Engelen, A. Freire, P. Hechler, B. I. Laksono, Iqbal, R. Jilderda, A. K. Foamouhoue, A. Kattenberg, R. Leander, R. M. Guingla, A. S. Mhanda, J. J. Nieto, Sunaryo, A. Suwondo, Y. S. Swarinoto, and G. Verver. 2015. International climate assessment & dataset: climate services across borders. Bulletin of the American Meteorological Society **96**:16-21.

Vanham, D., E. Fleischhacker, and W. Rauch. 2009. Impact of an extreme dry and hot summer on water supply security in an alpine region. Water Science and Technology **59**:469-477.

Varma, A. K. 2018. Measurement of Precipitation from Satellite Radiometers (Visible, Infrared, and Microwave): Physical Basis, Methods, and Limitations. Pages 223-248 *in* T. Islam, Y. Hu, A. Kokhanovsky, and J. Wang, editors. Remote Sensing of Aerosols, Clouds, and Precipitation. Elsevier, Amsterdam, Netherlands.

Vorosmarty, C. J., C.F-Jauregui, and M. C. Donoso. 1998. A Regional, Electronic Hydrometeorological Data Network for South America, Central America, and the Caribbean. University of New Hampshire, Durham, New Hampshire, U.S.

Wang, T., A. Hamann, D. L. Spittlehouse, and T. Q. Murdock. 2012. ClimateWNA—High-resolution spatial climate data for Western North America. Journal of Applied Meteorology and Climatology **51**:16-29.

Wang, T., A. Hamann, D. Spittlehouse, and C. Carroll. 2016. Locally downscaled and spatially customizable climate data for historical and future periods for North America. PLOS ONE **11**:e0156720. DOI: 0156710.0151371/journal.pone.0156720.

Willmott, C. J. 1982. Some comments on the evaluation of model performance. Bulletin of the American Meteorological Society **63**:1309-1313.

WMO. 1996. Climatological Normals (CLINO) for the period 1961-1990. World Meteorological Organization. Geneva, Switzerland.

Xie, P., and P. A. Arkin. 1997. Global precipitation: a 17-year monthly analysis based on gauge observations, satellite estimates, and numerical model outputs. Bulletin of the American Meteorological Society **78**:2539-2558.

Chapter 4. A comprehensive database of historical and projected future climate for Latin America

4.1. Summary

Analysis of climate change impacts and planning of adaptation strategies requires accurate historical climate databases and projections of future climate conditions. Although such data is generally widely available, the data formats, projection of grids, temporal coverage, spatial resolution, and spatial extent are highly variable. As a consequence, customized datasets suitable for research or management applications are only accessible to expert GIS users, and preparing the data can be complex and time consuming. The objective of this chapter is to contribute a collection of selected databases for Latin America that can be accessed through an easy-to-use software solution that applies lapse-rate based down-scaling of temperature variables to higher resolutions, and overlays anomaly layers for historical monthly data and future projections. Climate estimates resulting from interpolation and down-scaling were validated against weather station records. For the 1961-1990 average climate normal, we find a mean absolute error (MAE) of 0.6°C for annual temperature, and an 8% error for annual precipitation, compared to observed values. For estimates of individual years from 1901-2010, we find an average MAE of 0.7 for temperature, and an average 11% error for precipitation. The database also includes future projections for the 2020s, 2050s, and 2080s based on 15 AOGCMs from the CMIP5 project. To guide the selection of future projections, regional rankings of different scenarios with respect to the magnitude of their temperature and precipitation projections are provided. We provide estimates for 80 monthly, seasonal, annual, and bioclimatic variables for five climate normals, 11 decades, 113 years, and three future time periods for a total of 18,000 data layers, which can be interactively queried for point locations or read out as grids for a user-defined spatial extent, resolution and time period.

4.2. Introduction

Research and management in the context of climate change requires various types of historical climate data as well as future projections for a suite of relevant climate variables. These include monthly precipitation and temperature estimates, and also derived variables that have relevance for natural systems or infrastructure planning, such as growing degree days, frost-free periods, heating and cooling degree days, drought indices, etc. These variables need to be estimated for different time periods, such as: (1) 30-year climate normal averages that serve as reference points; (2) historical time series to study past responses to climate variability and climate trends, e.g. dendrochronological studies, (e.g., Suarez et al. 2015); (3) regional climate surfaces for specific time periods, e.g. to map suitability for crop production (e.g., Alkimim et al. 2015); (4) long term averages of climate conditions for sample locations, e.g. to climatically characterize census data for species distribution models (e.g., Sarkinen et al. 2013); and (5) projected future climates to plan for, or to adapt to climate change (e.g., Ramirez-Villegas et al. 2014).

Although gridded climate data products are available for Latin America (mostly through global products), they lack either high spatial or high temporal resolution. Data products with monthly data for the last century typically have a relatively low resolution of 0.5°, including the databases of Wilmott & Matsura (Willmott and Matsuura 1995, Willmott and Robeson 1995), the Climate Research Unit (CRU TS v3.21) (Mitchell and Jones 2005, Harris et al. 2014), or the Global Precipitation Climatology Centre (GPCC) (Becker et al. 2013). Because of their low spatial resolution, the absolute climate values are unreliable in mountainous regions where both temperature and precipitation vary considerably along elevation gradients and across topographic barriers. In contrast, gridded climate data with high spatial resolution tend to lack good temporal historical coverage. For example, the data layers developed by Hijmans et al. (2005) for the WorldClim project were generated at resolutions of 30 arc-

seconds (approximately 900 m at the equator), but there is only one historical climate normal layer available for the 1971-2000 period (Fick and Hijmans 2017).

The above databases are sufficient for many applications. For example, WorldClim is widely used for climate change impact assessments on species distributions, regional food productivity, urban planning, or regional expansion of tropical diseases. The temporally explicit database CRU is widely used for correlative models that predict land use changes, food security assessments, analysis of historical energy use, etc. Nevertheless, sometimes accuracy is required in both temporal and spatial resolution, for example when studying plant-climate interactions based on historical data in complex landscapes. An example is comparative dendroecological research that aims to identify vulnerable species and populations (Swetnam et al. 1999, Paritsis and Veblen 2011). Accurate time series estimates, including accuracy in absolute climate values are required for these types of research.

The problem of high spatial and high temporal resolution climate data is that quickly results in a database with an unmanageable size. For example, the WorldClim layers for one climate normal period with 19 bioclimatic and 36 monthly variables is approximately 20 GB for a global extent. If that data was provided for individual years from 1901-2015, the size would be 2.3 TB, which is difficult to handle by normal users. The same limitation applies to projections of future climate. Providing data for 60 AOGCM projections included in the CMIP5 multimodel dataset, four different emission scenarios (RCP2.6, RCP 4.5, 6.0 and 8.5), perhaps three future periods (e.g., 2020s, 2050s, and 2080s), and for 36 monthly variables and 19 biocliamtic variables, amounts to 39,000 spatial layers (or around 15 TB of data).

Furthermore, climatic characterization of sample points is not optimally solved with grid-based climate data products. In order to characterize sample points climatically, data is normally extracted from climate grids based on their location. However, location information for samples prior to the widespread use of global positioning systems is often only reported to

the nearest arcminute or the nearest 10 arcminutes (e.g. older botanical records or other census and inventory data). This leads to location errors of several 100m to several km. In mountainous terrain, this can result in substantial errors in the climate estimate if the elevation of the sampling location and the elevation of the grid cell to derive a climate estimate are substantially different.

Both problems, database size and characterization of sample points with inaccurate location information, have been addressed by Wang et al. (2006). Their approach relies on a medium resolution (2.5 arcminute) baseline climate normal dataset, low resolution (0.5 degree) anomaly surfaces that represent historical data, and low resolution future projections from AOGCMs (resampled to a common resolution of 1 degree). For precipitation variables, the medium resolution baseline layer is enough to accurately capture the interaction between topography and the global prevailing winds that drive precipitation (Daly 2006). For temperature variables, very high resolution surfaces can be created from the medium resolution baseline dataset with empirical lapse-rate based elevation adjustments. Lapse-rates vary considerably by location and by climate variable, and can be estimated as a mathematical derivative of how climate locally varies as a function of elevation (Hamann and Wang 2005). This technique also can be used for local downscaling of temperature variables, and is also useful for estimating climate values for sample locations where the location information is only approximate but an elevation is reported. Using this approach of relying on medium and low-resolution layers and on-demand down-sampling for points or local grids, a comprehensive database for North America can be packaged into a 1GB uncompressed database that can be easily queried (Wang et al. 2016). The statistical accuracy of local estimates are comparable or better than high resolution gridded data (Mbogga et al. 2010, Wang et al. 2016).

Here, we contribute a similar database package for Latin America, building on the methodology developed by Wang et al. (2016). This database and software package provides

scale-free climate data for temperature and precipitation at monthly, seasonal, and annual time steps, from 1901 to 2015, as well as decadal averages, and 30-year climate normal estimates. Also included are future projections for the 2020s, 2050s, and 2080s from 15 selected AOGCMs of the CMIP5 multimodel dataset. For all the above time periods, we provide a comprehensive set of monthly and bioclimatic variables. In total, the database includes approximately 18,000 data layers that can be interactively queried through a custom software front-end. We document the accuracy of this database by estimating mean absolute errors of the gridded surfaces and point estimates. For future projections, we provide guidance for researchers and managers how to best select AOGCMs that represent contrasting or median projections for their area of interest.

4.3. Methods

4.3.1. Baseline climate data

The main baseline climate normal layer consists of interpolated data for monthly minimum temperature, monthly maximum temperature and monthly precipitation for the 1961-1990 normal period. The precipitation layers were developed with a universal kriging interpolation based on 45,800 weather stations for the 1961-1990 climate normal period (Chapter 2 of this thesis). As covariate for the interpolation, an exposure metric was developed based on wind speed, wind direction, slope, and aspect. This exposure layer simulates how prevailing winds interact with the mountainous terrain causing effects such as orographic lift and rain shadows (Chapter 3 of this thesis). The temperature layers for the 1961-1990 normal period were derived from the 30 arcsecond WorldClim dataset developed by Hijmans et al. (2005). Since the original WorldClim layers were estimated for the 1971-2000 period, we adjusted the values to correspond to the 1961-1990 climate normal period using CRU TS data and the delta method (Mitchell and Jones 2005). Subsequently, we resampled the dataset to a target resolution of 2.5 arcminute that matches seamlessly with 2.5 arcminute PRISM data that Wang et al. (2016) used for their North American database.

71

4.3.2. Historical and future climate anomalies

To estimate historical climate values for the 1901-2013 period, we rely on the CRU-TS 3.12 database (Harris et al. 2014) that was developed by Mitchell and Jones (2005). While the database reports absolute climate values for individual years, the interpolations of the CRU-TS database are based on weather station data expressed as anomalies relative to a climate normal period. We recover the anomaly values for annual CRU grids by subtracting the normal value for the 1961 to 1990 period.

For future climate projections based on the CMIP5 multimodel dataset, we also calculate anomalies relative to 1961-1990 for the normal periods of 2011-2040 (hereafter referred to as 2020s), 2041-2070 (2050s), and 2071-2100 (2080s). The CMIP5 multimodel dataset includes approximately 60 Atmosphere-Ocean General Circulation Models (AOGCMs). Instead of including all 60 AOGCMs, we selected 15 AOGCMs intended to represent the major clusters of AOGCMs by Knutti et al. (2013). Within clusters, we selected models that had the highest validation statistics in their CMIP3 equivalents (Wang et al. 2007, Gleckler et al. 2008, Walsh et al. 2008, Chen et al. 2011, Scherrer 2011, Fasullo and Trenberth 2012). The selected AOGCMs were CanESM2, ACCESS1.0, IPSL-CM5A-MR, MIROC5, MPI-ESM-LR, CCSM4, HadGEM2-ES, CNRM-CM5, CSIRO Mk 3.6, GFDL-CM3, INM-CM4, MRI-CGCM3, MIROC-ESM, CESM1-CAM5, GISS-E2R. For each of these AOGCMs we provide estimates for two different Representative Concentration Pathways (RCPs). We selected RCP 4.5, which assumes that radiative forcing by greenhouse gasses will stabilize by the end of the century as the result of significant efforts in reducing greenhouse gas emissions. The other scenario we selected is RCP 8.5, which assumes that greenhouse gas emissions will continue to increase throughout the current century (Rogelj et al. 2012). Since AOGCMs projections are generated by different research centers around the world, and their

spatial resolutions vary from 0.75° to 2.85°, we resample the projections to a common resolution of 1° for use as anomaly layers in our software package.

The software overlays the historical or future anomaly layers over the 1961-1990 baseline layer to arrive to absolute climate values for the 36 monthly variables. Subsequently, the final output is generated for a user-defined sample point, or a user-defined resolution and spatial extent. This final downscaling is informed by the elevation for the points of interest or from a high resolution digital elevation model (DEM) for a study area in xyz-triplet format (i.e. latitude, longitude, elevation). This elevation adjustment is based on a regression approach and uses local derivative equations that estimate the change in temperature due to a change in elevation depending on the latitude, longitude and elevation of the point (Hamann and Wang 2005). In other words, if a point of interest or a grid cell of a high-resolution DEM is above the elevation of the 2.5 arcminute grid cell used to estimate the 1961-1990 baseline climate value, the temperature variable values will be adjusted according to the local lapse rate equation (usually becoming colder). For a point of interest below the elevation of the corresponding 2.5 arcminute tile, the adjustment would normally be upwards for a temperature value.

4.3.3. Estimation of bioclimatic variables

All interpolation, overlays, and elevation adjustment steps are performed on the 36 monthly variables, which are 12 average monthly minimum temperature variables, and 12 average monthly maximum temperature variables, and 12 monthly precipitation variables (no lapse rate adjustments are carried out on precipitation variables, however). From these values a number of bioclimatic variables can simply be calculated, such as seasonal and annual summaries for temperature and precipitation. This includes the following periods: December to February (DJF, Winter in the Northern hemisphere and Summer in the Southern hemisphere), March to May (MAM, Spring and Autumn, respectively), June to August (JJA,

Summer and Winter, respectively), and September to November (SON, Autumn and Spring, respectively). For each of these seasonal periods, mean temperature (°C), mean maximum temperature (°C), mean minimum temperature (°C), and precipitation (mm) are calculated. Annual summaries include mean annual temperature (MAT), mean warmest month temperature (MWMT), mean coldest month temperature (MCMT), mean annual precipitation (MAP). A simple annual heat moisture index (AHM) is calculated as MAT+10/MAP in units of meters, and a simple index of continentality is calculated as the difference between MWMT and MCMT or temperature difference (TD).

While the previous variables can be directly estimated from monthly summaries, other bioclimatic variables require daily data in principle, but can still be estimated through linear and non-linear regression approaches from the 36 monthly climate variables included as a baseline in this software package. For more details on the equations and algorithms to estimate derived climate variables that normally require daily data, refer to Wang et al. (2006) and Wang et al. (2016). The derived variables include degree days below 0°C (DD<0), degree days above 5°C (DD>5), degree days below 18°C (DD<18), degree days above 18°C (DD>18), number of frost free days (NFFD), precipitation as snow between January and December (PAS), expected extreme minimum temperature over 30 years (EMT), Hargreaves reference evaporation (Eref), and Hargreaves climatic moisture deficit (CMD). The degree days below 0°C is an indicator of the severity of winters. The degree days above 5°C are describe the growing season and are a commonly used criterion for crop selection. Degree days below and above 18°C are used in infrastructure planning to estimate the amount of energy used to heat or cool buildings (Vaughn 2005).

4.3.4. Error estimation and validation

To test the statistical precision and accuracy of the data generated as outlined above, we compare the elevation-adjusted climate estimates against weather station data obtained from

two historical databases, the Global Historical Climatology Network Monthly version two for precipitation (Peterson and Vose 1997) and the Global Historical Climatology Network Monthly version three for temperature (Lawrimore et al. 2011). While we previously reported validation statistics for the 1961-1990 normal period (Chapter 3 of this thesis), here we focus on the accuracy of historical climate estimates for individual months, seasons, and years from 1901 to 2010. Weather station coverage varies over this time period (Fig 4.1) and the validation statistics for different years are therefore based on different numbers of observations.

We report variance explained (R^2), as well as mean absolute error (MAE). The MAE is obtained by averaging the difference, independent of sign, between observed and predicted climate values for each weather station (Willmott 1982). However, for precipitation variables, we also express this error as percentage of the observed precipitation, to scale the error relative to the magnitude of the precipitation value. This makes it easier to compare the accuracy of monthly versus seasonal versus annual precipitation, or to compare accuracy of high precipitation values in tropical rainforests with low precipitation values in dry areas. We report R^2 and MAE statistics for the 1961-1990 normal period, and for each year of the 1901-2013 period for six variables, including temperature and precipitation for January (representing accuracy of a monthly variable), temperature and precipitation for the December-January-February period (seasonal variable), mean annual temperature and annual precipitation (annual variable). To detect any differences in statistical accuracy for difficult to model mountainous regions compared to plains areas, we divided the evaluation between weather stations with an elevation >1000m ASL and stations located <1000m ASL.
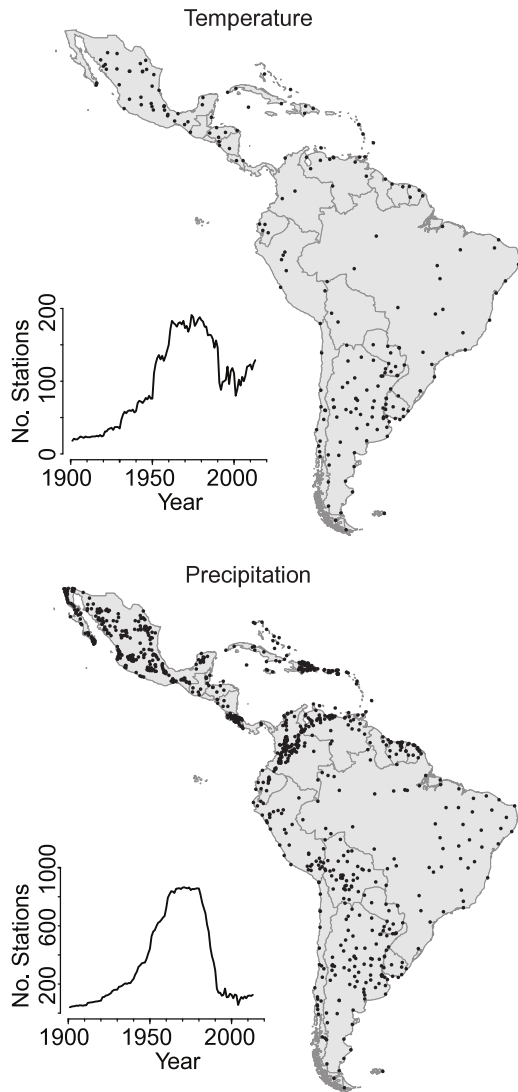
Fig. 4.1. Distribution of weather stations with temperature and precipitation records with at least 20 years of observations between 1900 and 2015 used for validation.

4.3.5. Summaries of future projections

To help managers, professionals, and researchers who need to develop adaptation strategies for climate change, and who need estimates of the range and median of climate change projections from multiple AOGCMs for a specific region, we classify different future projections by their direction and magnitude. However, given the broad extent of Latin America, individual AOGCM projections vary significantly by region (i.e. an AOGCM may

predict a reduction of precipitation of 5% for mountainous regions, affecting temperate forest all over the continent, but this decrease might be negligible in the Amazon rain forests). Therefore, we first grouped climate projections into geographic regions that are generally similar in type and magnitude of projected climate change according to an ensemble model that is an average of the 15 AOGCMs included in the software. Once these regions were defined, we grouped individual AOGCMs based on their individual projection for each region.

For the first step, regional groupings with similar ensemble projections, we cluster individual grid cells of future projections based on seasonal temperature and precipitation variables (Dec-Jan-Feb, Mar-Apr-May, Jun-Jul-Aug, Sep-Oct-Nov). Clustering is performed on the differences (anomalies) between the 1961-1990 normal period and the 2050s projections for the RCP 4.5 emission scenario for the 15 AOGCMs listed above. The anomalies for temperature were expressed as degree Celsius, while the anomalies for precipitation were expressed as percentage of change compared to the 1961-1990 reference normal period. We grouped grid cells for Latin America with a hierarchical cluster analysis implemented with the *hclust* function with the default Euclidean distance matrix option of the base R programming environment (R Core Team 2016).

As the basis for grouping the 15 individual AOGCMs, we then use projections of seasonal variables (as above), but with variables for the cluster analysis now broken up by four regional projections, obtained from the first step (i.e. 8 seasonal variables × 4 geographic regions = 32 variables for the second clustering step). The resulting table with 4 geographic regions × 32 climate variables, clustered by similarity and colored with a heatmap function can be used to select "optimistic", "pessimistic", or median AOGCM projections for different regions of Latin America. For a more local selection of AOGCMs we also provide the same table broken down by country × region of similar projected climate change.

4.4. Results & Discussion

4.4.1. Observed versus interpolated climate data

In general, both the variance explained and the accuracy of interpolated surfaces increases for variables that average larger time periods, either when comparing variables that cover different time periods, i.e. a month, a season, or a year, (Table 4.1), or when comparing validation statistics for single year averages versus 30-year climate normal averages (Fig. 4.2). Both our R^2 and MAE values seem comparable to what other studies report for non-independent validations. Mbogga et al. (2009) evaluated the PRISM surfaces for Western Canada for the 1961-1990 climate normal period, and reported R^2 values of 0.97 for both annual temperature and precipitation for the 1961-1990 period. Our results are similar for temperature (0.96), but explain less variance for precipitation (0.93) for Latin America (Fig. 4.2). Similarly, Wang et al. (2011) report R^2 values of 0.98 and 0.96 for monthly temperature and precipitation for western North America. WorldClim, for the entire world reports R^2 values for monthly temperature of 0.99, and like in our study, lower values for monthly precipitation $R^2=0.74$, but in their case the evaluation has been done with an independent dataset withheld for validation (Fick and Hijmans 2017).

We also provide an additional contrast between estimates for mountainous areas above 1000m ASL versus weather stations below 1000mASL. The mean absolute error (MAE) values for mountainous areas are almost double compared to the lower elevations, while errors of temperature estimates increase only by about 0.2°C for mountainous areas (Table 4.1). These differences in the accuracy of predictions for temperature and precipitation reflect the difficulty associated with modeling precipitation for mountainous areas (Daly 2006, Daly et al. 2008). In contrast, temperature estimates that included a lapse-based elevation adjustment can be made with high accuracy even in mountainous areas (Mbogga et al. 2009, Wang et al. 2016).

For historical time series, the accuracy of the temperature estimates increase slightly from the beginning of the century to the present time, but they are generally high with estimates for the 30-year normal period only slightly more precise (about 0.2°C) than for individual years (Fig 4.2, upper panel). The increase in precision over time is likely due to sparse weather station coverage prior to the 1950s (Menne et al. 2012). In contrast, for precipitation the accuracy can degrade substantially for individual years depending on the variable (Fig. 4.2, lower panel). Notably, error of monthly precipitation estimates for individual years have more than twice the error as estimates of the same variable for the 30-year climate normal period. The difference becomes less pronounced for seasonal and annual precipitation. This is due the highly stochastic nature of precipitation events. The longer the period over which precipitation events are summed up or averaged, the more reliable those estimates become (New et al. 2001, Arguez and Vose 2011).

Table 4.1. R^2 values and average deviation in absolute values, and for precipitation also as percentage from observed values, to compare the quality of estimates for the 1961-1990 climate normal from ClimateSA and from observed weather station data. The dataset was divided into plains regions (<1,000m ASL), and mountainous regions (>1,000m ASL).

Variable	<1,000m ASL		>1,000m ASL	
	R^2	MAE	R^2	MAE
January Temperature	0.97	0.59°C	0.94	0.73°C
Dec-Jan-Feb Temperature	0.97	0.56°C	0.94	0.71°C
Mean Annual Temperature	0.99	0.53°C	0.94	0.74°C
January Precipitation	0.95	10mm (9%)	0.80	17mm (15%)
Dec-Jan-Feb Precipitation	0.95	26mm (7%)	0.83	51mm (15%)
Mean Annual Precipitation	0.96	101mm (5%)	0.90	211mm (12%)
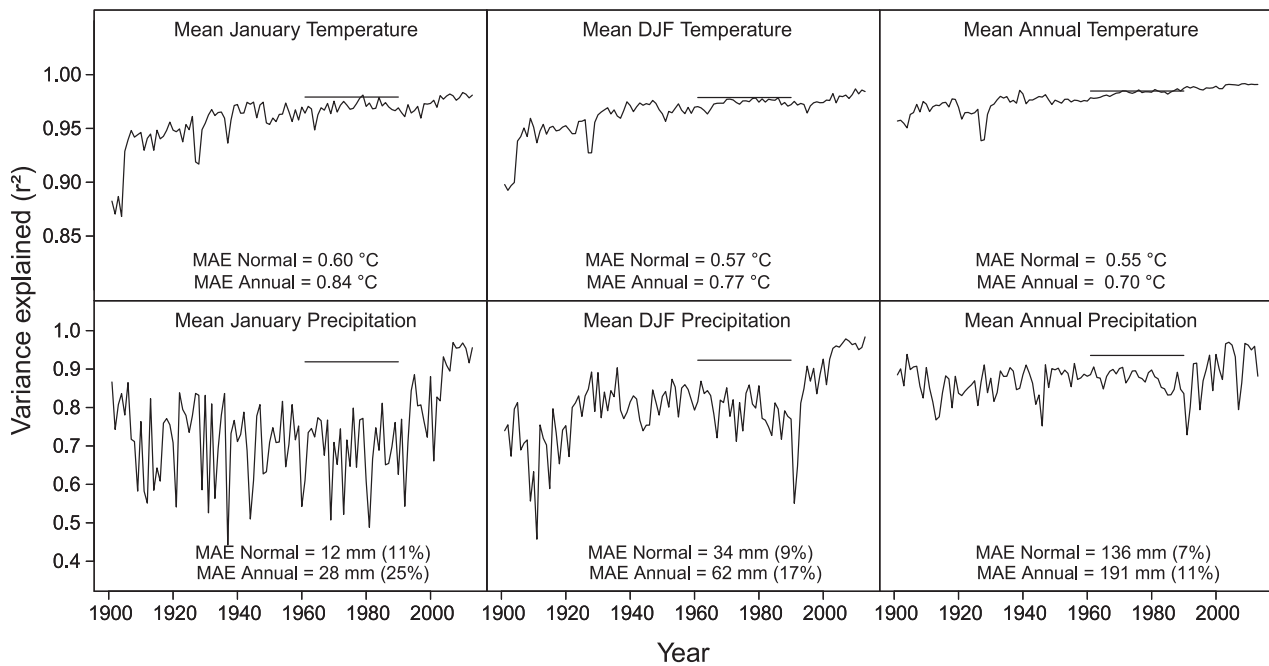
Fig. 4.2. Statistical accuracy of climate estimates expressed as variance explained (r^2) by ClimateSA estimates against weather station data, and expressed as mean absolute error (MAE) of climate estimates for the 1961-1990 normal period (non-zonal bar) and the average annual error from 1901 – 2013. DJF=December-January-February.

4.4.2. Future climate projections for Latin America

Regional patterns of projected climate change based on eight seasonal temperature and precipitation variables show that the regional groupings of climate change projections are mostly driven by precipitation (Fig. 4.3). The first split distinguishes Region 1 and 2, where precipitation is expected to decrease on average, versus Region 3 and 4, where precipitation is expected to increase, explaining 30% of the variance in regional climate change projections across Latin America. Subsequent splits explain less variance, with Region 1 characterized by strong projected precipitation reductions in the southern hemisphere summer season (December-February). This applies to North and Central Mexico, Guyana, Surinam, French Guiana, Southern Chile, and Southern Argentina (Fig. 4.4, white).
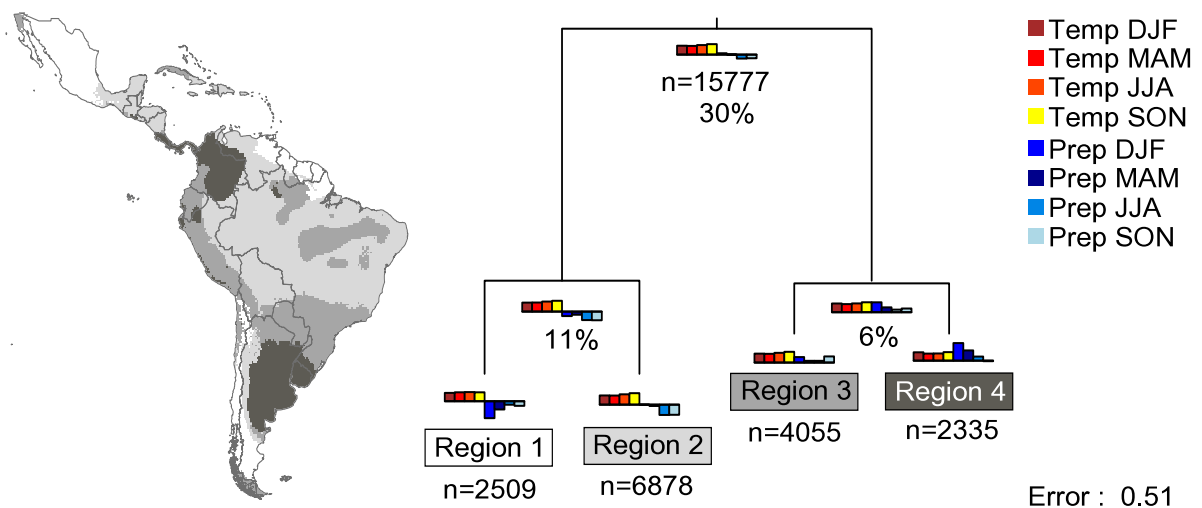
Fig. 4.3. Clustering of grid cells of Latin America that show similar projected climate changes. Temperature and precipitation anomalies for each season of the year were obtained with an ensemble of 15 AOGCMs of the CMIP5 multi-model project, for the 2050s climate normal period, relative to the 1961-1990 climate normal. DJF= December-January-February; MAM= March-April-May; JJA= June-July-August; SON= September-October-November.

For Region 1, average expected decreases of precipitation are 15% for the December-February period, 7% for the March-May period, 3% for the June-August period, and 4% for the Sept-Nov period. For North and Central Mexico this means that the dry season is going to be more severe, and there will be a slight decrease of precipitation during the rainy season. For Guyana, Surinam and French Guiana this decline in precipitation will apply mostly to one of their two rainy seasons. For Southern Chile and for the Patagonia desert, the most severe precipitation reduction coincides with their dry season and highest temperatures during the southern hemisphere summer months.

For Group 2, precipitation is predicted to decrease primarily between June and November, comprising Southern Mexico, northern Central America, the Caribbean Islands, the dry northern coast of Venezuela, the Amazon basin (Fig. 4.3, light gray). Here, precipitation is predicted to decrease by 9% on average for periods of Jun-Aug and Sep-Nov. This decrease primarily applies to the wetter seasons of the year for southern Mexico, northern Central

America, and the Caribbean Islands. For the Amazon basin, this means less rain when precipitation is lowest and temperatures are highest in the second half of the calendar year.

Southern Brazil, Paraguay, northern Argentina, and the Atacama Desert form Group 3 (Fig. 4.3, medium gray) with largely stable precipitation projections or slight increases. Lastly, substantial increases in southern hemisphere winter precipitation are expected for Group 4, comprising Costa Rica, Panama, Colombia, and the Uruguayan and Argentine Pampa (Fig. 4.3, dark gray). This group is characterized by average projected increases of precipitation of 16% and 9% for the periods of Dec-Feb and March-May, respectively. For southern Central America and Colombia this means precipitation increases during the dry season, while for Uruguayan and Argentinean Pampa the precipitation increase coincides with the rainy season.

4.4.3. Selection of AOGCMs

While the above section summarizes average expectations of climate change projections across all AOGCMs, individual models vary substantially in their projections by region, visualized with the second cluster analysis of similar AOGCMs. In the first and second group are the models that could generally be considered "optimistic", predicting the lowest increments of temperature, and only slight changes to precipitation (Fig. 4.4, first 6 AOGCMs: MRI-CGCM3 to CNRM-CM5). In the third group, including four scenarios plus the 15-model average ensemble can be considered typical projections, with temperature increases around 2°C and precipitation decreases around 10% for Regions 1 and 2 (Fig. 4.4, MPI-ESM to HadGM2-ES). The fourth group, comprising four AOGCMs, projects stronger temperature increases and precipitation reductions than the previous group (Fig. 4.4, GFDL-CM3 to CSIRO-mk3). The last model (IPSL-CM5A-MR) stands out with unusual precipitation projections, particularly for Region 1 and 3.

Lastly, we provide an even finer breakdown of projected changes by country and region to help researchers, managers and decision makers to locally select scenarios that represent median, "optimistic" or "pessimistic" scenarios (Fig 4.5). The descriptions "optimistic" or

"pessimistic" imply values and therefore depend on the type of impact and climate vulnerabilities that are studied or planned for. For example, a "pessimistic" scenario for a natural ecosystem or agricultural region that is water limited would be an AOGCM that locally predicts the highest temperature increases and precipitation decreases during the growing season. While we provide projections for only a limited set of variables in Fig 4.5, the software front-end that we provide for our database can be queried for any of the 19 bioclimatic variables and 36 monthly temperature and precipitation variables for any specific location and any AOGCM.

a) Δ Temperature (°C)

Model	Region 1				Region 2				Region 3				Region 4			
	DJF	MAM	JJA	SON	DJF	MAM	JJA	SON	DJF	MAM	JJA	SON	DJF	MAM	JJA	SON
MRI_CGCM3	1.2	1.3	1.3	1.2	1.4	1.4	1.4	1.6	1.4	1.4	1.5	1.3	1.2	1.3	1.1	0.9
MIROC5	1.8	1.9	2.0	1.9	1.7	1.7	2.4	2.2	1.6	1.6	1.9	2.0	1.5	1.1	1.3	1.5
GISS_E2R	1.3	1.5	1.5	1.7	1.7	1.6	1.8	1.7	1.6	1.4	1.5	1.4	0.9	0.8	0.9	1.1
CESM1_CAM5	2.0	2.1	2.1	2.1	2.0	2.1	2.4	2.5	1.9	2.0	2.2	2.2	1.7	1.7	1.6	1.8
INM_CM4	0.8	1.1	1.1	1.0	1.1	1.1	1.2	1.1	1.1	1.2	1.3	1.1	1.2	1.2	1.2	1.1
CNRM_CM5	1.6	1.7	1.8	1.8	1.7	1.5	1.9	2.2	1.6	1.6	1.9	2.2	1.7	1.4	1.5	1.6
MPI_ESM_LR	1.8	1.9	2.1	2.0	2.2	2.3	2.3	2.7	2.2	2.3	2.3	2.6	2.1	1.9	1.8	2.1
CCSM4	1.8	1.8	1.8	1.8	1.7	1.7	2.0	2.1	1.7	1.8	1.9	2.0	1.7	1.7	1.6	1.6
Ensemble15	1.9	2.0	2.1	2.0	2.1	2.0	2.3	2.6	2.0	2.0	2.2	2.4	1.9	1.6	1.6	1.9
ACCESS1_0	2.0	2.1	2.0	2.2	2.3	2.1	2.3	2.6	2.1	1.9	2.2	2.4	2.0	1.6	1.6	1.6
HadGEM2_ES	2.3	2.6	2.2	2.2	2.3	2.0	2.4	3.4	2.5	1.7	2.3	3.4	2.8	0.8	1.5	2.7
GFDL_CM3	2.4	2.4	2.8	2.9	2.7	2.5	3.1	4.5	2.7	2.4	3.1	4.1	2.5	2.2	2.5	3.5
CanESM2	2.5	2.6	2.7	2.6	3.2	3.4	3.5	3.6	3.1	3.0	3.1	3.3	2.7	2.6	2.4	2.8
MIROC_ESM	2.0	2.4	2.5	2.3	2.3	2.6	3.0	3.0	1.8	2.1	2.5	2.7	1.9	1.5	1.7	2.0
CSIRO_Mk3_6_0	2.1	2.3	2.3	2.2	2.4	2.4	3.0	3.2	2.3	2.4	2.8	2.8	1.9	1.9	2.1	2.3
IPSL_CM5A_MR	2.3	2.3	2.5	2.3	2.3	2.2	2.1	2.4	2.5	2.4	2.1	2.6	2.3	2.1	1.6	2.2

b) Δ Precipitation (%)

Model	Region 1				Region 2				Region 3				Region 4			
	DJF	MAM	JJA	SON	DJF	MAM	JJA	SON	DJF	MAM	JJA	SON	DJF	MAM	JJA	SON
MRI_CGCM3	-17	2	3	-3	4	5	-11	-1	8	4	-4	4	38	13	16	4
MIROC5	-14	-8	-3	-5	7	1	11	-1	5	2	16	4	32	15	-3	1
GISS_E2R	-3	-5	-3	-6	-6	-1	2	-7	-1	6	10	1	14	17	7	8
CESM1_CAM5	-13	-10	-3	-7	-2	2	0	-8	4	7	15	3	9	12	3	-1
INM_CM4	-7	-11	1	0	-2	2	1	1	-1	6	4	4	2	5	14	4
CNRM_CM5	-4	3	3	15	0	0	1	-2	5	3	5	11	13	3	5	9
MPI_ESM_LR	-19	-18	-12	-9	-5	-5	-11	-13	2	3	2	12	4	5	10	1
CCSM4	-11	-8	-5	-6	-2	-4	-13	-8	2	0	-8	-2	1	4	0	2
Ensemble15	-15	-7	-3	-4	0	-1	-9	-9	5	2	2	6	16	9	4	0
ACCESS1_0	-25	-7	0	-5	1	-1	-5	-9	5	2	5	4	10	3	6	-2
HadGEM2_ES	-24		4	-18	-1	-3	-21	-3	8	-6	-11	7	1	15	5	-4
GFDL_CM3	-12	-5	-11	-11	-3	7	-31	-48	0	2	-32	-34	11	13	-8	-16
CanESM2	-24	-11	-1	-11	-14	-17	-28	-39	-3	-3	-9	-22	8	0	-7	-15
MIROC_ESM	-7	2	2	-2	7	2	-19	-11	9	0	-22	-13	33	12	-15	-5
CSIRO_Mk3_6_0	-18	-4	-15	-3	4	-3	-18	-27	-5	-6	-3	-10	31	2	-8	-7
IPSL_CM5A_MR	-29	-24	-5	14	9	-1	7	40	36	5	56	114	28	19	31	15

Fig. 4.4. Temperature and precipitation anomalies for the 2050s, relative to the 1961-1990 normal period predicted by 15 AOGCMs of the CMIP5 model generation, corresponding to the 5th IPPC Assessment Report (AR5). Seasonal changes are shown for clusters of grid cells that show similar projected climate change patterns.

Table 1 (ATG–DOM)

Country	ATG	ARG				BHS	BLZ	BOL			BRA				CHL				COL			CRI		CUB		DOM
Region	1	1	2	3	4	3	2	1	2	3	1	2	3	4	1	2	3	4	2	3	4	2	4	2	3	2
MRI_CGCM3	1.1	0.9	1.0	1.0	0.8	1.1	1.3	1.8	1.6	1.7	1.3	1.5	1.5	1.1	1.0	1.2	1.2	1.7	1.4	1.4	1.5	1.3	1.3	1.2	1.2	1.5
MIROC5	1.5	1.3	1.5	1.4	1.1	1.5	2.0	2.1	2.3	2.0	1.9	2.0	1.9	1.1	1.2	1.4	1.4	1.9	1.7	1.5	1.7	1.4	1.4	1.4	1.5	1.7
GISS_E2R	1.1	1.3	1.1	0.9	0.4	1.3	1.4	2.0	1.6	1.8	1.3	1.8	1.6	0.7	1.3	1.2	1.4	1.8	1.6	1.5	1.6	1.3	1.3	1.3	1.4	1.3
CESM1_CAM5	1.3	1.8	2.0	1.9	1.4	1.5	1.9	2.5	2.5	2.3	2.1	2.2	2.1	1.9	1.8	2.1	1.9	2.3	2.0	1.9	2.0	1.7	1.7	1.7	1.8	1.7
INM_CM4	0.8	1.0	1.3	1.4	1.3	0.7	1.1	1.6	1.5	1.4	0.8	1.1	1.1	1.2	1.2	1.4	1.4	1.9	0.9	1.0	0.9	1.1	1.1	0.8	0.7	1.1
CNRM_CM5	1.0	1.6	1.9	1.8	1.5	1.1	1.4	2.0	1.9	1.9	1.7	1.8	1.8	1.7	1.7	1.9	1.7	1.9	1.8	1.5	1.7	1.3	1.3	1.3	1.2	1.4
MPI_ESM_LR	1.5	1.4	2.1	2.3	1.7	1.5	1.8	3.0	2.6	2.8	2.0	2.4	2.4	2.3	1.6	2.2	1.9	2.9	2.2	2.1	2.3	1.8	1.7	1.6	1.6	1.6
CCSM4	1.2	1.6	1.8	1.8	1.5	1.3	1.6	2.0	2.1	2.0	1.7	1.8	1.9	1.8	1.6	1.7	1.7	2.0	1.7	1.7	1.8	1.4	1.4	1.5	1.5	1.4
Ensemble15	1.4	1.6	1.8	1.9	1.5	1.5	1.9	2.5	2.5	2.4	2.0	2.3	2.2	1.8	1.6	1.9	1.8	2.4	2.2	1.9	2.1	1.8	1.7	1.6	1.6	1.7
ACCESS1_0	1.6	1.5	1.6	1.6	1.3	1.6	2.1	2.5	2.2	2.3	2.5	2.4	2.4	1.7	1.4	1.7	1.7	2.3	2.3	1.9	2.2	1.9	1.9	1.8	1.7	1.9
HadGEM2_ES	1.6	1.7	1.9	2.1	1.6	1.7	2.1	2.8	2.4	2.6	2.5	2.6	2.7	2.1	1.7	2.0	2.0	2.6	2.4	2.2	2.4	2.0	2.0	1.9	1.9	2.0
GFDL_CM3	2.1	2.1	2.6	2.8	2.2	2.3	2.3	3.2	3.8	3.4	2.5	3.2	3.0	2.8	2.2	2.9	2.4	3.2	3.9	2.9	3.3	2.4	2.5	2.4	2.3	2.3
CanESM2	1.8	2.2	2.7	3.0	2.1	2.0	2.5	3.4	3.7	3.1	2.7	3.5	3.3	2.7	2.3	2.9	2.7	3.4	3.8	2.7	3.4	2.4	2.5	1.9	1.9	2.3
MIROC_ESM	1.8	1.3	2.0	2.2	1.7	1.8	2.8	2.6	3.0	2.7	2.4	2.9	2.4	1.7	1.5	1.9	1.7	2.2	2.3	1.8	1.8	2.3	2.1	1.9	1.9	1.9
CSIRO_Mk3_6_0	1.7	1.6	2.1	2.3	1.6	1.8	2.2	3.0	3.1	2.9	2.3	2.8	2.6	2.1	1.7	2.2	2.2	2.9	3.0	2.0	2.7	2.4	2.3	1.9	2.0	1.9
IPSL_CM5A_MR	1.4	2.0	2.2	2.4	1.9	1.5	2.1	2.8	2.5	2.8	2.2	2.2	2.4	2.2	1.8	1.8	1.8	2.2	2.1	2.2	2.3	1.7	1.8	1.9	1.9	1.8

Table 2 (ECU–NIC)

Country	ECU			SLV		GUF		FLK	GLP	GTM			GUY			HTI	HND	JAM	MTQ	MEX			SUR			NIC		
Region	2	3	4	2	4	1	2	3	1	2	3	4	1	2	3	2	2	2	1	1	2	3	1	2	3	2	3	4
MRI_CGCM3	1.4	1.4	1.4	1.3	1.3	1.2	1.3	0.5	1.1	1.5	1.3	1.4	1.2	1.3	1.3	1.4	1.3	1.1	1.2	1.4	1.3	1.2	1.2	1.3	1.3	1.4	1.3	1.4
MIROC5	1.7	1.6	1.7	1.8	1.9	1.8	1.9	0.8	1.5	2.2	1.8	1.9	2.0	2.2	2.2	1.6	1.8	1.5	1.5	2.2	2.0	2.1	1.9	2.0	2.1	1.6	1.5	1.5
GISS_E2R	1.7	1.5	1.4	1.7	1.8	1.2	1.5	0.7	1.1	1.6	1.5	1.7	1.2	1.6	1.7	1.2	1.5	1.2	1.1	1.7	1.5	1.3	1.4	1.7	1.8	1.4	1.2	1.3
CESM1_CAM5	2.2	2.0	2.0	2.0	1.9	2.1	2.6	1.3	1.3	2.1	1.8	1.8	2.2	2.3	2.4	1.7	2.0	1.5	1.3	2.2	2.2	2.1	2.4	2.6	2.7	1.8	1.6	1.9
INM_CM4	0.9	0.9	0.9	1.4	1.3	0.8	0.9	0.8	0.8	1.3	1.1	1.3	0.9	0.9	0.8	1.1	1.2	0.8	0.8	1.0	1.2	1.2	0.8	0.8	0.8	1.2	1.1	1.2
CNRM_CM5	1.8	1.6	1.5	1.5	1.5	1.7	1.8	1.1	1.0	1.6	1.4	1.4	1.6	1.9	2.0	1.4	1.4	1.2	1.1	1.8	1.5	2.0	1.7	1.8	2.0	1.4	1.3	1.4
MPI_ESM_LR	2.2	2.1	2.0	2.3	2.4	1.8	2.2	0.5	1.5	2.4	2.4	2.4	2.1	2.6	2.9	1.6	2.0	1.6	1.5	2.2	2.0	1.9	2.1	2.4	2.7	2.0	1.7	1.8
CCSM4	1.8	1.7	1.6	1.7	1.7	1.7	1.9	1.4	1.1	1.8	1.7	1.7	1.8	2.0	2.0	1.4	1.6	1.3	1.2	1.9	1.8	1.7	1.8	1.9	2.0	1.5	1.3	1.4
Ensemble15	2.2	1.9	1.9	2.0	2.0	1.9	2.2	1.0	1.4	2.2	2.0	2.0	2.0	2.3	2.4	1.7	2.0	1.6	1.5	2.2	2.0	2.1	2.1	2.3	2.4	1.9	1.8	1.8
ACCESS1_0	2.2	2.0	2.0	2.1	2.1	2.8	2.9	0.7	1.6	2.3	2.0	2.0	2.5	2.6	2.6	1.8	2.2	1.7	1.7	2.2	2.0	2.3	2.8	2.8	2.8	2.1	1.9	1.9
HadGEM2_ES	2.3	2.1	2.1	2.2	2.3	2.5	2.7	1.2	1.5	2.5	2.2	2.3	2.6	2.8	2.8	1.9	2.3	1.7	1.6	2.6	2.3	2.6	2.7	2.8	2.9	2.3	2.2	2.2
GFDL_CM3	4.0	3.0	3.0	2.3	2.4	2.6	2.8	1.4	2.1	2.4	2.5	2.4	2.7	3.2	3.3	2.2	2.3	2.3	2.1	2.9	2.5	3.0	2.8	3.0	3.0	2.4	2.4	2.4
CanESM2	3.7	2.7	2.7	2.7	2.6	2.4	2.8	1.4	1.8	2.8	2.7	2.6	2.4	3.0	3.1	2.1	2.5	2.0	1.8	2.8	2.6	2.5	2.5	2.8	2.9	2.4	2.4	2.5
MIROC_ESM	2.0	2.0	2.0	2.6	2.7	2.4	2.9	1.2	1.8	3.1	2.6	2.8	3.2	3.3	3.6	1.8	2.7	1.9	1.9	2.6	2.5	2.4	3.3	3.9	4.7	2.6	2.5	2.4
CSIRO_Mk3_6_0	2.5	2.3	2.4	2.5	2.5	2.2	2.5	1.2	1.7	2.5	2.3	2.4	2.4	2.7	2.8	1.9	2.5	1.8	1.8	2.5	2.3	2.6	2.4	2.6	2.7	2.5	2.4	2.5
IPSL_CM5A_MR	2.6	2.2	2.2	2.1	2.2	2.0	2.2	1.0	1.4	2.4	2.2	2.2	1.9	1.9	2.0	1.8	2.0	1.6	1.5	2.8	2.2	2.6	1.8	1.9	2.1	1.9	1.7	1.8

Fig. 4.5. Temperature and precipitation anomalies for the 2050s, relative to the 1961-1990 normal period predicted by 15 AOGCMs of the CMIP5 model generation, corresponding to the 5th IPPC Assessment Report (AR5). Annual changes are shown for each country, and clusters of grid cells that show similar projected climate change patterns within each country.

Table 1 — Temperature anomalies

Country	PRY			PER			PAN	PRI	TTO	URY	VCT	VEN			VGB	VIR
Region	2	3	4	2	3	4	4	2	1	4	1	1	2	4	2	2
MRI_CGCM3	1.5	1.3	1.1	1.4	1.5	1.4	1.3	1.1	1.2	0.9	1.2	1.2	1.4	1.6	1.1	1.0
MIROC5	1.6	1.5	1.1	1.9	1.9	1.8	1.5	1.6	1.6	0.9	1.5	2.0	1.9	1.8	1.6	1.5
GISS_E2R	1.1	0.8	0.4	1.7	1.8	1.6	1.3	1.1	1.1	0.4	1.1	1.4	1.6	1.7	1.1	1.1
CESM1_CAM5	2.2	1.9	1.8	2.4	2.2	2.1	1.6	1.4	1.4	1.6	1.3	2.2	2.3	2.3	1.4	1.3
INM_CM4	1.7	1.7	1.6	1.0	1.1	1.1	0.9	0.8	0.8	1.4	0.8	1.1	1.1	1.0	0.8	0.8
CNRM_CM5	2.0	1.9	1.9	1.9	2.1	1.6	1.2	1.1	1.2	1.3	1.1	1.6	1.7	1.7	1.1	1.0
MPI_ESM_LR	2.7	2.6	2.3	2.3	2.4	2.2	1.8	1.6	1.5	1.9	1.5	2.2	2.7	2.7	1.6	1.6
CCSM4	2.2	2.0	1.9	2.0	1.9	1.7	1.3	1.2	1.2	1.7	1.2	1.7	1.9	2.0	1.2	1.2
Ensemble15	2.3	2.2	1.9	2.3	2.2	2.1	1.7	1.5	1.6	1.5	1.5	2.0	2.2	2.3	1.5	1.4
ACCESS1_0	1.7	1.8	1.7	2.3	2.2	2.1	1.8	1.6	1.8	1.3	1.7	2.3	2.3	2.4	1.6	1.5
HadGEM2_ES	1.9	2.4	2.3	2.4	2.4	2.2	1.9	1.7	1.7	1.7	1.6	2.4	2.5	2.8	1.7	1.6
GFDL_CM3	3.7	3.5	3.1	4.1	3.4	3.2	2.5	2.1	2.2	2.3	2.1	2.7	3.2	3.3	2.2	2.1
CanESM2	4.1	3.8	3.1	3.9	2.9	3.1	2.4	1.9	2.1	2.0	1.8	2.5	3.3	3.6	1.9	1.9
MIROC_ESM	2.9	2.1	1.7	2.5	2.2	2.1	1.4	1.9	2.2	1.3	1.9	2.4	2.2	2.3	1.9	1.9
CSIRO_Mk3_6_0	2.9	2.7	2.3	3.1	2.9	2.7	2.1	1.7	1.8	1.6	1.8	2.4	2.8	2.9	1.7	1.7
IPSL_CM5A_MR	2.6	2.7	2.7	2.4	2.6	2.3	1.7	1.5	1.8	2.1	1.6	2.1	2.1	2.5	1.5	1.4

Table 2 — Precipitation anomalies

Country	ATG	ARG				BHS	BLZ	BOL			BRA				CHL				COL			CRI		CUB		DOM
Region	1	1	2	3	4	3	2	1	2	3	1	2	3	4	1	2	3	4	2	3	4	2	4	2	3	2
MRI_CGCM3	21	-3	6	14	9	7	1	-11	3	3	-2	-1	4	8	-2	24	9	3	2	1	28	8	9	-1	7	-14
MIROC5	-1	-9	-8	3	6	1	-3	-1	2	0	-1	1	3	7	-11	-13	1	-8	9	5	8	24	26	-6	-2	3
GISS_E2R	-5	-2	12	14	25	-3	0	-1	3	0	3	-6	0	13	-4	7	8	18	-5	-2	-4	-7	-1	-4	-3	-3
CESM1_CAM5	-14	-1	6	9	10	-13	-10	5	4	8	-17	-1	4	5	-6	-9	-4	-4	0	7	3	-11	-9	-11	-12	-14
INM_CM4	-13	-1	8	-1	9	-1	-24	6	0	0	6	2	2	5	-1	20	12	-19	1	-2	-1	-15	-13	-7	-6	-10
CNRM_CM5	-7	6	2	-1	7	5	-4	5	4	4	-5	0	0	3	2	10	25	24	1	0	5	-4	-5	2	2	-6
MPI_ESM_LR	-21	-6	-11	-1	4	2	-12	-14	0	-3	-38	-4	7	3	-13	-22	-8	-18	4	10	10	7	5	-2	-2	-11
CCSM4	-28	0	3	4	7	-11	-18	1	0	3	-7	-3	-1	3	-6	-7	-1	-5	-2	8	0	-18	-14	-15	-13	-21
Ensemble15	-7	-5	-3	2	7	-1	-5	-4	-3	0	-8	-3	4	6	-8	-10	2	4	-2	2	5	-2	0	-4	-3	-8
ACCESS1_0	0	-10	-9	5	3	12	-4	5	1	6	-24	-2	4	13	-11	-7	-1	-4	-1	2	1	7	4	4	7	-7
HadGEM2_ES	-16	-6	-5	2	2	2	-11	18	-3	6	-15	0	3	9	-4	-6	3	23	0	8	5	2	9	-3	-5	-13
GFDL_CM3	2	-10	-7	-2	3	0	20	-3	-16	-6	-14	-16	-13	-6	-14	-31	-7	0	-12	-3	-3	11	11	4	5	2
CanESM2	-29	-7	-3	-6	2	-8	-22	27	-22	8	-50	-34	-23	-12	-11	-16	12	44	-34	-7	-25	-25	-14	-20	-12	-37
MIROC_ESM	13	-7	-13	-1	1	7	44	-18	-12	-9	1	-8	-5	0	-14	-35	-13	-28	3	-3	9	26	26	18	10	23
CSIRO_Mk3_6_0	-3	-9	-15	-5	4	3	-15	-53	-6	-23	-23	-12	-11	-1	-16	-24	-15	-9	-12	2	-7	-14	-5	2	1	1
IPSL_CM5A_MR	-11	-14	-8	-4	8	-13	-27	-30	-10	6	48	24	74	32	-23	-48	10	9	7	5	37	-28	-27	-25	-18	-21

Figure 4.5 (continued). Temperature and precipitation anomalies for the 2050s, relative to the 1961-1990 normal period predicted by 15 AOGCMs of the CMIP5 model generation, corresponding to the 5th IPPC Assessment Report (AR5). Annual changes are shown for each country, and clusters of grid cells that show similar projected climate change patterns within each country.

Table 1

Country	ECU			SLV		GUF		FLK	GLP	GTM			GUY			HTI	HND	JAM	MTQ	MEX			SUR			NIC		
Region	2	3	4	2	4	1	2	3	1	2	3	4	1	2	3	2	2	2	1	1	2	3	1	2	3	2	3	4
MRI_CGCM3	15	11	22	7	7	3	2	-4	28	1	5	5	9	16	8	-12	7	1	31	-3	-1	-7	8	9	6	1	-2	8
MIROC5	6	14	35	0	0	-4	4	-2	-3	-6	3	0	-9	-5	-2	6	6	5	-7	-3	-4	-10	-3	2	4	17	22	25
GISS_E2R	-8	2	5	-21	-19	4	-3	-5	-4	-4	-5	-12	5	-5	-4	-9	-8	-6	-1	-8	0	-4	1	-8	-8	-7	-1	-5
CESM1_CAM5	-7	3	9	-11	-11	-20	-23	1	-15	-11	-5	-10	-18	-11	-8	-15	-12	-7	-16	-3	-6	-2	-19	-19	-16	-11	-10	-12
INM_CM4	3	2	-1	-15	-15	2	5	-1	-15	-18	-16	-15	-4	-2	0	-9	-20	-7	-16	-4	-16	4	0	3	3	-19	-13	-15
CNRM_CM5	5	3	10	40	170	-8	-5	4	-7	1	23	188	-9	-8	-7	-6	2	1	-7	11	-6	50	-7	-6	-5	-3	-3	-4
MPI_ESM_LR	12	17	33	-3	1	-42	-40	-2	-23	-7	4	5	-39	-29	-28	-11	-9	-10	-21	-5	-7	5	-43	-40	-35	-1	7	9
CCSM4	-2	2	4	-20	-19	-10	-8	0	-29	-14	-7	-16	-15	-8	-6	-23	-19	-18	-30	-5	-11	0	-10	-8	-6	-22	-20	-17
Ensemble15	-1	5	15	-1	7	-13	-8	-1	-7	-4	1	10	-12	2	4	-7	-3	-3	-7	-2	-5	2	-10	-6	-2	-3	-1	-2
ACCESS1_0	3	6	23	1	1	-34	-21	-3	1	2	6	2	-25	-11	-7	-2	-2	-1	1	9	6	-2	-27	-17	-11	0	0	2
HadGEM2_ES	2	11	24	6	1	-20	-10	0	-16	-7	4	1	-18	2	2	-6	-4	2	-14	0	-7	5	-14	-4	-1	0	-3	-4
GFDL_CM3	-15	-7	1	19	13	-18	-16	-1	-1	15	10	13	-14	-6	-8	4	24	-1	-5	-2	7	-1	-16	-14	-10	27	9	11
CanESM2	-22	-6	4	-38	-35	-39	-49	-2	-33	-25	-20	-28	-25	-36	-43	-39	-25	-20	-37	-1	-14	-3	-31	-34	-34	-22	-17	-23
MIROC_ESM	1	1	12	40	37	-7	3	3	15	47	38	40	-4	4	12	21	44	21	13	9	28	3	0	8	14	31	35	31
CSIRO_Mk3_6_0	-1	11	25	-13	-11	-20	-24	0	2	-13	-7	-8	-27	-28	-22	-2	-17	4	1	-3	-10	-6	-22	-22	-19	-21	-3	-11
IPSL_CM5A_MR	-7	7	5	-14	-17	12	50	-4	-9	-29	-24	-17	13	143	162	-21	-19	-21	-14	-26	-29	-11	27	58	85	-19	-18	-27

Table 2

Country	PRY			PER			PAN	PRI	TTO	URY	VCT	VEN			VGB	VIR
Region	2	3	4	2	3	4	4	2	1	4	1	1	2	4	2	2
MRI_CGCM3	7	8	14	6	11	18	7	-5	4	9	10	17	38	29	-3	0
MIROC5	5	9	13	11	12	14	22	3	-16	5	-9	-4	2	3	5	4
GISS_E2R	9	18	27	0	-2	-4	11	-4	5	15	0	-5	-12	-9	-5	-4
CESM1_CAM5	9	8	10	1	12	7	0	-12	-16	5	-18	-16	-7	-5	-11	-12
INM_CM4	-3	0	3	4	8	12	-5	-10	-11	8	-15	-12	-10	-2	-9	-10
CNRM_CM5	2	1	-1	4	30	18	3	-6	-4	10	-6	-6	-2	6	-6	-6
MPI_ESM_LR	-8	0	7	4	3	11	9	-13	-39	10	-26	-32	-12	2	-13	-14
CCSM4	-2	1	4	1	4	4	-5	-24	-26	5	-31	-17	-12	-14	-23	-24
Ensemble15	-2	1	6	-1	7	9	5	-7	-15	7	-11	-12	-4	11	-7	-7
ACCESS1_0	2	9	20	2	3	-1	10	-5	-4	10	2	-17	-8	-4	-4	-4
HadGEM2_ES	-5	-2	9	1	13	15	11	-14	-18	8	-18	-13	-4	2	-12	-14
GFDL_CM3	-10	-10	-6	-16	-5	2	8	0	-18	-2	-7	-12	0	2	1	1
CanESM2	-24	-15	-7	-35	4	4	0	-29	-36	5	-44	-34	-43	-31	-23	-27
MIROC_ESM	-16	-3	5	1	3	6	16	23	-9	0	4	5	12	11	18	18
CSIRO_Mk3_6_0	-6	-3	1	-7	-7	-4	-1	-4	-27	3	-3	-32	-18	-10	-7	-5
IPSL_CM5A_MR	-3	0	-2	-2	10	16	-15	-15	-21	18	-15	-5	4	177	-13	-14

Figure 4.5 (continued). Temperature and precipitation anomalies for the 2050s, relative to the 1961-1990 normal period predicted by 15 AOGCMs of the CMIP5 model generation, corresponding to the 5th IPPC Assessment Report (AR5). Annual changes are shown for each country, and clusters of grid cells that show similar projected climate change patterns within each country.

4.5. Conclusions

The database and software front-end, ClimateSA that we developed in this study allows easy access by non-experts to a comprehensive set of historical and predicted climate variables such as growing degree days, frost-free periods, heating and cooling degree days, and drought indices. Temporal coverage includes monthly and annual data from 1901-2010, as well as decadal averages and 30-year climate normal periods between 1901-2010. Beside historical data, ClimateSA provides the same monthly, seasonal and annual variables for three future 30-year climate normals (2020s, 2050s, and 2080s) and two emission scenarios (RCP 4.5 and RCP 8.5) for 15 selected AOGCMs and an average ensemble projection. Users can query the database interactively for any location within Latin America, or develop gridded climate surfaces at any desired resolution, projection, and extent based on a digital elevation model.

Because it is quite straight forward to generate climate data at any resolution, including very high resolution local surfaces, we should note some important limitations of the database. Precipitation variables, including topographically-driven precipitation patterns, such as orographic lift and rain shadows, are modeled at a resolution of 2.5 arcminutes (approx. 4km). Any downscaling performed by the software to higher resolution is based on simple bi-linear interpolation and does not yield more accurate local estimates than a coarser 2.5 arcminute grid. Temperature variables, on the other hand, can be downscaled to much higher resolution using empirical lapse-rate formulas. Accuracy of estimates in steep, mountainous terrain can yield significant improvements up to a resolution of approximately 10 arcseconds (approx. 250m), while areas without significant topography are usually well characterized at 2.5 arcminutes (approx. 4km). For research that requires climate data with continental or sub-continental extent, we recommend a resolution of about 30 arcseconds (approx. 750m, depending on the latitude).

Sample-based research, and research that requires both high spatial and temporal resolution should benefit from the estimates provided by the ClimateSA software. Examples may include historical biology research, where the inter-annual climate variation is linked to a biological response recorded at monthly or annual timescales (e.g. dendroclimatology research, studies of plant phenology, or research on changes in the timing of animal behaviour, such as arrival and departure of migrating birds or insects). While the required time-series data can easily be generated, we should remind users that all estimates are ultimately based on standard weather station data, and consequently local microclimate effects that are driven by vegetation, slope or aspect beyond a resolution of 2.5 arcminutes are not accounted for. Only lapse-rate based temperature changes along elevation gradients are incorporated at resolutions finer than 2.5 arcminutes. Furthermore, historical estimates of time series data may have limited accuracy, specifically for monthly precipitation as quantified in Fig 4.2, with mean absolute errors of 25% of the total precipitation values for individual months of individual years.

The database and software is freely available from the website http://tinyurl.com/ClimateSA, and the software and database version corresponding to this paper have also been archived on the open-access repository Zenodo.org (links will be activated when this manuscript has undergone peer-review).

4.6. References

Alkimim, A., G. Sparovek, and K. C. Clarke. 2015. Converting Brazil's pastures to cropland: an alternative way to meet sugarcane demand and to spare forestlands. Applied Geography **62**:75-84.

Arguez, A., and R. S. Vose. 2011. The definition of the standard WMO climate normal: the key to deriving alternative climate normals. Bulletin of the American Meteorological Society **92**:699-U345.

Becker, A., P. Finger, A. Meyer-Christoffer, B. Rudolf, K. Schamm, U. Schneider, and M. Ziese. 2013. A description of the global land-surface precipitation data products of the Global Precipitation Climatology Centre with sample applications including centennial (trend) analysis from 1901–present. Earth System Science Data **5**:71-99.

Chen, W. L., Z. H. Jiang, and L. Li. 2011. Probabilistic Projections of Climate Change over China under the SRES A1B Scenario Using 28 AOGCMs. Journal of Climate **24**:4741-4756.

Daly, C. 2006. Guidelines for assessing the suitability of spatial climate data sets. International Journal of Climatology **26**:707-721.

Daly, C., M. Halbleib, J. I. Smith, W. P. Gibson, M. K. Doggett, G. H. Taylor, J. Curtis, and P. P. Pasteris. 2008. Physiographically sensitive mapping of climatological temperature and precipitation across the conterminous United States. International Journal of Climatology **28**:2031-2064.

Fasullo, J. T., and K. E. Trenberth. 2012. A Less Cloudy Future: The Role of Subtropical Subsidence in Climate Sensitivity. Science **338**:792-794.

Fick, S. E., and R. J. Hijmans. 2017. WorldClim 2: new 1-km spatial resolution climate surfaces for global land areas. International Journal of Climatology **37**:4302-4315.

Gleckler, P. J., K. E. Taylor, and C. Doutriaux. 2008. Performance metrics for climate models. Journal of Geophysical Research-Atmospheres **113**.

Hamann, A., and T. L. Wang. 2005. Models of climatic normals for genecology and climate change studies in British Columbia. Agricultural and Forest Meteorology **128**:211-221.

Harris, I., P. D. Jones, T. J. Osborn, and D. H. Lister. 2014. Updated high-resolution grids of monthly climatic observations – the CRU TS3.10 Dataset. International Journal of Climatology **34**:623-642.

Hijmans, R. J., S. E. Cameron, J. L. Parra, P. G. Jones, and A. Jarvis. 2005. Very high resolution interpolated climate surfaces for global land areas. International Journal of Climatology **25**:1965-1978.

Knutti, R., D. Masson, and A. Gettelman. 2013. Climate model genealogy: Generation CMIP5 and how we got there. Geophysical Research Letters **40**:1194-1199.

Lawrimore, J. H., M. J. Menne, B. E. Gleason, C. N. Williams, D. B. Wuertz, R. S. Vose, and J. Rennie. 2011. An overview of the Global Historical Climatology Network monthly mean temperature data set, version 3. Journal of Geophysical Research: Atmospheres **116**:D19121. doi:19110.11029/12011JD016187.

Mbogga, M. S., A. Hamann, and T. Wang. 2009. Historical and projected climate data for natural resource management in western Canada. Agricultural and Forest Meteorology **149**:881-890.

Mbogga, M. S., X. Wang, and A. Hamann. 2010. Bioclimate envelope model predictions for natural resource management: dealing with uncertainty. Journal of Applied Ecology **47**:731-740.

Menne, M. J., I. Durre, R. S. Vose, B. E. Gleason, and T. G. Houston. 2012. An overview of the Global Historical Climatology Network-Daily database. Journal of Atmospheric and Oceanic Technology **29**:897-910.

Mitchell, T. D., and P. D. Jones. 2005. An improved method of constructing a database of monthly climate observations and associated high-resolution grids. International Journal of Climatology **25**:693-712.

New, M., M. Todd, M. Hulme, and P. Jones. 2001. Precipitation measurements and trends in the twentieth century. International Journal of Climatology **21**:1899-1922.

Paritsis, J., and T. T. Veblen. 2011. Dendroecological analysis of defoliator outbreaks on *Nothofagus pumilio* and their relation to climate variability in the Patagonian Andes. Global Change Biology **17**:239-253.

Peterson, T. C., and R. S. Vose. 1997. An Overview of the Global Historical Climatology Network Temperature Database. Bulletin of the American Meteorological Society **78**:2837-2849.

Ramirez-Villegas, J., F. Cuesta, C. Devenish, M. Peralvo, A. Jarvis, and C. A. Arnillas. 2014. Using species distributions models for designing conservation strategies of Tropical Andean biodiversity under climate change. Journal for Nature Conservation **22**:391-404.

Rogelj, J., M. Meinshausen, and R. Knutti. 2012. Global warming under old and new scenarios using IPCC climate sensitivity range estimates. Nature Climate Change **2**:248-253.

Sarkinen, T., P. Gonzales, and S. Knapp. 2013. Distribution models and species discovery: the story of a new Solanum species from the Peruvian Andes. Phytokeys **31**:1-20.

Scherrer, S. C. 2011. Present-day interannual variability of surface climate in CMIP3 models and its relation to future warming. International Journal of Climatology **31**:1518-1529.

Suarez, M., R. Villalba, I. Mundo, and N. Schroeder. 2015. Sensitivity of *Nothofagus dombeyi* tree growth to climate changes along a precipitation gradient in northern Patagonia, Argentina. Trees **29**:1053-1067.

Swetnam, T. W., C. D. Allen, and J. L. Betancourt. 1999. Applied historical ecology: Using the past to manage for the future. Ecological Applications **9**:1189-1206.

Team, R. D. C. 2016. R: A language and environment for statistical computing. R Foundation for Statistical Computing, Vienna, Austria. URL https://www.R-project.org/.

Vaughn, D. 2005. Degree Days. Pages 315-318 *in* J. Oliver, editor. Encyclopedia of World Climatology. Springer Netherlands, Dordretch Netherlands.

Walsh, J. E., W. L. Chapman, V. Romanovsky, J. H. Christensen, and M. Stendel. 2008. Global Climate Model Performance over Alaska and Greenland. Journal of Climate **21**:6156-6174.

Wang, M. Y., J. E. Overland, V. Kattsov, J. E. Walsh, X. D. Zhang, and T. Pavlova. 2007. Intrinsic versus forced variation in coupled climate model simulations over the Arctic during the twentieth century. Journal of Climate **20**:1093-1107.

Wang, T., A. Hamann, D. Spittlehouse, and C. Carroll. 2016. Locally downscaled and spatially customizable climate data for historical and future periods for North America. PLOS ONE **11**:e0156720. DOI: 0156710.0151371/journal.pone.0156720.

Wang, T., A. Hamann, D. L. Spittlehouse, and S. N. Aitken. 2006. Development of scale-free climate data for Western Canada for use in resource management. International Journal of Climatology **26**:383-397.

Wang, T., A. Hamann, D. L. Spittlehouse, and T. Q. Murdock. 2011. ClimateWNA—High-resolution spatial climate data for Western North America. Journal of Applied Meteorology and Climatology **51**:16-29.

Willmott, C. J. 1982. Some comments on the evaluation of model performance. Bulletin of the American Meteorological Society **63**:1309-1313.

Willmott, C. J., and K. Matsuura. 1995. Smart interpolation of annually averaged air temperature in the United States. Journal of Applied Meteorology **34**:2577-2586.

Willmott, C. J., and S. M. Robeson. 1995. Climatologically aided interpolation (CAI) of terrestrial air temperature. International Journal of Climatology **15**:221-229.

Chapter 5. Climate-based seed zones for Mexico: guiding reforestation under observed and projected climate change

5.1. Summary

Seed zones for forest tree species are a widely used tool in reforestation programs to ensure that seedlings are well adapted to their planting environments. Here, we propose a climate-based seed zone system for Mexico to address observed and projected climate change. The proposed seed zone classification is based on bands of climate variables often related to genetic adaptation of tree species, mean coldest month temperature (MCMT) and an aridity index (AHM). The overlay of the MCMT and AHM for the 1961-1990 period resulted in 63 climate-based zones. Climate change observed over the last three decades has resulted in an increase of +0.74 °C for MCMT and a shift toward overall drier conditions across Mexico. By the 2050s, MCMT is expected to increase by +1.7 °C and AHM shifts further towards drier conditions. We recommend moving seed sources from warm, dry locations towards currently wetter and cooler planting sites, to compensate for climate change that has already occurred and is expected to continue for the next decades. We contribute a straight-forward climate-based seed zone system that allows practitioners to match seed procurement regions with planting regions under observed and anticipated climate change. Our transfer recommendations using climate-based zones can be implemented within the existing seed zone system, which often span large climate gradients.

5.2. Introduction

Numerous common garden studies indicate that forest tree populations are fundamentally adapted through natural selection to their local climates, primarily cold temperatures and aridity (St Clair et al. 2005, St. Clair 2006, Chmura et al. 2011, Vizcaíno-Palomar et al. 2017). Seed zone delineation for forest tree species is essential to guide where seed may be collected and where corresponding planting stock may be deployed in reforestation programs (either for ecological restoration or commercial plantations), in order to appropriately match locally adapted genotypes to their corresponding environments (Johnson et al. 2004, Dutkowski et al. 2016). Such tasks have become more complicated due to climatic change (Aitken et al. 2008, Castellanos-Acuña et al. 2015, Dumroese et al. 2015).

Seed zones for important commercial forest trees in the United States and Canada are based to some degree on genetic testing using common garden studies and various methodological approaches to delineate seed zones or breeding regions of similarly adapted genotypes (Ying and Yanchuk 2006, Hamann et al. 2011). An alternative approach to manage seed movement is to indicate a maximum climatic or geographic transfer distance between the seed origin and the planting site (Rehfeldt 1988, Parker 1992, Lesser and Parker 2006). Ideally, both delineation of locally adapted populations and population transfer guidelines are based on knowledge from reciprocal provenance trial series that test genotypes over multiple environments (Taïbi et al. 2014, Benito-Garzón and Fernández-Manjarrés 2015). Such data, however, are only available for a few important tree species, and typically only for the portions of their natural range where commercial forestry operations take place.

For all other species, where only a few genecology studies or provenance trials are available to estimate genetic population differentiation, or where long-term field trials are lacking,

reforestation is guided by proxy information (Potter and Hargrove 2012). Because forest trees are normally adapted to landscape-scale climatic and physiogeographic features, seed zone delineations are often first drawn based on ecosystem delineations or administrative boundaries, and later refined as genetic information from long-term provenance trials becomes available (Morgenstern 1996, Ying and Yanchuk 2006). More recently, provisional seed zones have been based on macro-climatic regions rather than ecosystem delineations (Potter and Hargrove 2012). The rationale for this change is that climatic regions can be re-drawn under observed and projected climate change to match genotypes to new environmental conditions. Examples of climate-based seed zones include delineations that largely reflect climatic gradients in minimum temperature and precipitation for the United States (Bower et al. 2014), minimum temperatures in Canada, where this climate aspect is of overwhelming importance (McKenney et al. 2001), or multivariate techniques that translate ecosystem delineations to climatic zones (Gray and Hamann 2011, Potter and Hargrove 2012).

In Mexico, there are still few long term common garden experiments for a limited number of species that would allow the delineation of individual seed zones (Hodge and Dvorak 2014), and current seed zones are largely based on physiographic provinces and sub-provinces (CONAFOR 2014). Seeds are normally collected in natural stands (seed orchards in general are not available) and deployed in most cases within the natural range of the species although not necessarily within the same seed zone. In some cases, planting stock production is based on seed collections in adjacent zones because seed production facilities are limited even for the main tree species. Although physiographic provinces and sub-provinces reflect climatic gradients to some degree, the current zonation (CONAFOR 2014) may include large climatic differences in elevation even within the finest classification.

Here, we propose an alternative climate-based provisional seed zone delineation for Mexico, based on overlapping GIS layers of minimum temperature and an aridity index, similar to a zonation developed for native plants in the United States (Bower et al. 2014). Taking advantage of the capability of climate-based seed zones to be re-drawn under climate change scenarios, we evaluate the changes in the spatial extent of these zones under climate change observed over the last three decades as well as under climate change projections for the 2050s, aiming to provide foresters with a perspective of how seed source and planting regions have already shifted with respect to their climate conditions, and may further shift in the medium-term future in a forestry planning context.

5.3. Methods

We followed the methodology of Bower et al. (2014) to delineate seed zones as areas of similar climate based on mean coldest month temperature (MCMT) and annual heat:moisture index (AHM), a measure of aridity that is calculated as (mean annual temperature+10)/(mean annual precipitation/1000) (Rehfeldt et al. 1999). Cold temperature tends to be an important driver of genetic differentiation even in sub-tropical regions (Morgenstern 1996, Gapare et al. 2015), and Mexico's main forestry regions in the Sierra Madre and the Volcanic Belt regions experience frost conditions in the winter months. Annual heat:moisture index is indicative of evapotranspirative demand, a variable that governs tree growth under limited moisture conditions. Temperature and water availability are often largely independent, i.e., for many landscapes we have all combinations of dry/wet and cool/warm climates. In combination, minimum temperatures and water availability have proven useful to explain both the genetic differentiation among trees populations and the phenotypic plasticity of tree populations in response to climate (Saenz-Romero et al. 2017).

For climatic characterization that largely predates anthropogenic climate change, we used a reference period (the 1961-1990 climate normal) to represent climate to which forest tree populations are putatively adapted. The period was chosen because it largely predates a strong anthropogenic warming signal and has good weather station coverage. We use intervals of 3°C for MCMT and intervals of AHM that are approximately equal width under a log-transformation, rounded to the nearest unit of five, and open-ended for the highest and lowest values. An approximate log-scaling is useful for variables related to water availability that have a skewed distribution, so that not too many intervals are used to classify a very small portion of the study area. We should note that depending on the size of the study area, one may choose larger or smaller intervals. This would not qualitatively influence the results of climate region shifts. For Mexico, the intervals we selected allow for a good visualization of climate regions at the full scale of the study area as well as for more local visualizations. In total, we have ten classes of MCMT that were intersected with seven classes of AHM to represent 70 potential seed zones for Mexico. The data for these climate variables for Mexico was obtained from interpolated climate data for North America (Wang et al. 2016) that is publicly available (*http://tinyurl.com/ClimateNA*).

We repeated the zoning process, using the same MCMT and AHM interval values, but using as input climate projections for the 2041-2070 period (hereafter referred to as 2050s), using an average ensemble projection across 15 CMIP5 models (CanESM2, ACCESS1.0, IPSL-CM5A-MR, MIROC5, MPI-ESM-LR, CCSM4, HadGEM2-ES, CNRM-CM5, CSIRO Mk 3.6, GFDL-CM3, INM-CM4, MRI-CGCM3, MIROC-ESM, CESM1-CAM5, GISS-E2R). The models were implemented under two Representative Concentration Pathways (RCP) of radiative forcing due to greenhouse gasses: 4.5 watts/m^2 (resulting in approximately 2°C warming in global temperature by the end of the century) and 8.5 watts/m^2 (approximately 4 ºC warming). The projected climate data are based on the delta method, overlaying an ensemble of CMIP5 climate change projections for the 2050s on the high-resolution 1961-1990 reference period, described in detail by (Wang et al. 2016), also publicly available (*http://tinyurl.com/ClimateNA*).

To show the climate change over the last approximately 30 years, we calculate the difference between the 1961-1990 normal reference period and an average climate for the 1991-2015 (25 years, rather than a 30 year normal period). We used the updated CRU-TS 3.22 dataset (Harris et al. 2014) originally developed by Mitchell and Jones (2005), to calculate a medium spatial resolution (0.5°) anomaly layer between the two periods, which was subsequently overlaid on the high resolution 1961-1990 reference layers described above, using the delta method as well. The mid-point of the two periods are 1975 and 2003, thus it represents 28 years of observed climate change. Our chosen future projection (2050s) represents another approximately 50 years of climate warming relative to the midpoint of the 1991-2015 period.

We overlaid the (CONAFOR 2014) regions and subregions and the Level III ecoregions of Omernik and Griffith (2014). The comparison with CONAFOR regions and subregions allows us to evaluate differences to the current approach to guiding seed movement in México's reforestation programs, and to make recommendations about how the climate-based seed transfer might complement the current system. The comparison with the Level III ecoregion classification system allows us to evaluate the ecological relevance of the climate variables that we have chosen for our climate-based seed zone delineations.

5.4. Results & Discussion

5.4.1. Climate-based seed zone delineations

Maps of mean coldest month temperature (MCMT) and annual heat moisture index (AHM) show relatively independent geographic distributions throughout Mexico (Fig 5.1). MCMT primarily reflects elevational gradients with warm areas on the coasts and colder areas in the mountains along the Mexican Trans-Volcanic Belt, the Sierra Madre Oriental, and the Sierra Madre

Occidental, as well as in the high elevation deserts of the Central-Northwest Plateau in northern Mexico. In contrast, AHM intervals exhibit more complex patterns. Lower elevation areas in the southern areas have low AHM values. Although temperatures are high, high precipitation throughout the year results in an evapotranspiration surplus. The highest moisture surplus occurs on the leeward side of the Sierra Madre Oriental, facing the Gulf of Mexico. Other mountain ranges also show low AHM values with adequate moisture and lower temperatures. High AHM values with an evapotranspiration deficit, on the other hand, are found at low elevation areas around the Gulf of California and in the central and northern interior plateaus of Mexico in the rainshadow of the Sierra Madre Occidental (Fig. 5.1).
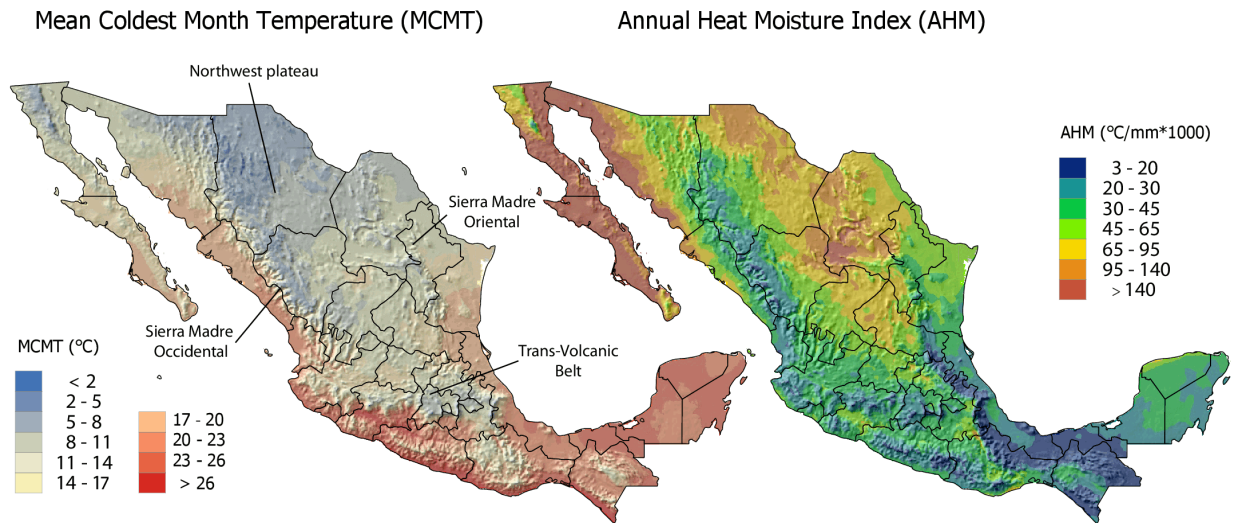
Fig. 5.1. Mean coldest month temperature (MCMT) and annual heat moisture index (AHM) bands. The 10 MCMT bands correspond to 2.8 ºC intervals (except for those containing lowest and upper extreme values; map labels rounded to 3 ºC for simplicity). AHM was calculated as mean annual temperature (MAT, ºC) plus 10 ºC (to obtain positive values) divided by mean annual precipitation in meters.

The overlay of the MCMT and AHM classification bands resulted in 63 seed zones in Mexico (of a potential of 70 zones) (Fig 5.2). Of those, 32 bands are present on at least 1% of the total land area (color codes highlighted with bold rectangles in the legend of Fig 5.2). Most of the

small or missing zones belong to the extreme ranges of environmental conditions (very cold or very dry), and have been omitted from the legend for Fig 5.2.

A visual comparison of climate-based zones and ecological zones shows a fairly high correspondence. For example, in Panel A of Fig. 5.2, dark blue colors coincide with the conifer forests dominated by *Abies religiosa* (a high altitude conifer) in the Monarch Butterfly Biosphere Reserve (Ramírez et al. 2003, Tucker 2004, Saenz-Romero et al. 2012). Panel B of Fig. 5.2 accurately reflects the ecosystem transitions from the high altitude conifer forest on the Sierra Madre Oriental (dark blue) and the pine-oak forest of the Sierra Norte of Oaxaca (dark green and light blue) to the humid, warm tropical areas on slopes facing the Gulf of Mexico (orange and reddish colors) (Castellanos-Bolaños et al. 2010, Sáenz-Romero et al. 2010, Zacarías-Eslava and Castillo 2010). In the northwestern portion of the country, purple and blue colors, accurately represent coniferous forests where (at the border between Chihuahua and Durango states) spruce occurs (Ledig et al. 2000, Ledig et al. 2010).

Climate-based seed zones (1961-1990 reference climate)

AHM	MCMT								
	2-5	5-8	8-11	11-14	14-17	17-20	20-23	23-26	>26
2 - 20	21	31	41	51	61	71	81	91	101
20 - 30	22	32	42	52	62	72	82	92	102
30 - 45	23	33	43	53	63	73	83	93	103
45 - 65	24	34	44	54	64	74	84	94	104
65 - 95	25	35	45	55	65	75	85	95	105
95 - 140	26	36	46	56	66	76	86	96	106
>140	27	37	47	57	67	77	87	97	107
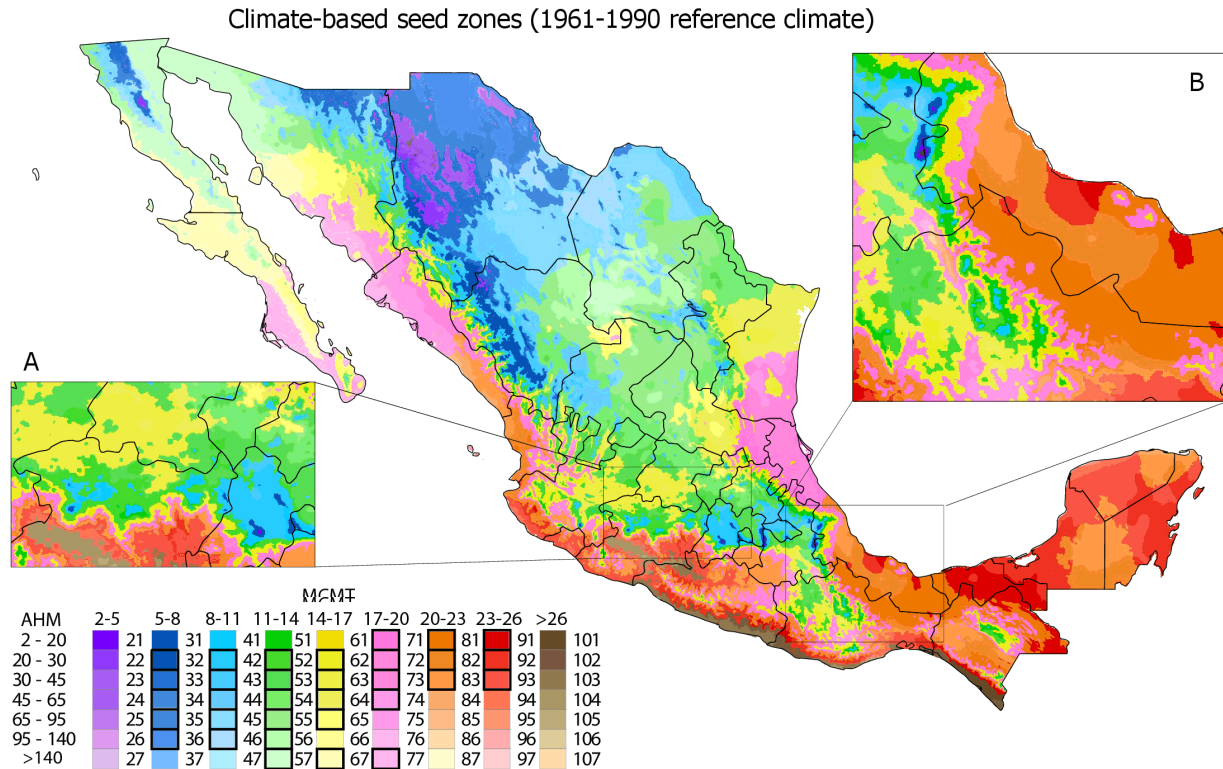
Fig. 5.2. Proposed climate-based seed zones for México, based on intervals of the variable mean temperature of the coldest month (columns in the legend) and on seven aridity index intervals (rows). Boxes with thick lines in the color legend are seed zones that represent at least 1% of the land area. The first column of the legend (MCMT of –1 to 2°C) was omitted. Lines indicate state boundaries.

5.4.2. Comparison to ecoregions and CONAFOR seed zones

A comparison with Omernik's Level III ecoregions shows relatively high correspondence to our climate-based zones, indicating that our two-variable method of climate region delineation produces zones that are ecologically relevant (Fig. 5.3). In areas of low topographic complexity the CONAFOR seed zones also track climatic regions reasonably well, e.g. pink and red areas along the coasts (Fig 5.3). However, it appears that CONAFOR subregions are too coarse for areas with high topographic complexity that include high climatic variation related to elevation gradients, as for example CONAFOR zones III.1, III.2 and III.3, that are crossed by Sierra

Madre Occidental. To decrease the risks of an excessive seed movement inside each zone, seed transfer rules for CONAFOR seed zones included a restricted altitudinal movement from the seed source to planting site of no more than 300 m upwards or 150 m downwards to ensure adapted plantations.

Elevation is considered in the delineation of Level III ecoregions (Omernik and Griffith 2014); thus, Level III ecoregions shows a high degree of similarity to our climate-based zones (Fig 5.3). Level III ecoregions could be used as a proxy to our climate-based seed zones for the purpose of collection of seed and deployment of planting stock without additional transfer-rules within seed zones. However, this requires the assumption of constant climate conditions. In other words, the existing zonation systems (CONAFOR and Ecoregions) are not amenable to assisted migration. Climate-based delineations such as those developed in this study allow seed zones to be redrawn using observed climate change and under future climate change projections.
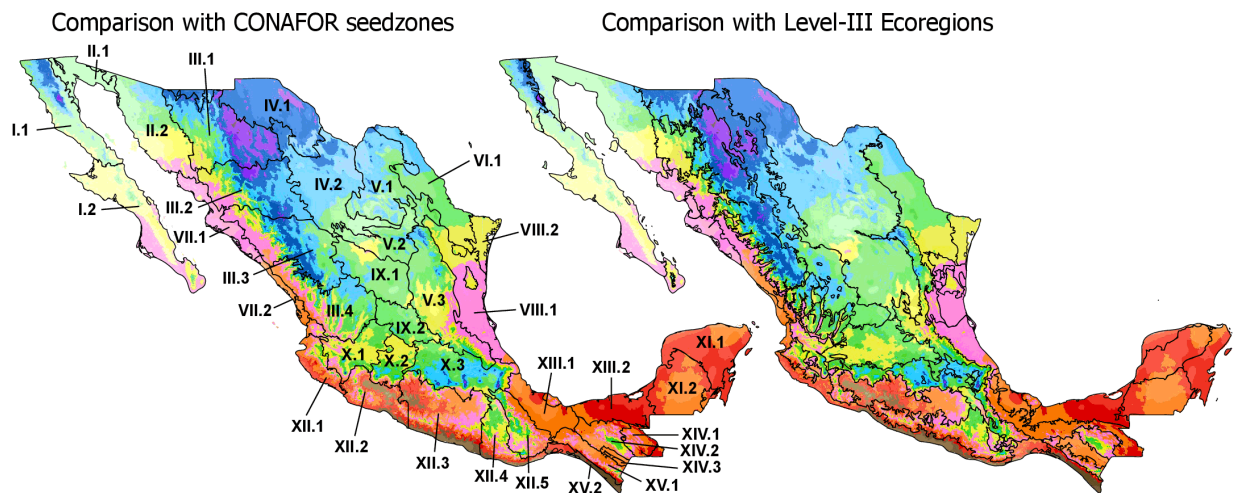
Fig. 5.3. Comparison of CONAFOR regions (left) and Level-III Ecoregions by Omernik and Griffith (right), both indicated by black lines, with the proposed climate-based seed zones for the 1961-1990 climate reference period (indicated by colors as in Fig. 2).

5.4.3. Seed zone shifts under climate change

Mean annual temperature in Mexico has increased 0.66 °C over the last three decades according to our analysis, an estimate consistent with previous analyses (Pavia et al. 2009, Cuervo-Robayo et al. 2014). Estimates for changes in precipitation are more variable among regions. Areas facing the Gulf of Mexico have seen increases in precipitation, while the west coast has seen decreases. Current reforestation programs do not have a mechanism to address these changes. The general approach of these programs is to collect seeds from a given seed zone, produce seedlings in a nursery, and reforest sites within the same zone. Current Mexican rules require that seed sources and planting sites are within the same CONAFOR seed zone. Matching seed sources with new environmental conditions under projected climate change will require a modified approach. Seedlings should be deployed in the same climate-based zone, but they would be re-mapped to account for observed climate change or future climate change projections (Fig. 5.4). In other words, assisted migration could be implemented by collecting seed in current procurement areas (delineated under 1961-1990 climate), and then deploying seedlings in the same climate-based zones although delineated under observed climate trends (1991-2015 climate) or under projected future climate (2050s climate).
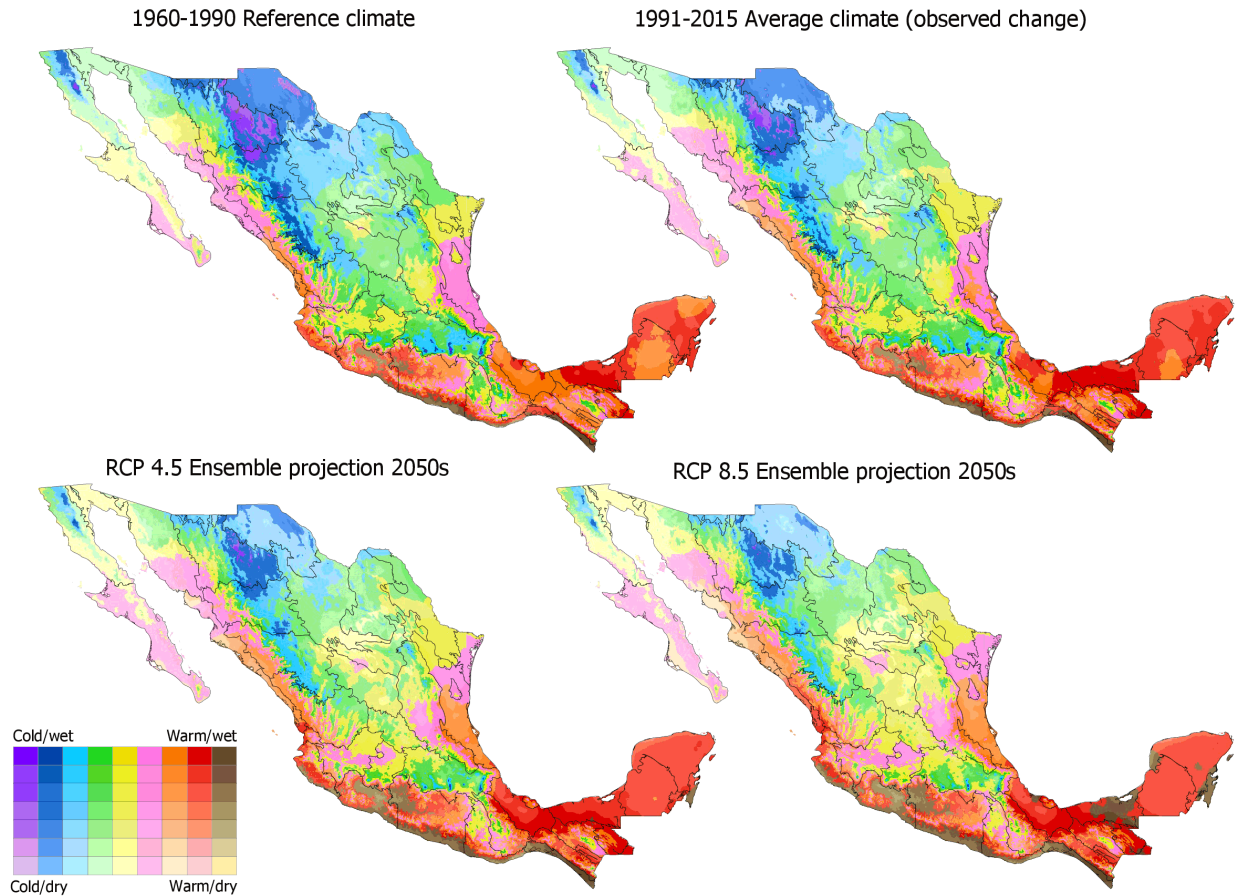
Fig. 5.4. Shift of climatic seedzones under observed and predicted climate change. The CONAFOR regions, indicated by black lines, are included as a reference. The 1991-2015 observed climate average is the result of climate change observed over the last three decades. The bottom row shows climate seed zone shifts for the 2050s under a moderate greenhouse gas forcing scenario (RCP 4.5), and a more pessimistic greenhouse gas emission scenario (RCP 8.5).

With respect to the two variables used for climate-based seed zone delineation, we find that mean coldest month temperature (MCMT) has increased 0.74 °C over the last three decades. For annual heat moisture (AHM), we observe an average +0.09 band shift toward drier conditions across Mexico, where bands refer to AHM intervals shown in Figs. 5.1 and 5.2. For projections for the 2050s, MCMT is predicted to increase by 1.7 °C relative to 1961-1990 reference period, and AHM is predicted to shift by +0.23 intervals for RCP 4.5 projections. For the more pessimistic RCP 8.5 projections, MCMT is predicted to increase by 2.4 °C and AHM is expected to shift 0.33 intervals toward drier conditions, relative to the 1961-1990 reference climate period.

Observed climate change for MCMT over the last three decades (from the mid-point of the 1961-1990 to the mid-point of the 1991-2015 average) represents approximately 44% of the expected climate change by the 2050s for the RCP 4.5 scenario and 31% of the RCP 8.5 scenario relative to the 1961-1990 baseline. Similarly, observed changes in AHM are already equivalent to 39% of the 2050s climate projections. The consistency of the observed trend with future projections suggests that managers should already be moving populations. Collecting seed from locations that are currently warmer and/or drier and moving it to historically cooler and/or wetter climates, would compensate for climate change that has already occurred and is predicted to continue in the future. Such prescriptions may be guided by maps or tables describing regional seed zone shifts (Fig 5.4, Table 5.1). Maps of observed change, as well as projections, show an increase of warmer and drier areas at the expense of colder and more humid areas. In particular, the reduction or disappearance of mountain-top climatic regions can already be observed for the recent time period 1991-2015 compared to the past (Fig. 5.4, loss of dark purple and dark blue regions). An increase in yellow and light blue areas representing the increase of dry and warm conditions across the interior plateau is only moderate for the observed climate but much more prevalent for both 2050s projections.

Changes have not occurred uniformly throughout Mexico. Table 5.1 shows the percent of the land area that has changed to a class of lower or higher for MCMT or AHM for each CONAFOR region. In terms of dryness, CONAFOR regions III, IV, and VI located in the east-facing slopes of the Sierra Occidental and the northern interior plateau show the highest increase in aridity (Table 5.1, column AHM+1). In contrast, the southern CONAFOR regions VIII, XI, and XII see overall more moist conditions (Table 5.1, column AHM–1), due to an increase in the intensity of hurricanes (Kang and Elsner 2015). Observed warming trends are less regionalized. All CONAFOR regions show a moderate change in their area to a class with higher MCMT values

(Table 5.1, MCMT+1). Future projections also show less regionally pronounced differences. For the RCP 4.5 and RCP 8.5 ensemble projection for the 2050s, all CONAFOR regions will experience some level of change towards a class of higher MCMT or AHM values.

Table 5.1. Change in climate bands as defined in Fig 5.2 for mean coldest month temperature (MCMT) and annual heat moisture index (AHM). The values represent the proportion (%) of the area in each seed zone that has changed to a warmer (1) interval or has remained the same (0). Similarly, changes to AHM are indicated towards a wetter (-1) or drier (1) interval (also visualized in Fig. 4). Columns with very low percentage values were omitted.

| CONAFOR | Change of intervals 2000s (observed) | | | | | Change of intervals 2050s (rcp4.5) | | | | Change of intervals 2050s (rcp8.5) | | | |
| | AHM | | | MCMT | | AHM | | MCMT | | AHM | | MCMT | |
	-1	0	1	0	1	0	1	0	1	0	1	0	1
I	1	92	7	59	40	96	4	35	65	89	11	13	87
II	0	82	18	70	30	89	11	28	72	77	23	4	96
III	0	76	24	68	32	73	27	34	66	54	46	6	94
IV	0	80	20	74	26	74	26	25	75	64	36	2	98
V	4	85	11	74	23	77	23	33	67	70	30	7	93
VI	0	71	29	42	58	83	17	31	69	74	26	5	95
VII	0	85	14	64	35	85	14	46	54	74	26	4	96
VIII	11	87	2	72	28	82	18	36	64	75	25	12	88
IX	0	92	8	89	9	72	28	35	65	63	37	6	94
X	1	87	12	86	14	70	30	35	65	62	38	10	90
XI	12	87	0	70	30	65	35	59	41	58	42	50	50
XII	9	88	3	90	10	76	24	41	59	69	31	21	79
XIII	5	95	0	71	29	76	24	50	50	69	31	21	79
XIV	5	95	0	62	38	87	13	37	63	87	13	19	81
XV	7	91	1	69	31	81	19	39	61	79	21	28	75

5.4.4. Applications and recommendations

Given the concordance of observed and projected climate change towards warmer and drier conditions, we propose that the movement of locally adapted seeds and seedlings towards colder

and wetter environments than their origins would be justified and in fact likely required to ensure good survival and growth of the deployed seedlings on the coming decades (Aitken et al. 2008, Dumroese et al. 2015, Potter et al. 2017). For the climate variables used in this study, we have already experienced approximately 37% of the climate change (over three decades) that is on average projected for the 2050s (over eight decades) relative to the 1961-1990 reference period. Thus, the rate of observed climate change over 30 years is almost exactly the proportion of change that would be expected based on 2050s projections, namely 0.25 °C per decade. Given the long growing period of tree plantations, it seems prudent to start moving seed sources to compensate for climate change that has already occurred.

Current CONAFOR seed zones are meant to ensure adaptation of planting stock by preventing seed movement across climates that are too dissimilar. However, current guidelines allow some flexibility for forest managers to address observed and projected climate change by implementing the climate-based seed zones we propose here. For example, seed sources for planting in the dark blue areas in seed zone VI.1 could come from the light blue regions further south within the same seed zone (Fig 5.5A, left panel). This choice would be guided by projections of the light blue climate-based seed zone under predicted climate change (Fig 5.5A, right panel). Similarly, seed sources for planting in the green areas in seed zone X.3 (Fig. 5.5B, left panel) could come from populations in the yellow regions from the adjacent X.2 region (Fig 5.5B, left panel) in order to compensate for the shift from contemporary colder and moister green areas to dryer and warmer yellow areas by the 2050s (Fig 5.5B, right panel).

Implementing seed movement based on any zone-based system, such as the CONAFOR seed zones or our climate-based seed zones, has some fundamental limitations. Zones delineated across a continuum of climate conditions or a continuum of a genetic variation should not be interpreted as distinct climate types or genetically distinct populations. Rather, the purpose of the maps we provide is to visualize where climate regions to which trees are putatively adapted have been in the past, and are predicted to be in the future. For the practitioner, they provide general

106

guidance where seed of any species may be sourced by tracking their historic climate niche without the need of more complex focal-point seed transfer systems (Parker 1992). Note that we do not recommend that a class change be used as decision criterion whether seed movement is required or not. To expand on the previous example for seedzone X.3 in Figure 5.5B: For a planting site in the green climate zone, close to the boundary to the warmer yellow zone (bottom right panel 2050s climate), the maps would suggest that no seed transfer is required (i.e. the site did not change from being green in the 1961-1990 left panel). However, the correct prescription would be to transfer seed from a source location close to the yellow/green boundary in the 1961-1990 reference map, the climate to which populations are putatively adapted.
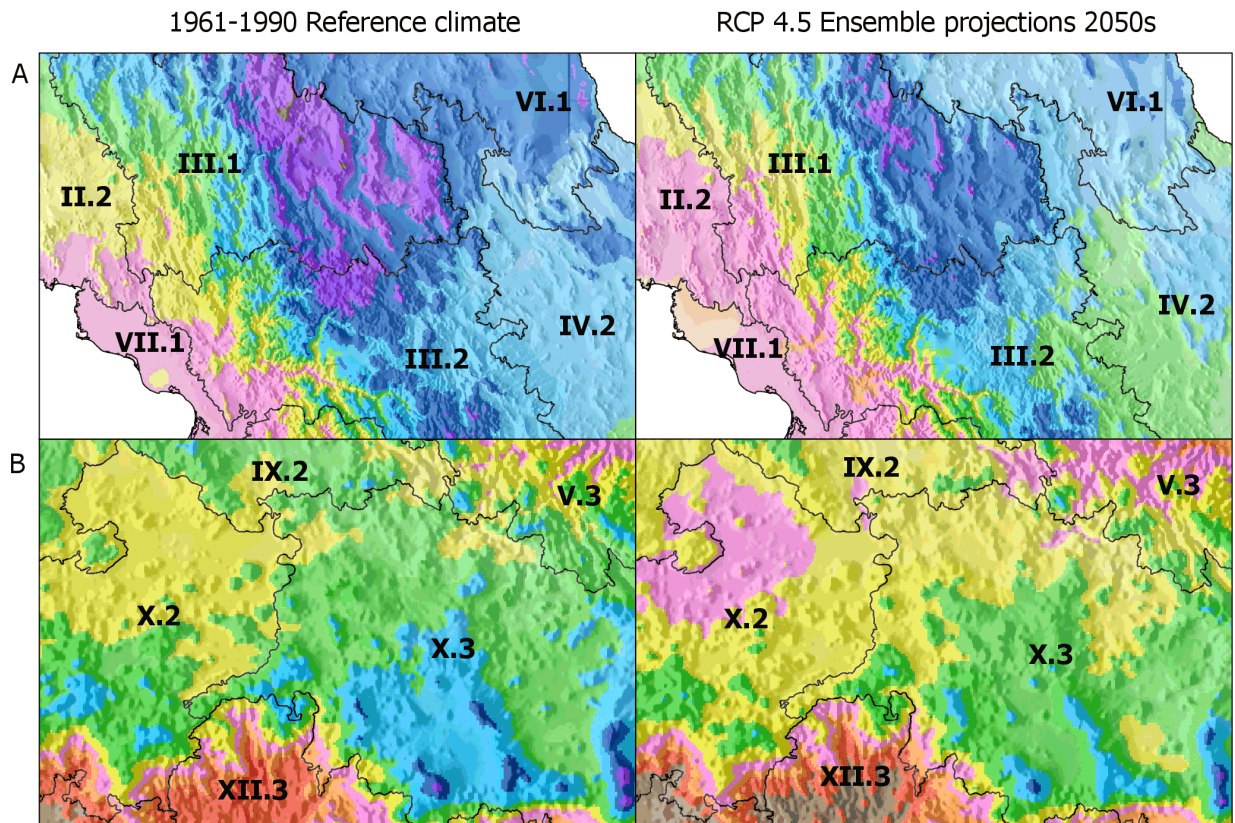
Fig. 5.5. Detail of climate-based seed zone shifts within CONAFOR regions, indicated by black lines. Practitioners should often be able to collect seed within the same seedzone that is predicted to become suitably adapted. For example, light blue collections in seed zone VI.1 (panel A, left) could be used further north in the same seedzone under predicted climate change (panel A, right).

Given the amount of observed and projected climate change, a simple and practical interim rule that also conforms to current Mexican legislation would be to move seeds one half of the seed zone intervals used here towards adjacent wetter and/or cooler climate-based seed zones, preferably within the same CONAFOR seed zone. This can be implemented based on the climate-based seed zones delineated in Fig 5.2, which GIS files are available through an open access database (*https://doi.org/10.5281/zenodo.1052141*). While this cannot fully address the anticipated climate shifts shown in Fig. 5.4, it would be a practical first step in the right direction, compensating for a general trend toward classes with a lower moisture index and higher temperatures. Such a first step would still comply with current legislation and significantly improve on status-quo management practices. Our proposed approach to track climate conditions to which organisms are putatively adapted could be refined with information on climatic tolerances from provenance testing. For species and populations with narrow climate tolerances it will be more important to track their optimum niche closely.

5.5. References

Aitken, S. N., S. Yeaman, J. A. Holliday, T. Wang, and S. Curtis-McLane. 2008. Adaptation, migration or extirpation: climate change outcomes for tree populations. Evolutionary Applications **1**:95-111.

Benito-Garzón, M., and J. F. Fernández-Manjarrés. 2015. Testing scenarios for assisted migration of forest trees in Europe. New Forests **46**:979-994.

Bower, A. D., J. B. S. Clair, and V. Erickson. 2014. Generalized provisional seed zones for native plants. Ecological Applications **24**:913-919.

Castellanos-Acuña, D., R. Lindig-Cisneros, and C. Sáenz-Romero. 2015. Altitudinal assisted migration of Mexican pines as an adaptation to climate change. Ecosphere **6**:1-16.

Castellanos-Bolaños, J. F., E. J. Treviño-Garza, O. A. Aguirre-Calderón, J. Jiménez-Pérez, and A. Velázquez-Martínez. 2010. Diversidad arbórea y estructura espacial de bosques de pino-encino en Ixtlán de Juárez, Oaxaca. Revista mexicana de ciencias forestales **1**:39-52.

Chmura, D. J., P. D. Anderson, G. T. Howe, C. A. Harrington, J. E. Halofsky, D. L. Peterson, D. C. Shaw, and J. Brad St.Clair. 2011. Forest responses to climate change in the northwestern United States: Ecophysiological foundations for adaptive management. Forest Ecology and Management **261**:1121-1142.

CONAFOR. 2014. Establecimiento de unidades productoras y manejo de germoplasma forestal-especificaciones tecnicas. NMX-AA-169-SCFI-2014. Comision Nacional Forestal, Guadalajara, Mexico.

Cuervo-Robayo, A. P., O. Téllez-Valdés, M. A. Gómez-Albores, C. S. Venegas-Barrera, J. Manjarrez, and E. Martínez-Meyer. 2014. An update of high-resolution monthly climate surfaces for Mexico. International Journal of Climatology **34**:2427-2437.

Dumroese, R. K., M. I. Williams, J. A. Stanturf, and J. B. S. Clair. 2015. Considerations for restoring temperate forests of tomorrow: forest restoration, assisted migration, and bioengineering. New Forests **46**:947-964.

Dutkowski, G., M. Ivković, W. J. Gapare, and T. A. McRae. 2016. Defining breeding and deployment regions for radiata pine in southern Australia. New Forests **47**:783-799.

Gapare, W. J., M. Ivković, K. J. Liepe, A. Hamann, and C. B. Low. 2015. Drivers of genotype by environment interaction in radiata pine as indicated by multivariate regression trees. Forest Ecology and Management **353**:21-29.

Gray, L. K., and A. Hamann. 2011. Strategies for reforestation under uncertain future climates: guidelines for Alberta, Canada. PLOS ONE **6**:e22977.

Hamann, A., T. Gylander, and P.-y. Chen. 2011. Developing seed zones and transfer guidelines with multivariate regression trees. Tree Genetics & Genomes **7**:399-408.

Harris, I., P. D. Jones, T. J. Osborn, and D. H. Lister. 2014. Updated high-resolution grids of monthly climatic observations – the CRU TS3.10 Dataset. International Journal of Climatology **34**:623-642.

Hodge, G. R., and W. S. Dvorak. 2014. Breeding southern US and Mexican pines for increased value in a changing world. New Forests **45**:295-300.

Johnson, G., F. C. Sorensen, J. B. St Clair, and R. C. Cronn. 2004. Pacific Northwest forest tree seed zones: a template for native plants? Native Plants Journal **5**:131-140.

Kang, N.-Y., and J. B. Elsner. 2015. Trade-off between intensity and frequency of global tropical cyclones. Nature Climate Change **5**:661-664.

Ledig, F. T., M. Mápula-Larreta, B. Bermejo-Velázquez, V. Reyes-Hernández, C. Flores-López, and M. A. Capó-Arteaga. 2000. Locations of endangered spruce populations in México and the demography of Picea chihuahuana. Madroño **47**:71-88.

Ledig, F. T., G. E. Rehfeldt, C. Sáenz-Romero, and C. Flores-López. 2010. Projections of suitable habitat for rare species under global warming scenarios. American Journal of Botany **97**:970-987.

Lesser, M. R., and W. H. Parker. 2006. Comparison of canonical correlation and regression based focal point seed zones of white spruce. Canadian Journal of Forest Research **36**:1572-1586.

McKenney, D. W., M. F. Hutchinson, J. L. Kesteven, and L. A. Venier. 2001. Canada's plant hardiness zones revisited using modern climate interpolation techniques. Canadian Journal of Plant Science **81**:129–143.

Mitchell, T. D., and P. D. Jones. 2005. An improved method of constructing a database of monthly climate observations and associated high-resolution grids. International Journal of Climatology **25**:693-712.

Morgenstern, K. 1996. Geographic Variation in Forest Trees. Genetic Basis and Application of Knowledge in Silviculture University of British Columbia Press, Vancouver, British Columbia.

Omernik, J. M., and G. E. Griffith. 2014. Ecoregions of the conterminous United States: evolution of a hierarchical spatial framework. Environmental Management **54**:1249-1266.

Parker, W. H. 1992. Focal point seed zones: site-specific seed zone delineation using geographic information systems. Canadian Journal of Forest Research **22**:267-271.

Pavia, E. G., F. Graef, and J. Reyes. 2009. Annual and seasonal surface air temperature trends in Mexico. International Journal of Climatology **29**:1324-1329.

Potter, K. M., and W. W. Hargrove. 2012. Determining suitable locations for seed transfer under climate change: a global quantitative method. New Forests **43**:581-599.

Potter, K. M., R. M. Jetton, A. Bower, D. F. Jacobs, G. Man, V. D. Hipkins, and M. Westwood. 2017. Banking on the future: progress, challenges and opportunities for the genetic conservation of forest trees. New Forests **48**:153-180.

Ramírez, M. I., J. G. Azcárate, and L. Luna. 2003. Effects of human activities on monarch butterfly habitat in protected mountain forests, Mexico. The Forestry Chronicle **79**:242-246.

Rehfeldt, G. E. 1988. Ecological genetics of *Pinus contorta* from the Rocky Mountains (USA): A synthesis. Silvae genetica **37**:131-135.

Rehfeldt, G. E., C. C. Ying, D. L. Spittlehouse, and D. A. Hamilton. 1999. Genetic responses to climate in *Pinus contorta*: niche breadth, climate change, and reforestation. Ecological Monographs **69**:375-407.

Saenz-Romero, C., J. B. Lamy, A. Ducousso, B. Musch, F. Ehrenmann, S. Delzon, S. Cavers, W. Chalupka, S. Dagdas, J. K. Hansen, S. J. Lee, M. Liesebach, H. M. Rau, A. Psomas, V. Schneck, W. Steiner, N. E. Zimmermann, and A. Kremer. 2017. Adaptive and plastic responses of *Quercus petraea* populations to climate across Europe. Global Change Biology **23**:2831-2847.

Sáenz-Romero, C., G. E. Rehfeldt, N. L. Crookston, P. Duval, R. St-Amant, J. Beaulieu, and B. A. Richardson. 2010. Spline models of contemporary, 2030, 2060 and 2090 climates for Mexico and their use in understanding climate-change impacts on the vegetation. Climatic Change **102**:595-623.

Saenz-Romero, C., G. E. Rehfeldt, P. Duval, and R. A. Lindig-Cisneros. 2012. Abies religiosa habitat prediction in climatic change scenarios and implications for monarch butterfly conservation in Mexico. Forest Ecology and Management **275**:98-106.

St Clair, J. B., N. L. Mandel, and K. W. Vance-Borland. 2005. Genecology of Douglas fir in western Oregon and Washington. Annals of Botany **96**:1199-1214.

St. Clair, J. B. 2006. Genetic variation in fall cold hardiness in coastal Douglas-fir in western Oregon and Washington. Canadian Journal of Botany **84**:1110-1121.

Taïbi, K., A. D. del Campo, J. M. Mulet, J. Flors, and A. Aguado. 2014. Testing Aleppo pine seed sources response to climate change by using trial sites reflecting future conditions. New Forests **45**:603-624.

Tucker, C. M. 2004. Community institutions and forest management in Mexico's Monarch Butterfly Reserve. Society & Natural Resources **17**:569-587.

Vizcaíno-Palomar, N., I. Ibáñez, M. Benito-Garzón, S. C. González-Martínez, M. A. Zavala, and R. Alía. 2017. Climate and population origin shape pine tree height-diameter allometry. New Forests **48**:363-379.

Wang, T., A. Hamann, D. Spittlehouse, and C. Carroll. 2016. Locally downscaled and spatially customizable climate data for historical and future periods for North America. PLOS ONE **11**:e0156720. DOI: 0156710.0151371/journal.pone.0156720.

Ying, C. C., and A. D. Yanchuk. 2006. The development of British Columbia's tree seed transfer guidelines: Purpose, concept, methodology, and implementation. Forest Ecology and Management **227**:1-13.

Zacarías-Eslava, Y., and R. F. d. Castillo. 2010. Comunidades vegetales templadas de la Sierra Juárez, Oaxaca: pisos altitudinales y sus posibles implicaciones ante el cambio climático. Boletín de la Sociedad Botánica de México **87**:13-28.

Chapter 6. General discussion and conclusions

This thesis primarily represents applied research and method development focused on supporting research and management on climate change adaptation. The applied objective of the thesis was to develop general climate-based seed zones for Mexico that can serve to guide seed movement in reforestation programs under observed and projected climate change scenarios. To meet this objective, I developed a comprehensive precipitation weather station databases with a global extent and global precipitation layers generated with a new interpolation approach. Subsequently, I compiled a comprehensive database for Latin America that comprises 18,000 data layers that can be interactively queried though a software front-end ClimateSA. Selected data was then used for the delineation of climate-based seed zones for Mexico, using a simple climate envelope modeling approach. This work required a number of choices with regards to data sources, interpolation methods, and climate envelope modeling that I will discuss in the subsequent paragraphs. I will point out general limitations of my chosen methods, alternative approaches that may be used to achieve similar objectives, and alternative data sources that researchers could consider when working on similar problems.

6.1. Temporal resolution of interpolated climate data

Regarding the temporal resolution for our gridded climate surfaces, I rely on climate data with a monthly temporal resolution. This is normally sufficient to adequately describe the habitat for any organism with respect to seasonality, water availability and growing conditions. Similarly, monthly data, or variables that can be derived from monthly data are often sufficient to describe climate dependency of human managed systems, such as the climatic suitability of an area for agricultural crops, forest tree species, or for selection of planting stock that is well adapted for a particular climate environment.

113

However, other applications may require higher temporal resolution. A detailed understanding of biological processes, and response of organisms to extreme events can benefit or even require data at a weekly or daily temporal resolution. Daily data is usually needed for mechanistic models of plant growth (e.g., Zhang et al. 2017), when analyzing the effect of past extreme events (Mctaggart-Cowan et al. 2007), or for describing climate conditions associated with risk of wildfires (Van Wagner 1987). Also, because of the highly stochastic nature of precipitation events, studies that focus on hydrology and streamflow almost always rely on daily precipitation records (Richardson et al. 2008, Jager et al. 2015, Ashouri et al. 2016).

Daily estimates of climate conditions have shown to be less accurate that monthly averages by a considerable margin. For example, daily temperature estimates have MAEs of around 2°C, more than double that of monthly estimates (Thornton et al. 1997). In the case of precipitation, substantially larger errors are not the only problem. Daily precipitation estimates of interpolated data will also be biased, with a tendency to underestimate the absolute values. This is due to a widely spaced weather station network regularly missing rare, local extreme precipitation events (Ashouri et al. 2015b, Miao et al. 2015).

6.2. Temporal resolution of future projections

The same issue of bias also applies to projections of climate variables, especially for precipitation from AOGCMs (Christensen et al. 2008). Even though AOGCMs work on a daily or hourly time step, the distribution of precipitation events is still not well modeled, with the number of wet days overestimated, and this leads to an underestimation of precipitation extremes (Frei et al. 2003, Räty et al. 2014). For studies that require precipitation data at a daily resolution, bias correction can be implemented with weather generators, which are mathematical models

that stochastically generate daily time series of weather for a location, based on average projections from AOGCMs on combination with observed daily data and its statistical characteristics (Wilks and Wilby 1999).

Another approach to arrive at unbiased estimates of daily climate grids is the interpolation of ratios of wet/dry days derived from ground-based meteorological stations and gridded surfaces (Di Luzio et al. 2008). This method outperformed methods of direct interpolation of daily data to develop grids of retrospective temperature and precipitation values. These ratios in turn can also inform weather generators to obtain projections of daily precipitation patterns for the future.

In my research, issues of bias are generally reduced or eliminated when averaging precipitation events over long periods of time. When averaging daily precipitation events over a 30-year period at weather stations, there are enough precipitation events captured to reliably estimate mean monthly averages that can be interpolated directly. Similarly, AOGCM projections used in this study were generated by averaging monthly time series provided by AOGCMs over 30-year normal periods, which were subsequently overlaid with the delta method over 30-year climate normal data. This approach, although primarily based on avoidance of bias through the use of long-term average has been described by some authors as a simple form of bias correction (Maraun 2016).

For some applications that require information normally obtained from daily data, derived summary variables can capture the key aspects of daily data. For example, some of the derived variables in ClimateSA were created with this intent, including: an estimate of frost free period, growing and chilling degree days, extreme max and min temperatures expected over a 30 year period. These types of variables that describe patterns and extremes of daily records over longer periods of time can often be estimated with high accuracy from monthly data by correlating the

frequency, sums, or minima and maxima of daily records to monthly means. This normally requires non-linear and multivariate predictive approaches (Rehfeldt et al. 2006, Wang et al. 2006, Wang et al. 2016).

6.3. Spatial resolution of future projections

In order to be able to run the weather generator at hourly time steps at a global scale, AOGCMs usually make the compromise of running at very coarse spatial scales. This has implications for future climate projections because they cannot model climate processes that occur at smaller scales. For example, areas on the windward versus the leeward side of a mountain range may warm at different rates or even directions. Similarly, ocean and adjacent coastal land areas regularly experience different rates of climate change.

This shortcoming can be solved by dynamic downscaling methods that work by using the AOGCM at its native resolution, but for a specific area of interest a higher resolution window models the climate patterns at a higher resolution that allows the incorporation of local topography or water bodies (Xu et al. 2019). A main limitation of this approach to obtaining regional AOGCM projections at higher resolution is computational capacity. As a consequence, relatively few model runs tend to be available for regional AOGCMs and only a subset of emission scenarios is usually covered. Further, the highest resolutions available for dynamic downscaling methods is in the order of 0.5°, still relatively coarse to resolve effects of topography on climate. Finally, dynamic downscaling models are essentially identical to AOGCMs, and will not produce information that is qualitatively different from the coarse resolution AOGCMs from which they are derived (Castro et al. 2005).

Regional AOGCMs for South America are not widely and comprehensively available, and we have not included regional AOGCMs in the ClimateSA data package. However, users can add anomaly grids obtained with the dynamic downscaling up to a resolution of 0.5° as they become available.

6.4. Alternative data sources: remote sensing

The development of satellite technology over the last decades provides an alternative way of observing weather conditions over large geographic areas where weather station coverage is sparse. However, climate data derived from satellites also has substantial limitations. Temperature is estimated from Microwave Sounding Units (MSUs), that measure microwave radiation from the atmosphere at different elevations (Weng et al. 2014). MSU sensors had a resolution on the ground of around 200km, while the newer Advanced (AMSUs) have a resolution of 50km. The difficulty is that this microwave radiation originates from throughout the entire height of the troposphere, and can also be influenced by emissions from the surface or water vapor in the troposphere. That is why deriving a temperature estimate for surface air temperature or any position in the troposphere is difficult.

In contrast, precipitation can be directly measured by passive microwave sensors on low orbiting satellites. Precipitation-size drops interact strongly with microwaves, whereas cloud droplets interact weekly, allowing the direct detection of precipitation (Varma 2018). The main limitations with these satellites is that they require a very low earth orbit, thereby sweeping only a relatively small area and also providing a temporally very incomplete record of precipitation envents. Alternatively, precipitation can be measured by infrared sensors (IR/VIS) on geostationary satellites, so they have a comprehensive temporal record for their region under observation (Varma 2018). Infrared sensors measure the temperature of clouds, with the

assumption that a colder cloud translates to precipitation, although this is not always true. These sensors can also be influenced by infrared radiation from the surface or the stratosphere, or water vapor in the troposphere. Due to the orbits of geostationary satellites, their data quality is best for the tropics and the mid latitudes, and degrades significantly for high latitude regions.

I tested the utility of two remote sensing products, PERSIANN-CDR (Ashouri et al. 2015a) and NASA's TRMM product (Huffman et al. 2007) as an alternative to interpolation for generating a baseline climate normal surface. However, validation statistics were low for both PERSIANN-CDR with a mean absolute error 17%, and for TRMM of 20% for mean annual precipitation, when expressed as proportion of the total observed precipitation value. This compares to a relative mean absolute error of 8% in our independent validation of precipitation surfaces developed in Chapter 3. Furthermore, a visual evaluation of the product with the highest resolution (0.04°), revealed significant artifacts reflecting the satellite orbits while still showing insufficient spatial definition of precipitation patterns in mountainous regions, and that should be visible at this resolution (Fig. 6.1).
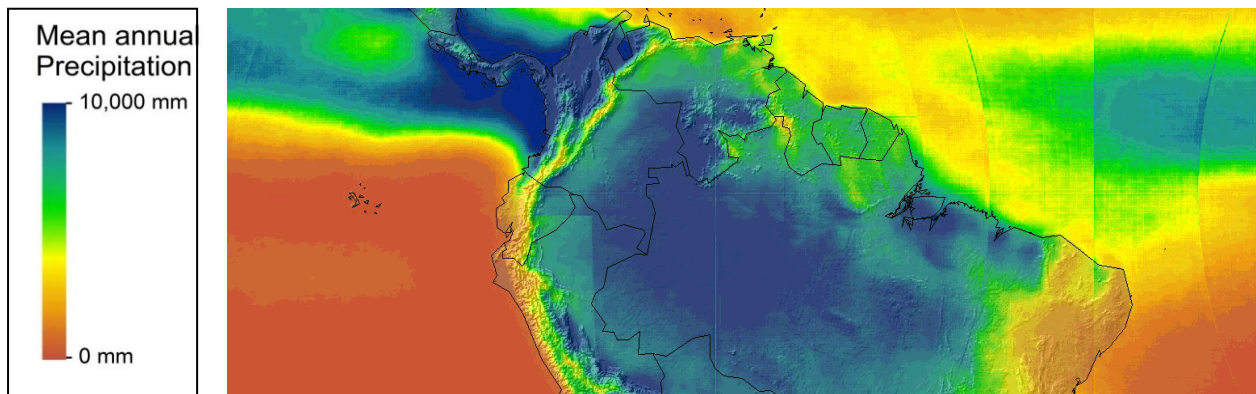
Figure 6.1. Mean annual precipitation for a long-term average from 2003-2015, near the equator where data quality was best. The image was derived from 3-hourly product of the 0.04° PERSIANN data product.

While the utility of remote sensed data for generating precipitation estimates with useful spatial resolution appears limited, a strength of this data is the temporal resolution. PERSIANN-CDR is available at 3-hourly resolution since 1980 at 0.25° and since 2003 at 0.04° resolution. Combined with a high-resolution baseline surface derived from interpolated weather station data, it could be useful to generate accurate time-series data at daily, weekly, or monthly time steps, when converted into anomaly surfaces and overlaid on a high-resolution baseline dataset. In the form of anomaly surfaces, artifacts or biases, as long as they are consistently generated over time, would cancel out.

6.5. Applications: climate change adaptation

Comprehensive climate databases including historical data for local evaluation of observed climate change trends are essential for climate change adaptation planning. While future projections give some broad range of the magnitude and directions of changes that we can expect, locally observed climate change trends represent the conditions that that we ultimately need to adapt to. Changes to management of natural resources should not rely on climate models alone, even if they uniformly agree that, for example, precipitation increases for a particular locality. If the observed long-term trend is actually toward drier conditions, then this cannot be ignored. Such discrepancies are very common due to the nature of very coarse scale climate projections that may be correct on average for a large grid cell, but will nevertheless not reflect local trends.

In general, I recommend the use of recent climate averages (e.g. the most recent 10, 20, or 30 years compared to a 1961-1990 normal period), or time series graphs in addition to future projections. One important consideration is that the shorter the historical time period under evaluation, the higher the probability that the climate difference or climate trend is not due to

directional climate change, but rather due to a random anomaly or cyclical climate event. Examples of such cyclical weather patterns that influence climate conditions in South America are the El Niño Southern Oscillation, the Quasi-biennial oscillation, and Schwabe cycle or sunspot cycle (Smith et al. 2012).

In chapter 5, I have chosen a 25-year period following our normal reference (1991-2015), which almost amounts to a normal period that should not be influenced significantly by cyclical or random climate anomalies. I found that observed trends for the most part matched or exceeded climate projections for the 2020s. Climate change for MCMT over the last three decades (from the mid-point of the 1961-1990 to the mid-point of the 1991-2015 average) represents approximately 44% of the expected climate change by the 2050s for the RCP 4.5 scenario, and 31% of the RCP 8.5 scenario relative to the 1961-1990 baseline. Similarly, observed changes in aridity are already equivalent to 39% of the 2050s climate projections.

Given the concordance of observed and projected climate change towards warmer and drier conditions, we propose that the movement of locally adapted seeds and seedlings towards colder and wetter environments than their origins would generally be justified for Mexico and in fact likely required to ensure survival and growth of the deployed seedlings on the coming decades. That said, the conclusion is generalized for Mexico, and the magnitude and direction of climate trends may locally vary. For any operational implementation in any particular locality, we recommend a check of long-term climate trends which can easily be generated with the time series functionality of the ClimateSA software package.

Thesis bibliography

Aitken, S. N., and J. B. Bemmels. 2016. Time to get moving: assisted gene flow of forest trees. Evolutionary Applications **9**:271-290.

Aitken, S. N., S. Yeaman, J. A. Holliday, T. Wang, and S. Curtis-McLane. 2008. Adaptation, migration or extirpation: climate change outcomes for tree populations. Evolutionary Applications **1**:95-111.

Alcamo, J., N. Dronin, M. Endejan, G. Golubev, and A. Kirilenkoc. 2007. A new assessment of climate change impacts on food production shortfalls and water availability in Russia. Global Environmental Change-Human and Policy Dimensions **17**:429-444.

Alkimim, A., G. Sparovek, and K. C. Clarke. 2015. Converting Brazil's pastures to cropland: an alternative way to meet sugarcane demand and to spare forestlands. Applied Geography **62**:75-84.

Allen, C. D., A. K. Macalady, H. Chenchouni, D. Bachelet, N. McDowell, M. Vennetier, T. Kitzberger, A. Rigling, D. D. Breshears, E. H. Hogg, P. Gonzalez, R. Fensham, Z. Zhang, J. Castro, N. Demidova, J. H. Lim, G. Allard, S. W. Running, A. Semerci, and N. Cobb. 2010. A global overview of drought and heat-induced tree mortality reveals emerging climate change risks for forests. Forest Ecology and Management **259**:660-684.

Anthony, K. W., T. S. von Deimling, I. Nitze, S. Frolking, A. Emond, R. Daanen, P. Anthony, P. Lindgren, B. Jones, and G. Grosse. 2018. 21st-century modeled permafrost carbon emissions accelerated by abrupt thaw beneath lakes. Nature Communications **9**:3262. DOI: 3210.1038/s41467-41018-05738-.

Arguez, A., and R. S. Vose. 2011. The definition of the standard WMO climate normal: the key to deriving alternative climate normals. Bulletin of the American Meteorological Society **92**:699-U345.

Ashouri, H., K.-L. Hsu, S. Sorooshian, D. K. Braithwaite, K. R. Knapp, L. D. Cecil, B. R. Nelson, and O. P. Prat. 2015a. PERSIANN-CDR: daily precipitation climate data record from multisatellite observations for hydrological and climate studies. Bulletin of the American Meteorological Society **96**:69-83.

Ashouri, H., K. L. Hsu, S. Sorooshian, D. K. Braithwaite, K. R. Knapp, L. D. Cecil, B. R. Nelson, and O. P. Prat. 2015b. PERSIANN-CDR: daily precipitation climate data record from multisatellite observations for hydrological and climate studies. Bulletin of the American Meteorological Society **96**:69-83.

Ashouri, H., P. Nguyen, A. Thorstensen, K.-l. Hsu, S. Sorooshian, and D. Braithwaite. 2016. Assessing the efficacy of high-resolution satellite-based PERSIANN-CDR precipitation product in simulating streamflow. Journal of Hydrometeorology **17**:2061-2076.

Bader, D., C. Covey, W. Gutowski, I. Held, K. Kunkel, R. Miller, R. Tokmakian, and M. Zhang. 2008. Climate models: an assessment of strengths and limitations. Geological and Atmospheric Sciences Reports. 3. Accessed March 6, 2017 at http://lib.dr.iastate.edu/ge_at_reports/3.

Bartsotas, N. S., E. N. Anagnostou, E. I. Nikolopoulos, and G. Kallos. 2018. Investigating satellite precipitation: uncertainty over complex terrain. Journal of Geophysical Research-Atmospheres **123**:5346-5359.

Beaubien, E., and A. Hamann. 2011. Spring Flowering Response to Climate Change between 1936 and 2006 in Alberta, Canada. Bioscience **61**:514-524.

Becker, A., P. Finger, A. Meyer-Christoffer, B. Rudolf, K. Schamm, U. Schneider, and M. Ziese. 2013. A description of the global land-surface precipitation data products of the Global Precipitation Climatology Centre with sample applications including centennial (trend) analysis from 1901–present. Earth System Science Data **5**:71-99.

Benito-Garzón, M., and J. F. Fernández-Manjarrés. 2015. Testing scenarios for assisted migration of forest trees in Europe. New Forests **46**:979-994.

Birdsey, R., and Y. D. Pan. 2011. Ecology: drought and dead trees. Nature Climate Change **1**:444-445.

Bogaert, P., P. Mahau, and F. Beckers. 1995. The Spatial Interpolation of Agro-Climatic Data. Cokriging software and source data. User's Manual v1.0b. Agrometeorology Series Working Paper 12. Environmental Information Management Service. Sustainable Development Department. Agrometeorology Group. FAO. Rome, Italy.

Boisvert-Marsh, L., C. Périé, and S. de Blois. 2014. Shifting with climate? Evidence for recent changes in tree species distribution at high latitudes. Ecosphere **5**:art83. doi:10.1890/ES1814-00111.00111.

Bower, A. D., J. B. S. Clair, and V. Erickson. 2014. Generalized provisional seed zones for native plants. Ecological Applications **24**:913-919.

Breshears, D. D., N. S. Cobb, P. M. Rich, K. P. Price, C. D. Allen, R. G. Balice, W. H. Romme, J. H. Kastens, M. L. Floyd, J. Belnap, J. J. Anderson, O. B. Myers, and C. W. Meyer. 2005. Regional vegetation die-off in response to global-change-type drought. Proceedings of the National Academy of Sciences 102:15144-15148.

Campbell, B. M., S. J. Vermeulen, P. K. Aggarwal, C. Corner-Dolloff, E. Girvetz, A. M. Loboguerrero, J. Ramirez-Villegas, T. Rosenstock, L. Sebastian, P. K. Thornton, and E. Wollenberg. 2016. Reducing risks to food security from climate change. Global Food Security-Agriculture Policy Economics and Environment **11**:34-43.

Castellanos-Acuña, D., R. Lindig-Cisneros, and C. Sáenz-Romero. 2015. Altitudinal assisted migration of Mexican pines as an adaptation to climate change. Ecosphere **6**:1-16.

Castellanos-Bolaños, J. F., E. J. Treviño-Garza, O. A. Aguirre-Calderón, J. Jiménez-Pérez, and A. Velázquez-Martínez. 2010. Diversidad arbórea y estructura espacial de bosques de pino-encino en Ixtlán de Juárez, Oaxaca. Revista mexicana de ciencias forestales **1**:39-52.

Castro, C. L., R. A. Pielke, and G. Leoncini. 2005. Dynamical downscaling: Assessment of value retained and added using the regional atmospheric modeling system (RAMS). Journal of Geophysical Research-Atmospheres **110**:D05108. DOI: 05110.01029/02004JD00472.

Chen, M., W. Shi, P. Xie, V. B. S. Silva, V. E. Kousky, R. Wayne Higgins, and J. E. Janowiak. 2008. Assessing objective techniques for gauge-based analyses of global daily precipitation. Journal of Geophysical Research: Atmospheres **113**:D04110. doi: 04110.01029/02007JD009132.

Chen, M., P. Xie, J. E. Janowiak, and P. A. Arkin. 2002. Global land precipitation: a 50-yr monthly analysis based on gauge observations. Journal of Hydrometeorology **3**:249-266.

Chen, W. L., Z. H. Jiang, and L. Li. 2011. Probabilistic Projections of Climate Change over China under the SRES A1B Scenario Using 28 AOGCMs. Journal of Climate **24**:4741-4756.

Chmura, D. J., P. D. Anderson, G. T. Howe, C. A. Harrington, J. E. Halofsky, D. L. Peterson, D. C. Shaw, and J. Brad St.Clair. 2011. Forest responses to climate change in the northwestern United States: Ecophysiological foundations for adaptive management. Forest Ecology and Management **261**:1121-1142.

Chou, C., J. Y. Tu, and P. H. Tan. 2007. Asymmetry of tropical precipitation change under global warming. Geophysical Research Letters **34**:Artn L17708, DOI:17710.11029/12007gl030327

Christensen, J. H., F. Boberg, O. B. Christensen, and P. Lucas-Picher. 2008. On the need for bias correction of regional climate change projections of temperature and precipitation. Geophysical Research Letters **35**:L20709, DOI:20710.21029/22008GL03569.

CONAFOR. 2014. Establecimiento de unidades productoras y manejo de germoplasma forestal-especificaciones tecnicas. NMX-AA-169-SCFI-2014. Comision Nacional Forestal, Guadalajara, Mexico.

Cook, B. I., J. S. Mankin, and K. J. Anchukaitis. 2018. Climate change and drought: from past to future. Current Climate Change Reports **4**:164-179.

Cuervo-Robayo, A. P., O. Téllez-Valdés, M. A. Gómez-Albores, C. S. Venegas-Barrera, J. Manjarrez, and E. Martínez-Meyer. 2014. An update of high-resolution monthly climate surfaces for Mexico. International Journal of Climatology **34**:2427-2437.

Daly, C. 2006. Guidelines for assessing the suitability of spatial climate data sets. International Journal of Climatology **26**:707-721.

Daly, C., W. P. Gibson, G. H. Taylor, G. L. Johnson, and P. Pasteris. 2002. A knowledge-based approach to the statistical mapping of climate. Climate Research **22**:99-113.

Daly, C., M. Halbleib, J. I. Smith, W. P. Gibson, M. K. Doggett, G. H. Taylor, J. Curtis, and P. P. Pasteris. 2008. Physiographically sensitive mapping of climatological temperature and precipitation across the conterminous United States. International Journal of Climatology **28**:2031-2064.

Derin, Y., and K. K. Yilmaz. 2014. Evaluation of multiple satellite-based precipitation products over complex topography. Journal of Hydrometeorology **15**:1498-1516.

Di Luzio, M., G. L. Johnson, C. Daly, J. K. Eischeid, and J. G. Arnold. 2008. Constructing retrospective gridded daily precipitation and temperature datasets for the conterminous United States. Journal of Applied Meteorology and Climatology **47**:475-497.

Dumroese, R. K., M. I. Williams, J. A. Stanturf, and J. B. S. Clair. 2015. Considerations for restoring temperate forests of tomorrow: forest restoration, assisted migration, and bioengineering. New Forests **46**:947-964.

Durre, I., M. J. Menne, B. E. Gleason, T. G. Houston, and R. S. Vose. 2010. Comprehensive automated quality assurance of daily surface observations. Journal of Applied Meteorology and Climatology **49**:1615-1633.

Dutkowski, G., M. Ivković, W. J. Gapare, and T. A. McRae. 2016. Defining breeding and deployment regions for radiata pine in southern Australia. New Forests **47**:783-799.

ESRI. 2008. ArcMap 9.3.

Estrada, F., P. Perron, and B. Martinez-Lopez. 2013. Statistically derived contributions of diverse human influences to twentieth-century temperature changes. Nature Geoscience **6**:1050-1055.

Fasullo, J. T., and K. E. Trenberth. 2012. A Less Cloudy Future: The Role of Subtropical Subsidence in Climate Sensitivity. Science **338**:792-794.

Fick, S. E., and R. J. Hijmans. 2017. WorldClim 2: new 1-km spatial resolution climate surfaces for global land areas. International Journal of Climatology **37**:4302-4315.

Flannigan, M. D., M. A. Krawchuk, W. J. de Groot, B. M. Wotton, and L. M. Gowman. 2009. Implications of changing climate for global wildland fire. International Journal of Wildland Fire **18**:483-507.

Flato, G., J. Marotzke, B. Abiodun, P. Braconnot, S. C. Chou, W. Collins, P. Cox, F. Driouech, S. Emori, V. Eyring, C. Forest, P. Gleckler, E. Guilyardi, C. Jakob, V. Kattsov, C.

Reason, and M. Rummukaine. 2013. Evaluation of Climate Models.*in* T. F. Stocker, D. Qin, G.-K. Plattner, M. Tignor, S. K. Allen, J. Boschung, A. Nauels, Y. Xia, V. Bex, and P. M. Midgley, editors. Climate Change 2013: The Physical Science Basis. Contribution of Working Group I to the Fifth Assessment Report of the Intergovernmental Panel on Climate Change. Cambridge University Press, Cambridge, UK.

Flato, G. M. 2011. Earth system models: an overview. Wiley Interdisciplinary Reviews: Climate Change **2**:783-800.

Frei, C., J. H. Christensen, M. Deque, D. Jacob, R. G. Jones, and P. L. Vidale. 2003. Daily precipitation statistics in regional climate models: Evaluation and intercomparison for the European Alps. Journal of Geophysical Research-Atmospheres **108**:4124, DOI:4110.1029/2002jd002287.

Gapare, W. J., M. Ivković, K. J. Liepe, A. Hamann, and C. B. Low. 2015. Drivers of genotype by environment interaction in radiata pine as indicated by multivariate regression trees. Forest Ecology and Management **353**:21-29.

Gelaro, R., W. McCarty, M. J. Suarez, R. Todling, A. Molod, L. Takacs, C. A. Randles, A. Darmenov, M. G. Bosilovich, R. Reichle, K. Wargan, L. Coy, R. Cullather, C. Draper, S. Akella, V. Buchard, A. Conaty, A. M. da Silva, W. Gu, G. K. Kim, R. Koster, R. Lucchesi, D. Merkova, J. E. Nielsen, G. Partyka, S. Pawson, W. Putman, M. Rienecker, S. D. Schubert, M. Sienkiewicz, and B. Zhao. 2017. The Modern-Era Retrospective Analysis for Research and Applications, Version 2 (MERRA-2). Journal of Climate **30**:5419-5454.

Gesch, D. B., K. L. Verdin, and S. K. Greenlee. 1999. New land surface digital elevation model covers the Earth. Eos, Transactions: American Geophysical Union **80**:69-70.

Giorgi, F., and L. O. Mearns. 2002. Calculation of average, uncertainty range, and reliability of regional climate changes from AOGCM simulations via the "reliability ensemble averaging" (REA) method. Journal of Climate **15**:1141-1158.

GISTEMP. 2019. GISS Surface Temperature Analysis (GISTEMP). NASA Goddard Institute for Space Studies. Dataset accessed 2019-04-10 at data.giss.nasa.gov/gistemp/.

Gleckler, P. J., K. E. Taylor, and C. Doutriaux. 2008. Performance metrics for climate models. Journal of Geophysical Research-Atmospheres **113**.

Graler, B., E. Pebesma, and G. Heuvelink. 2016. Spatio-Temporal Interpolation using gstat. R Journal **8**:204-218.

Gray, L. K., and A. Hamann. 2011. Strategies for reforestation under uncertain future climates: guidelines for Alberta, Canada. PLOS ONE **6**:e22977.

Guan, H. D., C. T. Simmons, and A. J. Love. 2009. Orographic controls on rain water isotope distribution in the Mount Lofty Ranges of South Australia. Journal of Hydrology **374**:255-264.

Guttman, N. B. 1989. Statistical descriptors of climate. Bulletin of the American Meteorological Society **70**:602-607.

Hamann, A., T. Gylander, and P.-y. Chen. 2011. Developing seed zones and transfer guidelines with multivariate regression trees. Tree Genetics & Genomes **7**:399-408.

Hamann, A., and T. L. Wang. 2005. Models of climatic normals for genecology and climate change studies in British Columbia. Agricultural and Forest Meteorology **128**:211-221.

Hamann, A., T. L. Wang, D. L. Spittlehouse, and T. Q. Murdock. 2013. A Comprehensive, High-Resolution Database of Historical and Projected Climate Surfaces for Western North America. Bulletin of the American Meteorological Society **94**:1307-1309.

Hansen, J., R. Ruedy, M. Sato, and K. Lo. 2010. Global Surface Temperature Change. Reviews of Geophysics **48**:RG4004.

Harris, I., P. D. Jones, T. J. Osborn, and D. H. Lister. 2014. Updated high-resolution grids of monthly climatic observations – the CRU TS3.10 Dataset. International Journal of Climatology **34**:623-642.

Hijmans, R. J., S. E. Cameron, J. L. Parra, P. G. Jones, and A. Jarvis. 2005. Very high resolution interpolated climate surfaces for global land areas. International Journal of Climatology **25**:1965-1978.

Hodge, G. R., and W. S. Dvorak. 2014. Breeding southern US and Mexican pines for increased value in a changing world. New Forests **45**:295-300.

Hoegh-Guldberg, O., and J. F. Bruno. 2010. The impact of climate change on the world's marine ecosystems. Science **328**:1523-1528.

Huffman, G. J., D. T. Bolvin, E. J. Nelkin, D. B. Wolff, R. F. Adler, G. Gu, Y. Hong, K. P. Bowman, and E. F. Stocker. 2007. The TRMM multisatellite precipitation analysis (TMPA): quasi-global, multiyear, combined-sensor precipitation estimates at fine scales. Journal of Hydrometeorology **8**:38-55.

Hughes, D. A. 2006. Comparison of satellite rainfall data with observations from gauging station networks. Journal of Hydrology **327**:399-410.

Hutchinson, M. F. 1995. Interpolating mean rainfall using thin-plate smoothing splines. International Journal of Geographical Information Systems **9**:385-403.

IPCC. 1990. Working Group I: Scientific Assesment of Climate Change. Cambridge University Press, Cambridge UK.

IPCC. 2014. Climate Change 2014: Synthesis Report. Contribution of Working Groups I, II and III to the Fifth Assessment Report of the Intergovernmental Panel on Climate Change [Core Writing Team, R.K. Pachauri and L.A. Meyer (eds.)]. IPCC, Geneva, Switzerland.

Jager, H. I., L. M. Baskaran, P. E. Schweizer, A. F. Turhollow, C. C. Brandt, and R. Srinivasan. 2015. Forecasting changes in water quality in rivers associated with growing biofuels in the Arkansas-White-Red river drainage, USA. Global Change Biology Bioenergy **7**:774-784.

Johnson, G., F. C. Sorensen, J. B. St Clair, and R. C. Cronn. 2004. Pacific Northwest forest tree seed zones: a template for native plants? Native Plants Journal **5**:131-140.

Jones, P. D., and M. E. Mann. 2004. Climate over past millennia. Reviews of Geophysics **42**.

Joseph, R., T. M. Smith, M. R. P. Sapiano, and R. R. Ferraro. 2009. A new high-resolution satellite-derived precipitation dataset for climate studies. Journal of Hydrometeorology **10**:935-952.

Kang, N.-Y., and J. B. Elsner. 2015. Trade-off between intensity and frequency of global tropical cyclones. Nature Climate Change **5**:661-664.

Kirtman, B., S.B. Power, J.A. Adedoyin, G.J. Boer, R. Bojariu, I. Camilloni, F.J. Doblas-Reyes, A.M. Fiore, M. Kimoto, G.A. Meehl, M. Prather, A. Sarr, C. Schär, R. Sutton, G.J. van Oldenborgh, G. Vecchi, and H. J. Wang. 2013. Near-term Climate Change: Projections and Predictability.*in* T. F. Stocker, D. Qin, G.-K. Plattner, M. Tignor, S. K. Allen, J. Boschung, A. Nauels, Y. Xia, V. Bex, and P. M. Midgley, editors. Climate Change 2013: The Physical Science Basis. Contribution of Working Group I to the Fifth Assessment Report of the Intergovernmental Panel on Climate Change. Cambridge University Press, Cambridge, UK.

Knutti, R., D. Masson, and A. Gettelman. 2013. Climate model genealogy: Generation CMIP5 and how we got there. Geophysical Research Letters **40**:1194-1199.

Koetse, M. J., and P. Rietveld. 2009. The impact of climate change and weather on transport: an overview of empirical findings. Transportation Research Part D-Transport and Environment **14**:205-221.

Koo, K. A., W. S. Kong, S. U. Park, J. H. Lee, J. Kim, and H. Jung. 2017. Sensitivity of Korean fir (*Abies koreana* Wils.), a threatened climate relict species, to increasing temperature at an island subalpine area. Ecological Modelling **353**:5-16.

Kurz, W. A., C. C. Dymond, G. Stinson, G. J. Rampley, E. T. Neilson, A. L. Carroll, T. Ebata, and L. Safranyik. 2008. Mountain pine beetle and forest carbon feedback to climate change. Nature **452**:987-990.

Lashof, D. A., and D. R. Ahuja. 1990. Relative Contributions of Greenhouse Gas Emissions to Global Warming. Nature **344**:529-531.

Lawrimore, J. H., M. J. Menne, B. E. Gleason, C. N. Williams, D. B. Wuertz, R. S. Vose, and J. Rennie. 2011. An overview of the Global Historical Climatology Network monthly mean temperature data set, version 3. Journal of Geophysical Research: Atmospheres **116**:D19121. doi:19110.11029/12011JD016187.

Lean, J. L. 2018. Observation-based detection and attribution of 21st century climate change. Wiley Interdisciplinary Reviews-Climate Change **9**:e511. DOI: 510.1002/wcc.1511.

Ledig, F. T., M. Mápula-Larreta, B. Bermejo-Velázquez, V. Reyes-Hernández, C. Flores-López, and M. A. Capó-Arteaga. 2000. Locations of endangered spruce populations in México and the demography of Picea chihuahuana. Madroño **47**:71-88.

Ledig, F. T., G. E. Rehfeldt, C. Sáenz-Romero, and C. Flores-López. 2010. Projections of suitable habitat for rare species under global warming scenarios. American Journal of Botany **97**:970-987.

Lenoir, J., J. C. Gegout, P. A. Marquet, P. de Ruffray, and H. Brisse. 2008. A significant upward shift in plant species optimum elevation during the 20th century. Science **320**:1768-1771.

Lesser, M. R., and W. H. Parker. 2006. Comparison of canonical correlation and regression based focal point seed zones of white spruce. Canadian Journal of Forest Research **36**:1572-1586.

Lewis, S. L., P. M. Brando, O. L. Phillips, G. M. F. van der Heijden, and D. Nepstad. 2011. The 2010 Amazon drought. Science **331**:554-554.

Liepe, K. J., A. Hamann, P. Smets, C. R. Fitzpatrick, and S. N. Aitken. 2016. Adaptation of lodgepole pine and interior spruce to climate: implications for reforestation in a warming world. Evolutionary Applications **9**:409-419.

Ljungqvist, F. C., P. J. Krusic, H. S. Sundqvist, E. Zorita, G. Brattstrom, and D. Frank. 2016. Northern Hemisphere hydroclimate variability over the past twelve centuries. Nature **532**:94-98.

Lwanga, J. S. 2003. Localized tree mortality following the drought of 1999 at Ngogo, Kibale National Park, Uganda. African Journal of Ecology **41**:194-196.

Maclean, I. M. D., and R. J. Wilson. 2011. Recent ecological responses to climate change support predictions of high extinction risk. Proceedings of the National Academy of Sciences USA **108**:12337-12342.

Magnuson, J. J., D. M. Robertson, B. J. Benson, R. H. Wynne, D. M. Livingstone, T. Arai, R. A. Assel, R. G. Barry, V. Card, E. Kuusisto, N. G. Granin, T. D. Prowse, K. M. Stewart, and

V. S. Vuglinski. 2000. Historical trends in lake and river ice cover in the Northern Hemisphere. Science **289**:1743-1746.

Manabe, S., and K. Bryan. 1969. Climate calculations with a combined ocean-atmosphere model. Journal of the Atmospheric Sciences **26**:786-&.

Manabe, S., and R. T. Wetherald. 1967. Thermal equilibrium of the atmosphere with a given distribution of relative humidity. Journal of the Atmospheric Sciences **24**:241-259.

Maraun, D. 2016. Bias Correcting Climate Change Simulations - a Critical Review. Current Climate Change Reports **2**:211-220.

Matyas, C. 2010. Forecasts needed for retreating forests. Nature **464**:1271-1271.

Mbogga, M. S., A. Hamann, and T. Wang. 2009. Historical and projected climate data for natural resource management in western Canada. Agricultural and Forest Meteorology **149**:881-890.

Mbogga, M. S., X. Wang, and A. Hamann. 2010. Bioclimate envelope model predictions for natural resource management: dealing with uncertainty. Journal of Applied Ecology **47**:731-740.

McDowell, N. G., D. J. Beerling, D. D. Breshears, R. A. Fisher, K. F. Raffa, and M. Stitt. 2011. The interdependence of mechanisms underlying climate-driven vegetation mortality. Trends in Ecology & Evolution **26**:523-532.

McKenney, D. W., M. F. Hutchinson, J. L. Kesteven, and L. A. Venier. 2001. Canada's plant hardiness zones revisited using modern climate interpolation techniques. Canadian Journal of Plant Science **81**:129–143.

Mctaggart-Cowan, R., L. F. Bosart, J. R. Gyakum, and E. H. Atallah. 2007. Hurricane Katrina (2005). Part I: Complex life cycle of an intense tropical cyclone. Monthly Weather Review **135**:3905-3926.

Meehl, G. A., C. Covey, T. Delworth, M. Latif, B. McAvaney, J. F. B. Mitchell, R. J. Stouffer, and K. E. Taylor. 2007. The WCRP CMIP3 multimodel dataset - A new era in climate change research. Bulletin of the American Meteorological Society **88**:1383-1394.

Meinshausen, M., S. J. Smith, K. Calvin, J. S. Daniel, M. L. T. Kainuma, J. F. Lamarque, K. Matsumoto, S. A. Montzka, S. C. B. Raper, K. Riahi, A. Thomson, G. J. M. Velders, and D. P. P. van Vuuren. 2011. The RCP greenhouse gas concentrations and their extensions from 1765 to 2300. Climatic Change **109**:213-241.

Memmott, J., P. G. Craze, N. M. Waser, and M. V. Price. 2007. Global warming and the disruption of plant-pollinator interactions. Ecology Letters **10**:710-717.

Mendelsohn, R., P. Kurukulasuriya, A. Basist, F. Kogan, and C. Williams. 2007. Climate analysis with satellite versus weather station data. Climatic Change **81**:71-83.

Menne, M. J., I. Durre, R. S. Vose, B. E. Gleason, and T. G. Houston. 2012. An overview of the Global Historical Climatology Network-Daily database. Journal of Atmospheric and Oceanic Technology **29**:897-910.

Miao, C., H. Ashouri, K.-L. Hsu, S. Sorooshian, and Q. Duan. 2015. Evaluation of the PERSIANN-CDR daily rainfall estimates in capturing the behavior of extreme precipitation events over China. Journal of Hydrometeorology **16**:1387-1396.

Michaelian, M., E. H. Hogg, R. J. Hall, and E. Arsenault. 2011. Massive mortality of aspen following severe drought along the southern edge of the Canadian boreal forest. Global Change Biology **17**:2084-2094.

Millar, C. I., N. L. Stephenson, and S. L. Stephens. 2007. Climate change and forests of the future: managing in the face of uncertainty. Ecological Applications **17**:2145-2151.

Min, S.-K., X. Zhang, F. W. Zwiers, and G. C. Hegerl. 2011. Human contribution to more-intense precipitation extremes. Nature **470**:378.

Mitchell, K. E., D. Lohmann, P. R. Houser, E. F. Wood, J. C. Schaake, A. Robock, B. A. Cosgrove, J. Sheffield, Q. Duan, L. Luo, R. W. Higgins, R. T. Pinker, J. D. Tarpley, D. P. Lettenmaier, C. H. Marshall, J. K. Entin, M. Pan, W. Shi, V. Koren, J. Meng, B. H. Ramsay, and A. A. Bailey. 2004. The multi-institution North American Land Data Assimilation System (NLDAS): Utilizing multiple GCIP products and partners in a continental distributed hydrological modeling system. Journal of Geophysical Research: Atmospheres **109**:D07S90. doi:10.1029/2003JD003823

Mitchell, T. D., and P. D. Jones. 2005. An improved method of constructing a database of monthly climate observations and associated high-resolution grids. International Journal of Climatology **25**:693-712.

Miura, H., M. Satoh, H. Tomita, A. T. Noda, T. Nasuno, and S. Iga. 2007. A short-duration global cloud-resolving simulation with a realistic land and sea distribution. Geophysical Research Letters **34**:Artn L02804. DOI: 02810.01029/02006gl027448.

Moorthi, S., and M. J. Suarez. 1992. Relaxed Arakawa-Schubert - a parameterization of moist convection for General-Circulation Models. Monthly Weather Review **120**:978-1002.

Morgenstern, K. 1996. Geographic Variation in Forest Trees. Genetic Basis and Application of Knowledge in Silviculture University of British Columbia Press, Vancouver, British Columbia.

Muller, C. J., and P. A. O'Gorman. 2011. An energetic perspective on the regional response of precipitation to climate change. Nature Climate Change **1**:266-271.

New, M., M. Hulme, and P. Jones. 1999. Representing twentieth-century space-time climate variability. Part I: Development of a 1961-90 mean monthly terrestrial climatology. Journal of Climate **12**:829-856.

New, M., M. Todd, M. Hulme, and P. Jones. 2001. Precipitation measurements and trends in the twentieth century. International Journal of Climatology **21**:1899-1922.

O'Neill, G., T. Wang, N. Ukrainetz, L. Charleson, L. McAuley, A. Yanchuk, and S. Zedel. 2017. A proposed climate-based seed transfer system for British Columbia. Prov. BC, Victoria. BC Tech. Rep. 099. www. for. gov. bc. ca/hfd/pubs/Docs/Tr/Tr099. htm.

Omernik, J. M., and G. E. Griffith. 2014. Ecoregions of the conterminous United States: evolution of a hierarchical spatial framework. Environmental Management **54**:1249-1266.

Osterkamp, T. E. 2007. Characteristics of the recent warming of permafrost in Alaska. Journal of Geophysical Research-Earth Surface **112**.

Pan, D.-M., and D. D. A. Randall. 1998. A cumulus parameterization with a prognostic closure. Quarterly Journal of the Royal Meteorological Society **124**:949-981.

Paritsis, J., and T. T. Veblen. 2011. Dendroecological analysis of defoliator outbreaks on *Nothofagus pumilio* and their relation to climate variability in the Patagonian Andes. Global Change Biology **17**:239-253.

Parker, W. H. 1992. Focal point seed zones: site-specific seed zone delineation using geographic information systems. Canadian Journal of Forest Research **22**:267-271.

Parmesan, C., and G. Yohe. 2003. A globally coherent fingerprint of climate change impacts across natural systems. Nature **421**:37-42.

Pavia, E. G., F. Graef, and J. Reyes. 2009. Annual and seasonal surface air temperature trends in Mexico. International Journal of Climatology **29**:1324-1329.

Pebesma, E. J. 2004. Multivariable geostatistics in S: the gstat package. Computers & Geosciences **30**:683-691.

Pedlar, J., D. McKenney, J. Beaulieu, S. Colombo, J. McLachlan, and G. O'Neill. 2011. The implementation of assisted migration in Canadian forests. The Forestry Chronicle **87**:766-777.

Pedlar, J. H., D. W. McKenney, I. Aubin, T. Beardmore, J. Beaulieu, L. Iverson, G. A. O'Neill, R. S. Winder, and C. Ste-Marie. 2012. Placing forestry in the assisted migration debate. BioScience **62**:835-842.

Penuelas, J., R. Ogaya, M. Boada, and A. S. Jump. 2007. Migration, invasion and decline: changes in recruitment and forest structure in a warming-linked shift of European beech forest in Catalonia (NE Spain). Ecography **30**:829-837.

Peterson, T. C., and R. S. Vose. 1997. An Overview of the Global Historical Climatology Network Temperature Database. Bulletin of the American Meteorological Society **78**:2837-2849.

Potter, K. M., and W. W. Hargrove. 2012. Determining suitable locations for seed transfer under climate change: a global quantitative method. New Forests **43**:581-599.

Potter, K. M., R. M. Jetton, A. Bower, D. F. Jacobs, G. Man, V. D. Hipkins, and M. Westwood. 2017. Banking on the future: progress, challenges and opportunities for the genetic conservation of forest trees. New Forests **48**:153-180.

Pravalie, R. 2018. Major perturbations in the Earth's forest ecosystems. Possible implications for global warming. Earth-Science Reviews **185**:544-571.

Ramirez-Villegas, J., A. J. Challinor, P. K. Thornton, and A. Jarvis. 2013. Implications of regional improvement in global climate models for agricultural impact research. Environmental Research Letters **8**:Artn 024018. DOI: 024010.021088/021748-029326/024018/024012/024018

Ramirez-Villegas, J., F. Cuesta, C. Devenish, M. Peralvo, A. Jarvis, and C. A. Arnillas. 2014. Using species distributions models for designing conservation strategies of Tropical Andean biodiversity under climate change. Journal for Nature Conservation **22**:391-404.

Ramírez, M. I., J. G. Azcárate, and L. Luna. 2003. Effects of human activities on monarch butterfly habitat in protected mountain forests, Mexico. The Forestry Chronicle **79**:242-246.

Randall, D., M. Khairoutdinov, A. Arakawa, and W. Grabowski. 2003. Breaking the cloud parameterization deadlock. Bulletin of the American Meteorological Society **84**:1547-1564.

Randall, D. A. 2010. The evolution of complexity in general circulation models.*in* L. Donner, W. Schubert, and R. C. J. Somerville, editors. The development of atmospheric general circulations models: complexity, synthesis, and computation. Cambridge University Press, Cambridge UK.

Räty, O., J. Räisänen, and J. S. Ylhäisi. 2014. Evaluation of delta change and bias correction methods for future daily precipitation: intermodel cross-validation using ENSEMBLES simulations. Climate Dynamics **42**:2287-2303.

Rehfeldt, G. E. 1988. Ecological genetics of *Pinus contorta* from the Rocky Mountains (USA): A synthesis. Silvae genetica **37**:131-135.

Rehfeldt, G. E. 2006. A spline model of climate for the Western United States. General Technical Report RMRS-GTR-165. Department of Agriculture, Forest Service, Rocky Mountain Research Station, Fort Collins, Colorado, U.S.

Rehfeldt, G. E., N. L. Crookston, M. V. Warwell, and J. S. Evans. 2006. Empirical analyses of plant-climate relationships for the Western United States. International Journal of Plant Sciences **167**:1123-1150.

Rehfeldt, G. E., C. C. Ying, D. L. Spittlehouse, and D. A. Hamilton. 1999. Genetic responses to climate in *Pinus contorta*: niche breadth, climate change, and reforestation. Ecological Monographs **69**:375-407.

Richardson, C. W., D. A. Bucks, and E. J. Sadler. 2008. The Conservation Effects Assessment Project benchmark watersheds: Synthesis of preliminary findings. Journal of Soil and Water Conservation **63**:590-604.

Rogelj, J., M. Meinshausen, and R. Knutti. 2012. Global warming under old and new scenarios using IPCC climate sensitivity range estimates. Nature Climate Change **2**:248-253.

Rosenzweig, C., D. Karoly, M. Vicarelli, P. Neofotis, Q. G. Wu, G. Casassa, A. Menzel, T. L. Root, N. Estrella, B. Seguin, P. Tryjanowski, C. Z. Liu, S. Rawlins, and A. Imeson. 2008. Attributing physical and biological impacts to anthropogenic climate change. Nature **453**:353-357.

Saenz-Romero, C., J. B. Lamy, A. Ducousso, B. Musch, F. Ehrenmann, S. Delzon, S. Cavers, W. Chalupka, S. Dagdas, J. K. Hansen, S. J. Lee, M. Liesebach, H. M. Rau, A. Psomas, V. Schneck, W. Steiner, N. E. Zimmermann, and A. Kremer. 2017. Adaptive and plastic responses of *Quercus petraea* populations to climate across Europe. Global Change Biology **23**:2831-2847.

Sáenz-Romero, C., G. E. Rehfeldt, N. L. Crookston, P. Duval, R. St-Amant, J. Beaulieu, and B. A. Richardson. 2010. Spline models of contemporary, 2030, 2060 and 2090 climates for Mexico and their use in understanding climate-change impacts on the vegetation. Climatic Change **102**:595-623.

Saenz-Romero, C., G. E. Rehfeldt, P. Duval, and R. A. Lindig-Cisneros. 2012. Abies religiosa habitat prediction in climatic change scenarios and implications for monarch butterfly conservation in Mexico. Forest Ecology and Management **275**:98-106.

Sarkinen, T., P. Gonzales, and S. Knapp. 2013. Distribution models and species discovery: the story of a new Solanum species from the Peruvian Andes. Phytokeys **31**:1-20.

Schär, C., and C. Frei. 2005. Orographic Precipitation and Climate Change. Pages 255-266 *in* U. M. Huber, H. K. M. Bugmann, and M. A. Reasoner, editors. Global Change and Mountain Regions: An Overview of Current Knowledge. Springer Netherlands, Dordrecht, Netherlands.

Scherrer, S. C. 2011. Present-day interannual variability of surface climate in CMIP3 models and its relation to future warming. International Journal of Climatology **31**:1518-1529.

Schneider, U., A. Becker, P. Finger, A. Meyer-Christoffer, M. Ziese, and B. Rudolf. 2014. GPCC's new land surface precipitation climatology based on quality-controlled in situ data and its role in quantifying the global water cycle. Theoretical and Applied Climatology **115**:15-40.

Scholl, M. A., and S. F. Murphy. 2014. Precipitation isotopes link regional climate patterns to water supply in a tropical mountain forest, eastern Puerto Rico. Water Resources Research **50**:4305-4322.

Schweikert, A., P. Chinowsky, X. Espinet, and M. Tarbert. 2014. Climate change and infrastructure impacts: comparing the impact on roads in ten countries through 2100. Humanitarian Technology: Science, Systems and Global Impact 2014 **78**:306-316.

Sharma, S., J. J. Magnuson, R. D. Batt, L. A. Winslow, J. Korhonen, and Y. Aono. 2016. Direct observations of ice seasonality reveal changes in climate over the past 320-570 years. Scientific Reports **6**:Artn 25061. DOI: 25010.21038/Srep25061

Smith, D. M., A. A. Scaife, and B. P. Kirtman. 2012. What is the current state of scientific knowledge with regard to seasonal and decadal forecasting? Environmental Research Letters **7**.

St Clair, J. B., N. L. Mandel, and K. W. Vance-Borland. 2005. Genecology of Douglas fir in western Oregon and Washington. Annals of Botany **96**:1199-1214.

St. Clair, J. B. 2006. Genetic variation in fall cold hardiness in coastal Douglas-fir in western Oregon and Washington. Canadian Journal of Botany **84**:1110-1121.

Stott, P. A., S. F. B. Tett, G. S. Jones, M. R. Allen, W. J. Ingram, and J. F. B. Mitchell. 2001. Attribution of twentieth century temperature change to natural and anthropogenic causes. Climate Dynamics **17**:1-21.

Suarez, M., R. Villalba, I. Mundo, and N. Schroeder. 2015. Sensitivity of *Nothofagus dombeyi* tree growth to climate changes along a precipitation gradient in northern Patagonia, Argentina. Trees **29**:1053-1067.

Suarez, M. L., L. Ghermandi, and T. Kitzberger. 2004. Factors predisposing episodic drought-induced tree mortality in Nothofagus - site, climatic sensitivity and growth trends. Journal of Ecology **92**:954-966.

Sun, Q. H., C. Y. Miao, Q. Y. Duan, H. Ashouri, S. Sorooshian, and K. L. Hsu. 2018. A review of global precipitation data sets: data sources, estimation, and intercomparisons. Reviews of Geophysics **56**:79-107.

Swetnam, T. W., C. D. Allen, and J. L. Betancourt. 1999. Applied historical ecology: Using the past to manage for the future. Ecological Applications **9**:1189-1206.

Taïbi, K., A. D. del Campo, J. M. Mulet, J. Flors, and A. Aguado. 2014. Testing Aleppo pine seed sources response to climate change by using trial sites reflecting future conditions. New Forests **45**:603-624.

Tank, A. M. G. K., J. B. Wijngaard, G. P. Konnen, R. Bohm, G. Demaree, A. Gocheva, M. Mileta, S. Pashiardis, L. Hejkrlik, C. Kern-Hansen, R. Heino, P. Bessemoulin, G. Muller-Westermeier, M. Tzanakou, S. Szalai, T. Palsdottir, D. Fitzgerald, S. Rubin, M. Capaldo, M. Maugeri, A. Leitass, A. Bukantis, R. Aberfeld, A. F. V. Van Engelen, E. Forland, M. Mietus, F. Coelho, C. Mares, V. Razuvaev, E. Nieplova, T. Cegnar, J. A. Lopez, B. Dahlstrom, A. Moberg, W. Kirchhofer, A. Ceylan, O. Pachaliuk, L. V. Alexander, and P. Petrovic. 2002. Daily dataset of 20th-century surface air temperature and precipitation series for the European Climate Assessment. International Journal of Climatology **22**:1441-1453.

Team, R. D. C. 2016. R: A language and environment for statistical computing. R Foundation for Statistical Computing, Vienna, Austria. URL https://www.R-project.org/.

Tett, S. F. B., P. A. Stott, M. R. Allen, W. J. Ingram, and J. F. B. Mitchell. 1999. Causes of twentieth-century temperature change near the Earth's surface. Nature **399**:569-572.

Thornton, P. E., S. W. Running, and M. A. White. 1997. Generating surfaces of daily meteorological variables over large regions of complex terrain. Journal of Hydrology **190**:214-251.

Tucker, C. M. 2004. Community institutions and forest management in Mexico's Monarch Butterfly Reserve. Society & Natural Resources **17**:569-587.

Van Den Besselaar, E. J. M., A. M. G. K. Tank, G. Van Der Schrier, M. S. Abass, O. Baddour, A. F. V. Van Engelen, A. Freire, P. Hechler, B. I. Laksono, Iqbal, R. Jilderda, A. K. Foamouhoue, A. Kattenberg, R. Leander, R. M. Guingla, A. S. Mhanda, J. J. Nieto, Sunaryo, A. Suwondo, Y. S. Swarinoto, and G. Verver. 2015. International climate assessment & dataset: climate services across borders. Bulletin of the American Meteorological Society **96**:16-21.

Van Wagner, C. E. 1987. Development and Structure of the Canadian Forest Fire Weather Index System. Forestry Technical Report 35. Canadian Forestry Service, Ottawa, ON.

Vanham, D., E. Fleischhacker, and W. Rauch. 2009. Impact of an extreme dry and hot summer on water supply security in an alpine region. Water Science and Technology **59**:469-477.

Varma, A. K. 2018. Measurement of Precipitation from Satellite Radiometers (Visible, Infrared, and Microwave): Physical Basis, Methods, and Limitations. Pages 223-248 *in* T. Islam,

Y. Hu, A. Kokhanovsky, and J. Wang, editors. Remote Sensing of Aerosols, Clouds, and Precipitation. Elsevier, Amsterdam, Netherlands.

Vaughn, D. 2005. Degree Days. Pages 315-318 *in* J. Oliver, editor. Encyclopedia of World Climatology. Springer Netherlands, Dordretch Netherlands.

Visser, M. E., and C. Both. 2005. Shifts in phenology due to global climate change: the need for a yardstick. Proceedings of the Royal Society Biological Sciences **272**:2561-2569.

Vizcaíno-Palomar, N., I. Ibáñez, M. Benito-Garzón, S. C. González-Martínez, M. A. Zavala, and R. Alía. 2017. Climate and population origin shape pine tree height-diameter allometry. New Forests **48**:363-379.

Vorosmarty, C. J., C.F-Jauregui, and M. C. Donoso. 1998. A Regional, Electronic Hydrometeorological Data Network for South America, Central America, and the Caribbean. University of New Hampshire, Durham, New Hampshire, U.S.

Walsh, J. E., W. L. Chapman, V. Romanovsky, J. H. Christensen, and M. Stendel. 2008. Global Climate Model Performance over Alaska and Greenland. Journal of Climate **21**:6156-6174.

Wang, M. Y., J. E. Overland, V. Kattsov, J. E. Walsh, X. D. Zhang, and T. Pavlova. 2007. Intrinsic versus forced variation in coupled climate model simulations over the Arctic during the twentieth century. Journal of Climate **20**:1093-1107.

Wang, T., A. Hamann, D. Spittlehouse, and C. Carroll. 2016. Locally downscaled and spatially customizable climate data for historical and future periods for North America. PLOS ONE **11**:e0156720. DOI: 0156710.0151371/journal.pone.0156720.

Wang, T., A. Hamann, D. L. Spittlehouse, and S. N. Aitken. 2006. Development of scale-free climate data for Western Canada for use in resource management. International Journal of Climatology **26**:383-397.

Wang, T., A. Hamann, D. L. Spittlehouse, and T. Q. Murdock. 2011. ClimateWNA—High-resolution spatial climate data for Western North America. Journal of Applied Meteorology and Climatology **51**:16-29.

Wang, T., A. Hamann, D. L. Spittlehouse, and T. Q. Murdock. 2012. ClimateWNA—High-resolution spatial climate data for Western North America. Journal of Applied Meteorology and Climatology **51**:16-29.

Weng, F., X. Zou, and Z. Qin. 2014. Uncertainty of AMSU-A derived temperature trends in relationship with clouds and precipitation over ocean. Climate Dynamics **43**:1439-1448.

Werner, R. A., E. H. Holsten, S. M. Matsuoka, and R. E. Burnside. 2006. Spruce beetles and forest ecosystems in south-central Alaska: A review of 30 years of research. Forest Ecology and Management **227**:195-206.

Westerling, A. L., H. G. Hidalgo, D. R. Cayan, and T. W. Swetnam. 2006. Warming and earlier spring increase western US forest wildfire activity. Science **313**:940-943.

Wiens, J. J. 2016. Climate-related local extinctions are already widespread among plant and animal species. Plos Biology **14**:ARTN e2001104. DOI:2001110.2001371/journal.pbio.2001104

Wilks, D. S., and R. L. Wilby. 1999. The weather generation game: a review of stochastic weather models. Progress in Physical Geography **23**:329-357.

Willmott, C. J. 1982. Some comments on the evaluation of model performance. Bulletin of the American Meteorological Society **63**:1309-1313.

Willmott, C. J., and K. Matsuura. 1995. Smart interpolation of annually averaged air temperature in the United States. Journal of Applied Meteorology **34**:2577-2586.

Willmott, C. J., and S. M. Robeson. 1995. Climatologically aided interpolation (CAI) of terrestrial air temperature. International Journal of Climatology **15**:221-229.

WMO. 1996. Climatological Normals (CLINO) for the period 1961-1990. World Meteorological Organization. Geneva, Switzerland.

Xie, P., and P. A. Arkin. 1997. Global precipitation: a 17-year monthly analysis based on gauge observations, satellite estimates, and numerical model outputs. Bulletin of the American Meteorological Society **78**:2539-2558.

Xu, Z. F., Y. Han, and Z. L. Yang. 2019. Dynamical downscaling of regional climate: A review of methods and limitations. Science China-Earth Sciences **62**:365-375.

Ying, C. C., and A. D. Yanchuk. 2006. The development of British Columbia's tree seed transfer guidelines: Purpose, concept, methodology, and implementation. Forest Ecology and Management **227**:1-13.

Zacarías-Eslava, Y., and R. F. d. Castillo. 2010. Comunidades vegetales templadas de la Sierra Juárez, Oaxaca: pisos altitudinales y sus posibles implicaciones ante el cambio climático. Boletín de la Sociedad Botánica de México **87**:13-28.

Zhang, N., C. Zhao, S. M. Quiring, and J. L. Li. 2017. Winter wheat yield prediction using normalized difference vegetative index and agro-climatic parameters in Oklahoma. Agronomy Journal **109**:2700-2713.

8. Appendices

Appendix 8.1. Climate based seed zones for Mexico: spatial grids to guide reforestation under observed and projected climate change

This seed zone classification is based on bands of two climate variables that have often been shown to drive genetic adaptation of tree species: mean coldest month temperature (MCMT), and an aridity index (AHM). MCMT was divided into ten bands of 3°C intervals, with the limits of these bands being, temperatures below <2°C, 2-5°, 5-8°, 8-11°, 11-14°, 14-17°, 17-20°, 20-23°, 23-26°, >26°C. AHM was divided into seven bands with intervals that are approximately equal width under a log-transformation: <20, 20-30, 30-45, 45-65, 65-95, 95-140, and >140 °C/mm.

High-resolution images are provided below, while corresponding GIS files can be downloaded from the open-access repository Zenodo.org (*https://doi.org/10.5281/zenodo.1052141*). The local maps for four regions shown below are drawn at a scale useful for forest managers to identify seed source locations for reforestation programs to address observed and projected climate change.
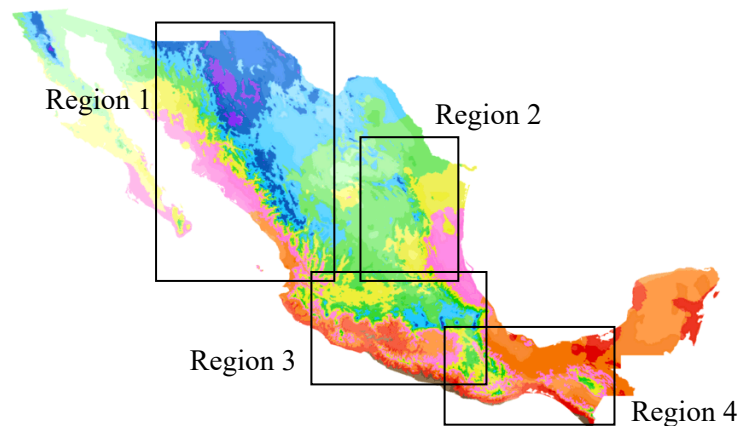
Region 1

1961-1990

1991-2015

139
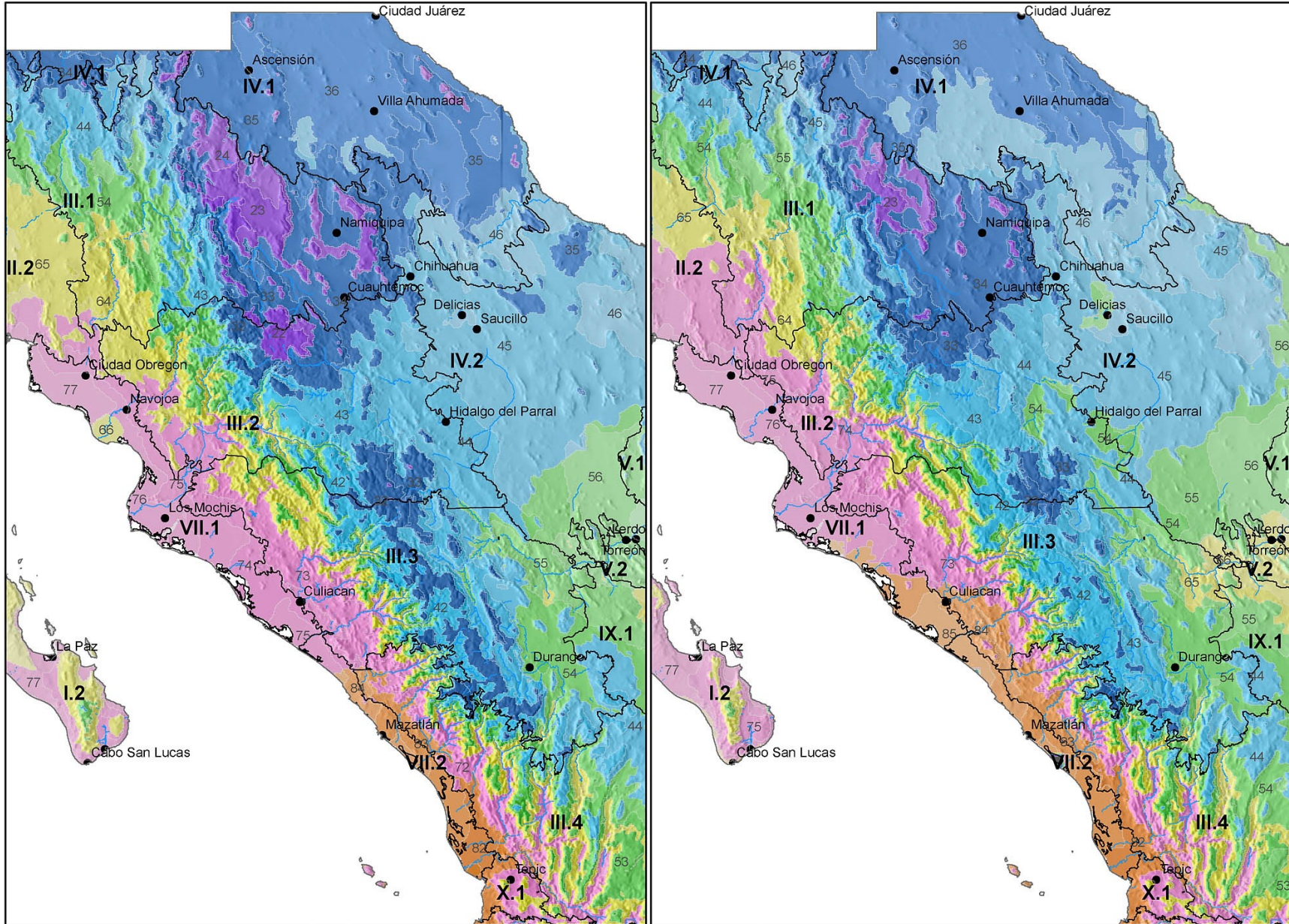
Region 1

2050 rcp 4.5

2050 rcp 8.5

140
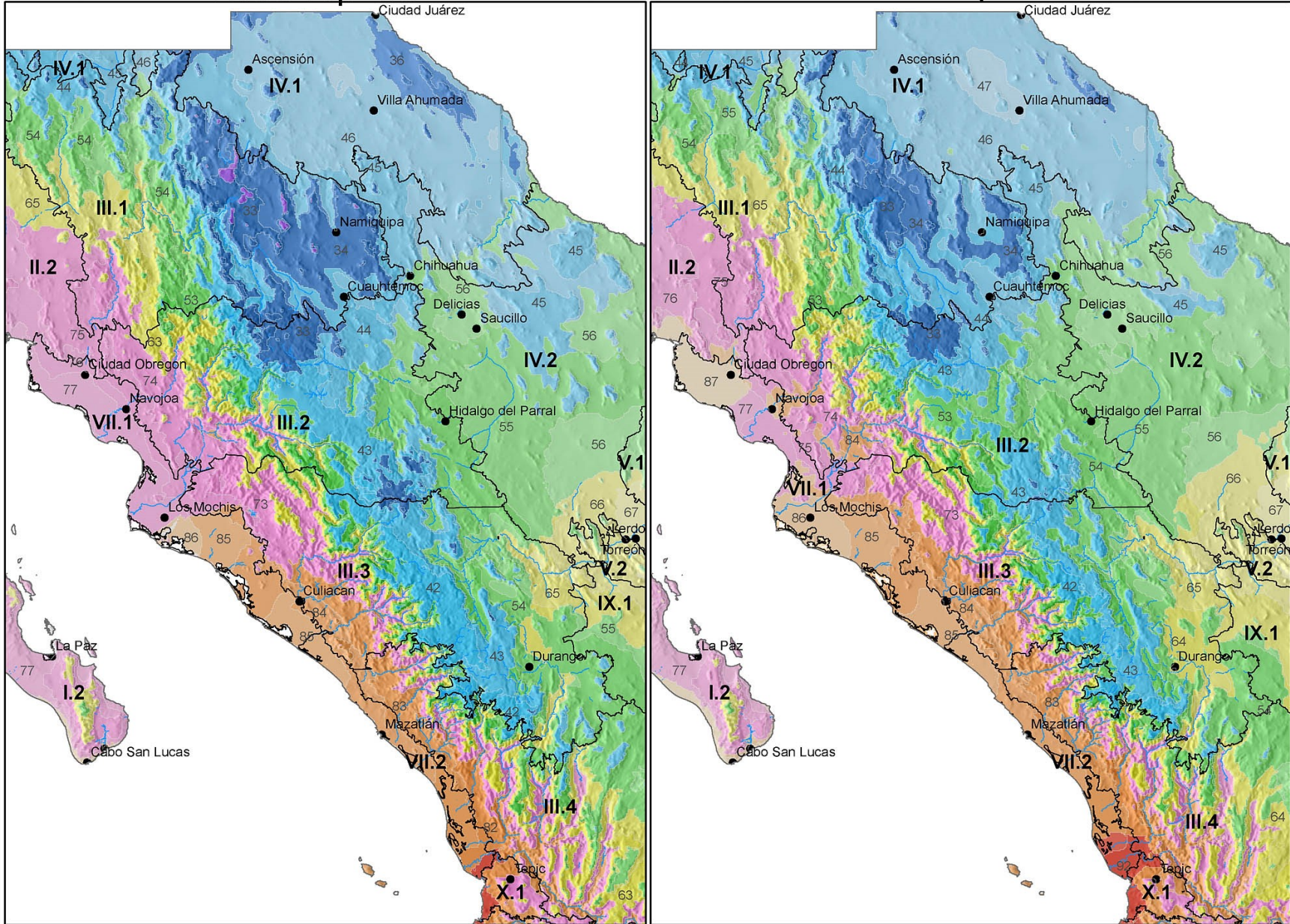
Region 2

1961-1990

1991-2015

141
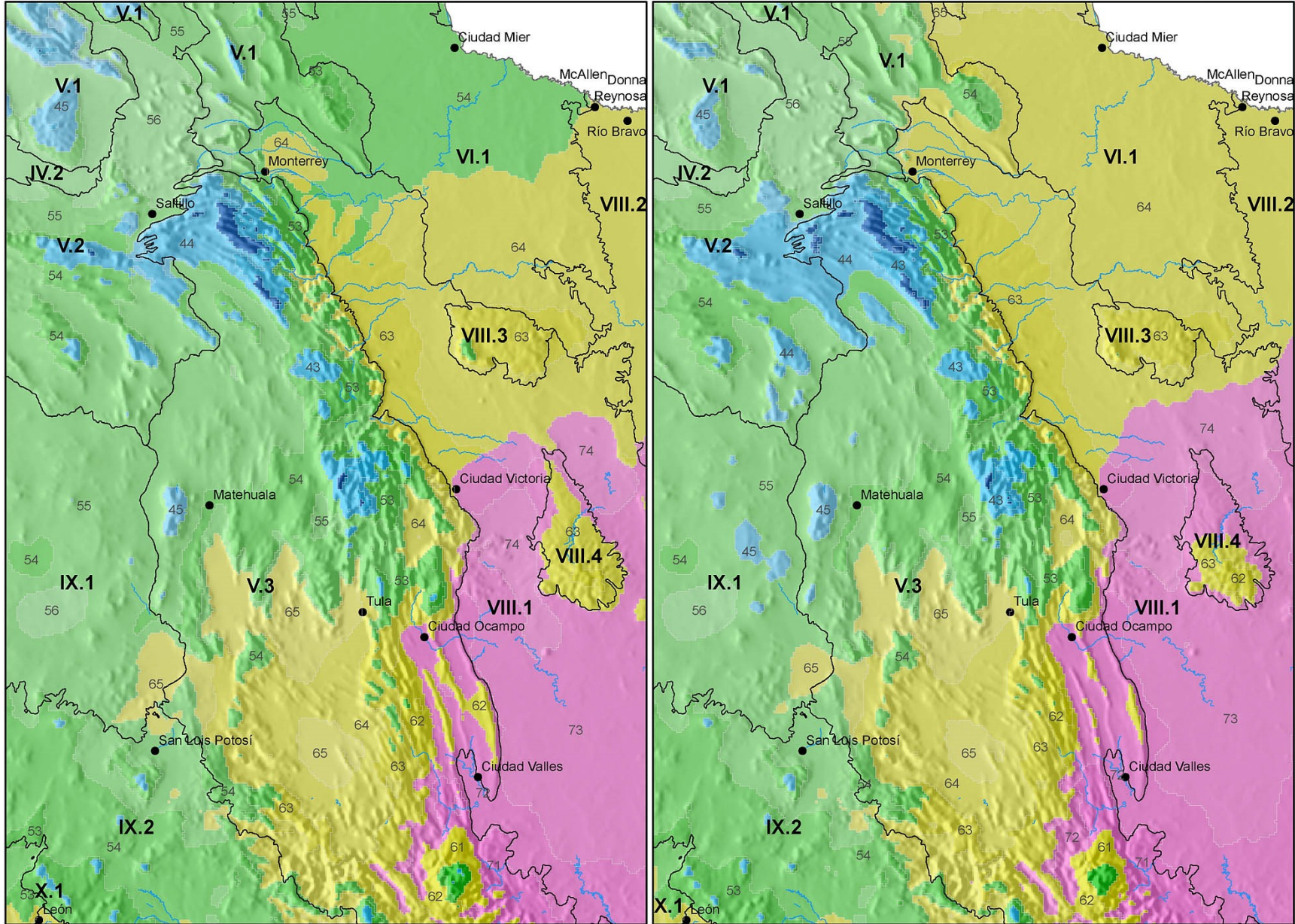
Region 2

2050 rcp 4.5

2050 rcp 8.5
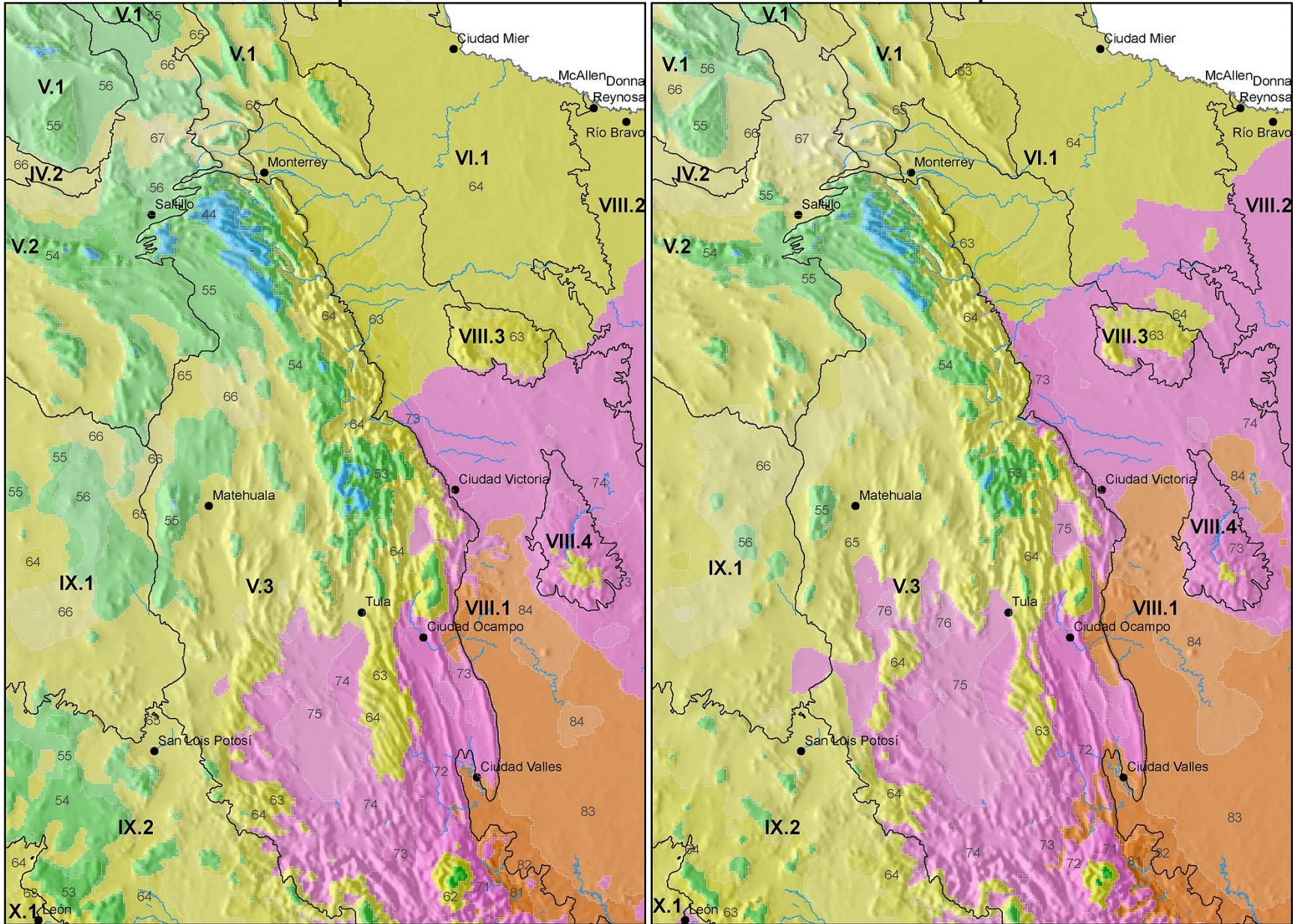
Region 3

1961-1990
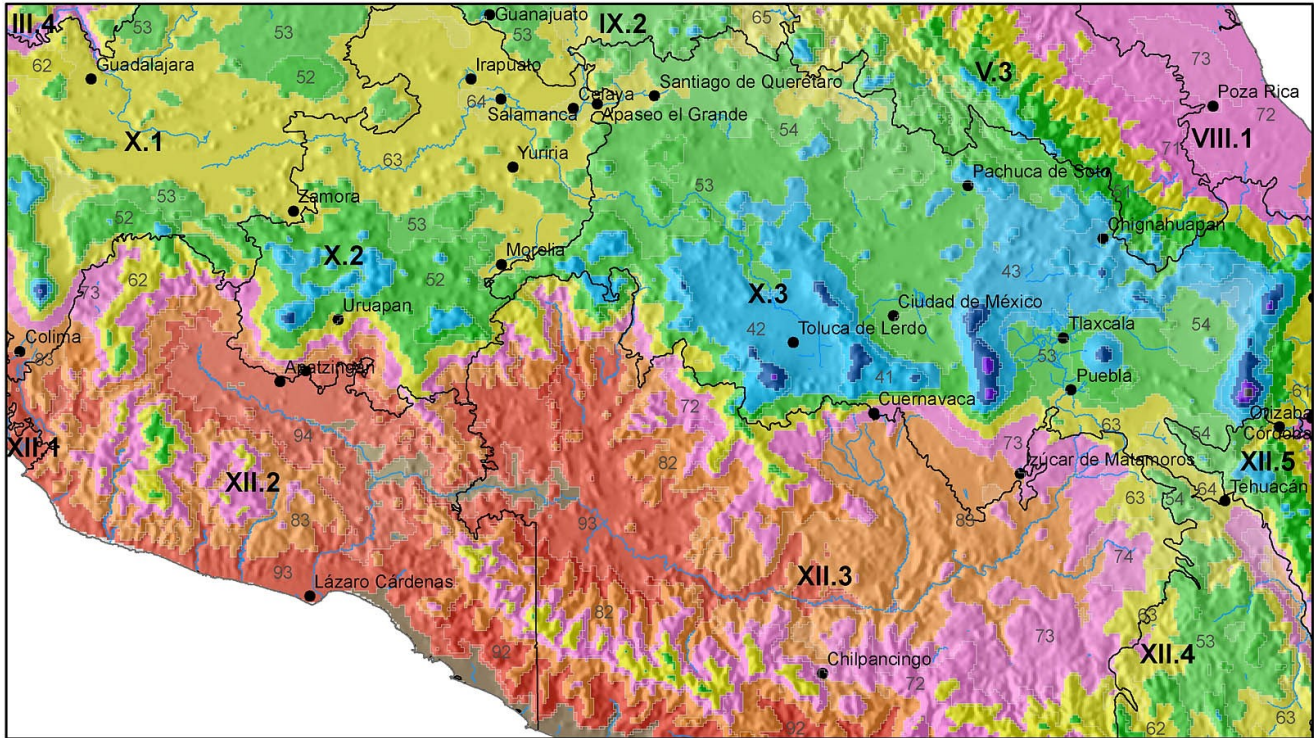
1991-2015
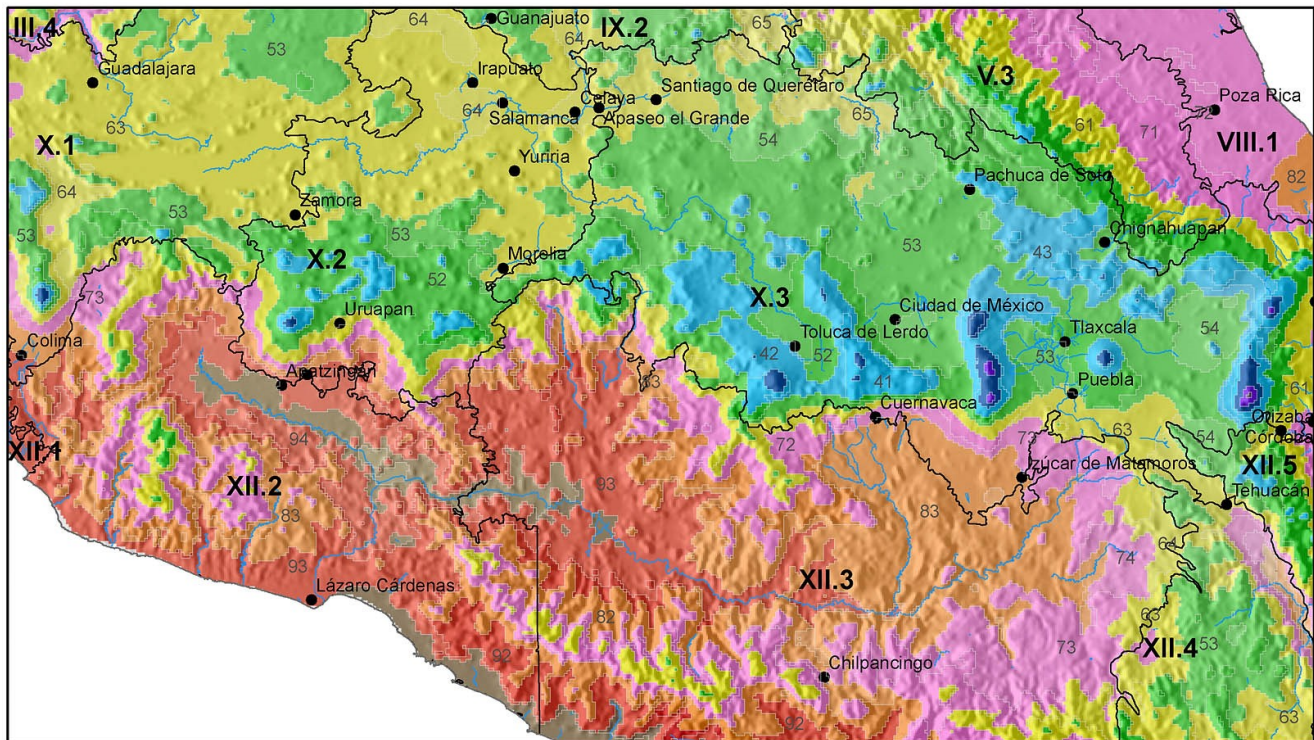
Region 3

2050 rcp 4.5

2050 rcp 8.5

Region 4

1961-1990
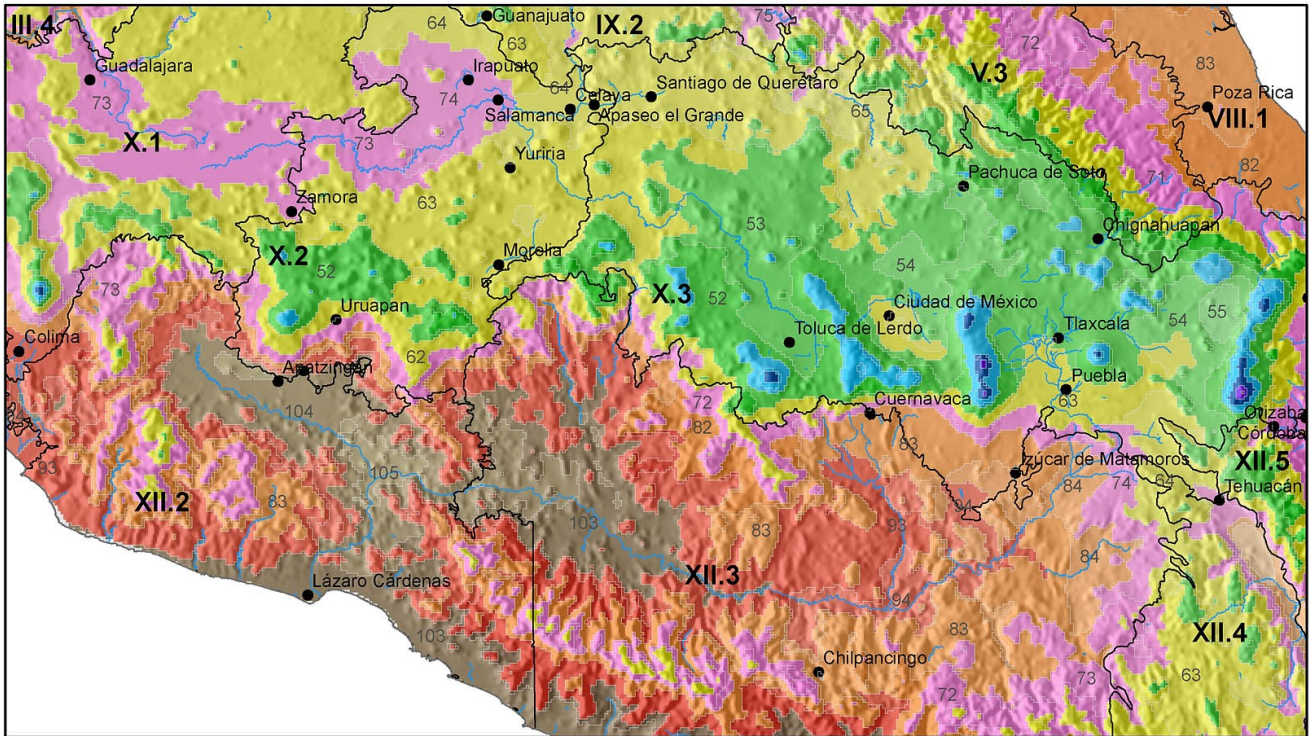
1991-2015
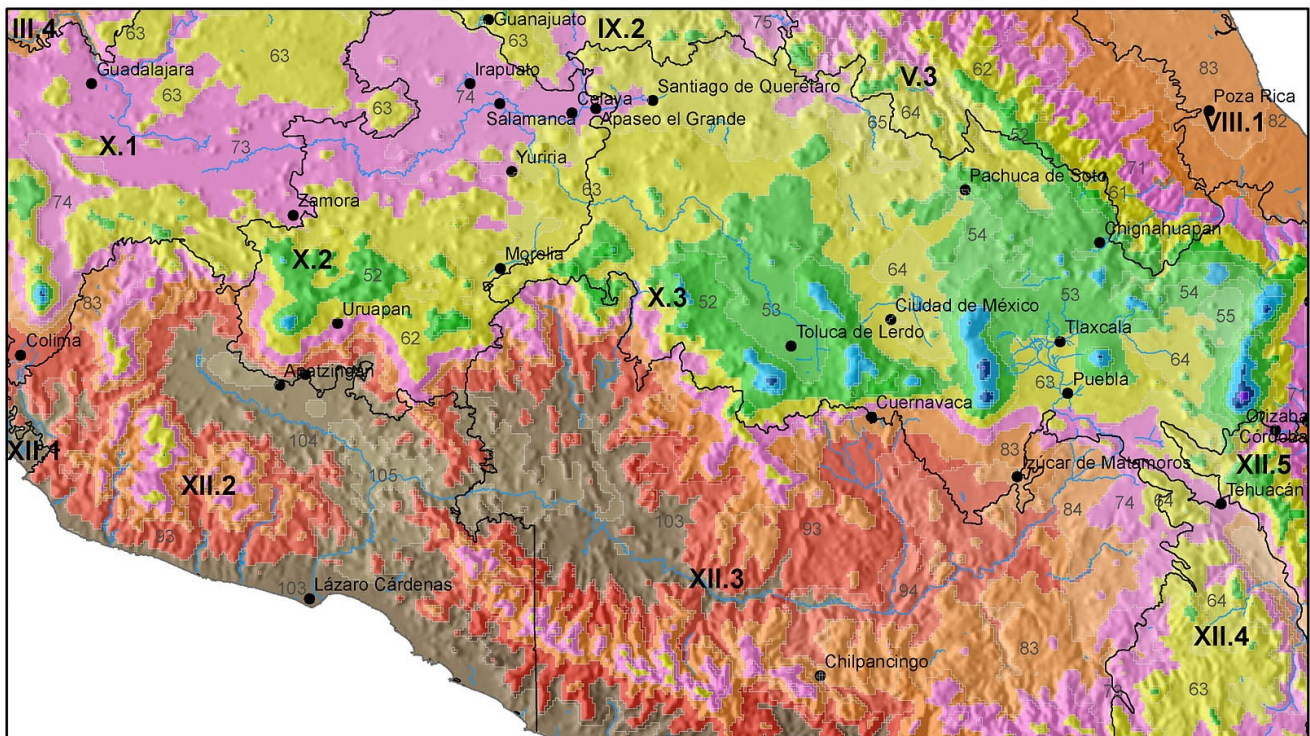
Region 4

2050 rcp 4.5

2050 rcp 8.5